UNIVERSITY OF HULL

Investigating the importance of CBX2's structural motifs for its chromatin interactions and pro-oncogenic epigenetic regulatory function in triple negative breast cancer.

By

Wojciech Dobrowinski

201841455

MSc by Research in Biomedical Science

Supervisor: Dr Mark Wade

Secondary Supervisor: Dr Cheryl Walter

December 2022

Acknowledgements

I would like to thank Dr Mark Wade for being a great supervisor and for all of his knowledge, support, guidance and patience. Especially at the start of the project when I was getting used to the laboratory work.

I would also like to thank Dr Cheryl Walter for training me in microbiological techniques and her valuable assistance throughout the whole project.

Additionally, I would like to thank Lucie Bilton for training me in the majority of the laboratory techniques, for her valuable advice and support.

I would also like to thank Thomas Francis for providing the flow cytometry training and his continued encouragement.

Also big thanks to Jun-ichi Nakayama (Nagoya City University) for kindly providing the plasmids used in this project.

Publications to date

Data enclosed in this thesis was published in the following research article:

Bilton, L. J., Warren, C., Humphries, R. M., Kalsi, S., Waters, E., Francis, T., Dobrowinski, W., Beltran-Alvarez, P., Wade, M. A. (2022). The Epigenetic Regulatory Protein CBX2 Promotes mTORC1 Signalling and Inhibits DREAM Complex Activity to Drive Breast Cancer Cell Growth. *Cancers*, *14*(14), 3491.

Abstract

Epigenetics is the study of the change in gene expression patterns that are not caused by direct alterations in the DNA nucleotide sequence but instead are as a result of the dynamic remodelling of the chromatin state. Regulation of the chromatin landscape is mediated via coordination between methylation of DNA and chemical modifications of the associated histone proteins. The activity and expression of the epigenetic regulatory proteins modulating the histone modifications has been shown to be dysregulated in a range of cancers, moreover, due to the reversible nature of the histone modifications these epigenetic regulatory proteins have emerged as potential therapeutic targets. CBX2 is an epigenetic regulatory protein shown to be overexpressed in triple negative breast cancer (TNBC) and to play a role in regulating TNBC cell growth. It functions as the chromatin interacting subunit of polycomb repressive complex 1 (PRC1) which condenses the chromatin and thus represses the transcription of genes. This study aimed to investigate which structural motifs of CBX2 are integral for its ability to interact with the chromatin in TNBC. Genotypic and phenotypic changes in TNBC cell line models were assessed following the overexpression of CBX2 and structural motif deficient CBX2 variants. The effect of rescue of CBX2 expression following siRNA mediated CBX2 knockdown with the CBX2 variants was also assessed. We identified the chromodomain of the CBX2 as the structural motif important for CBX2s ability to regulate TNBC cell growth, the catalytic activity of the PRC1 complex and regulation of its target genes. This suggests that therapeutically targeting the chromodomain of CBX2 may be a viable strategy for treating the aberrant epigenome created by CBX2 overexpression in hard-to-treat cancers such as TNBC.

Table of Contents

List of figures

List of Tables

Abbreviations

AcCoA – Acetyl coenzyme A

AR – Acidic residue

AURKA - Aurora kinase A

BP – Base pairs

BRD – Bromodomain

CBX – Chromobox

CD – Chromodomain

CDK – Cyclin dependent kinase

CSD – Chromo shadow domain

ddH2O – double distilled water

DNA – Deoxyribonucleic acid

DREAM - Dimerization partner, RB-like, E2F and multi-vulval class B

ERG1 – Early growth response protein

EZH2 - Enhancer of zeste homolog 2

FACS - Fluorescence-activated cell sorting

GBM - Glioblastoma multiforme

HAT – Histone acetyl transferase

HDAC – Histone deacetylase

HP – Heterochromatin protein

HPH – Human polyhometoic homologue

IF – Immunofluorescence

MAPK – Mitogen activated protein kinase

MMP – Matrix metalloproteinase

mTORC1 - Mammalian target of rapamycin complex 1

NFkB- Nuclear factor kappa B

P-TEFb – Positive transcription elongation factor

PcBox – Polycomb repressor box

PcG – Polycomb group

PCGF – Polycomb ring finger protein

PEV – Position effect variegation

PI3K - Phosphoinositide 3-kinases

PRC1 – Polycomb repressor complex 1

qPCR - quantitative polymerase chain reaction

RBL2 – Retinoblastoma-like protein 2

RISC – RNA – induced silencing complex

RNA - ribonucleic acid

ROS – Reactive oxygen species

SA – Serine rich and acidic residue

SDS-PAGE - Sodium dodecyl-sulfate polyacrylamide gel electrophoresis

shRNA – short hairpin RNA

siRNA – small interfering RNA

SR – Serine rich

SUMO - Small Ubiquitin-like Modifier

TDRD – Tudor domain containing protein

TNBC – Triple negative breast cancer

XIAP - X-linked inhibitor of apoptosis protein

Chapter 1. Introduction

1.1 Epigenetics

DNA in eukaryotic cells is packaged into chromatin, a dynamic and compact complex structure comprised of nucleosomes which are structural units consisting of 147 base pairs (bp) of DNA wrapped in a 1.75 super-helical turn around a histone octamer (Buocikova et al, 2020). Making up the histone octamer are two copies of the four core histone proteins: H2A, H2B, H3 and H4 which are all connected to a short strand of linker DNA (around 20bp) creating the beads on a string structure (Hergeth and Schneider, 2015). However, in order to form higher order structures like the 30nm chromatin fibre a fifth histone, linker H1, is required to bind to the entry and exit sites of DNA in order to stabilize the nucleosome (Brockers and Schneider, 2019). The histone proteins are able to bind to DNA as a result of their protruding N-terminal amino acid tails being enriched in arginine and lysine residues providing the histone proteins with a positive charge and thus, an affinity for the negatively charged DNA (Sher et al, 2020). Furthermore, these amino acid tails can be chemically modified inducing a change in the chromatin state and subsequently the gene expression pattern by altering the inter-nucleosomal interactions and the net charges of the histone proteins. Depending on the chemical modification, the chromatin can either be in a compact, highly condensed state (heterochromatin) where the transcriptional machinery won't have access to the promoter region of a gene or a more relaxed state (euchromatin) where a gene will be transcribed (Figure 1.1) (Kim and Kaang, 2017). Heterochromatin can be further classified into facultative, meaning it can be converted into euchromatin, and constitutive, meaning it's always highly condensed. Executing these chemical modifications, and thereby regulating the accessibility of the DNA, are histone modifying proteins that can be split into three broad subgroups: writer, eraser and reader proteins.

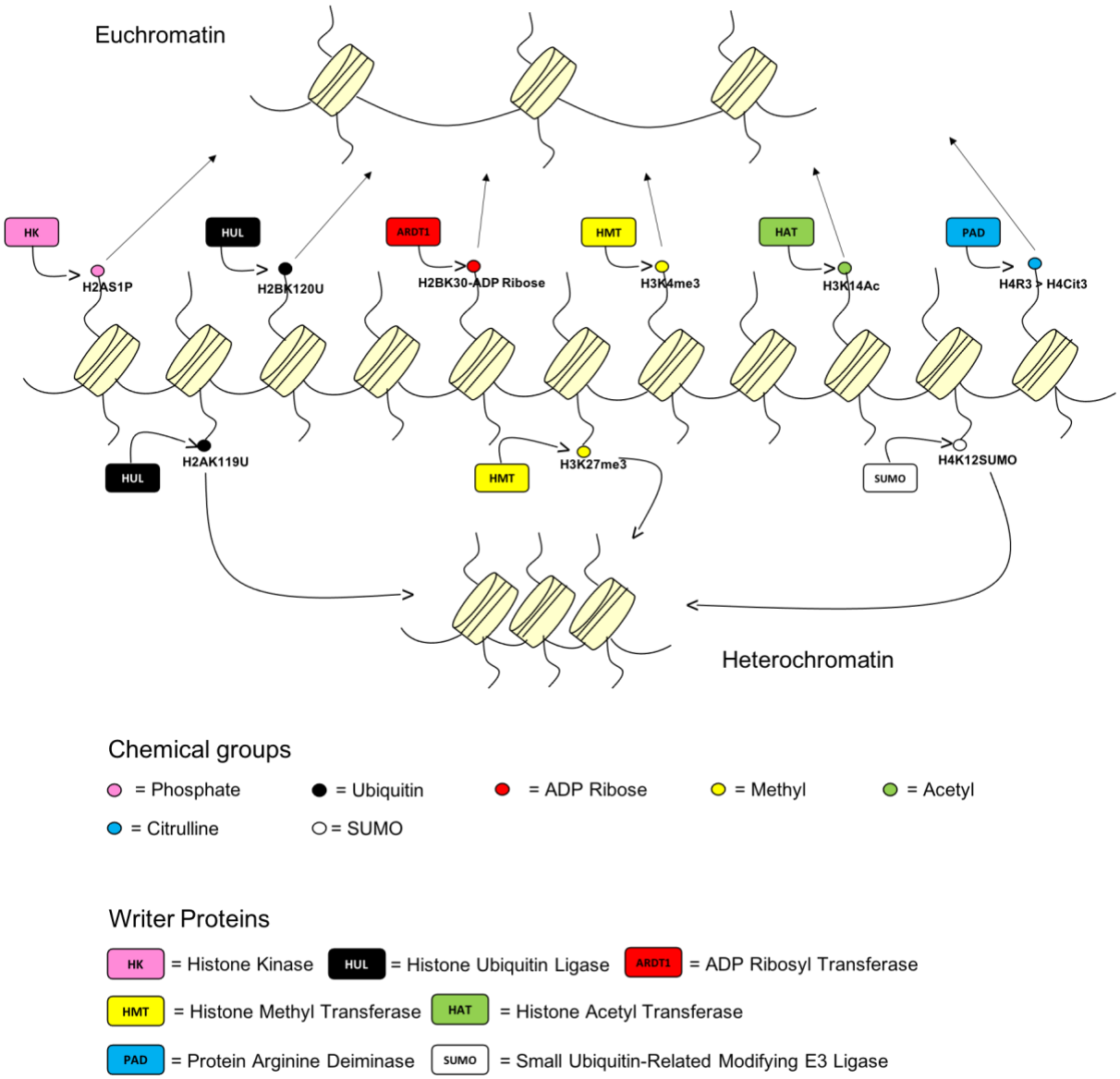

Figure 1.1 The chromatin state (heterochromatin or euchromatin) following writer protein mediated addition of different chemical groups to specific lysine (K), arginine (R) and serine (S) residues of the histone tails. The coloured boxes represent the writer proteins which in this figure add chemical groups (coloured circles) to the protruding amino acid histone tails of a specific histone (yellow cylinders). Which histone is modified at which amino acid is shown under each coloured circle using the histone modification nomenclature. Which describes the name of the histone that is being modified, followed by the single letter amino acid abbreviation, the position of the amino acid in the histone tail and the chemical group that is being added eg H3K14Ac. The specific writer proteins and chemical groups that enrich the histone tails illustrated in this figure are just a few examples out of the many others. The addition of a chemical group will either loosen the chromatin state (euchromatin) or condense it (heterochromatin) preventing transcription from taking place. Some chemical groups can both loosen or condense the chromatin depending on which amino acid of the histone tails gets modified (eg methylation).

1.2 Epigenetic Regulators

Writer proteins are enzymes that add chemical groups to the histone tails, they are split into classes based on the chemical modification they add. One of the classes are the histone acetyltransferases (HATs) which promotes the transcription of genes by adding acetyl groups to H3K14, H4K8 among other lysine residues (Haque et al, 2021). Based on their structural and biochemical properties HATs can be further split into five subfamilies: HAT1, Gcn5, MYST, p300 and Rtt109. All 5 subfamilies share varying carboxyl and amino terminals that surround their central core regions which interacts with the acetyl coenzyme A (AcCoA) cofactor that transfers the acetyl group to the ε-amino of a lysine side chain when conducting the catalytic mechanism (Marmostein and Zhou, 2014). Since acetyl groups carry a negative charge the addition of them to lysine residues of histone tails neutralises the lysine's positive charge, which weakens the histones' affinity for DNA resulting in euchromatin and allowing genes to be transcribed (Bannister and Kouzarides, 2011).

Opposing the effects of writer proteins by removing chemical modifications from the histone tails are eraser proteins. In the case of histone acetylation, it is the histone deacetylases (HDAC) which remove the acetyl group from the lysine residues of the histone tails. To date 18 HDACs have been identified and grouped into four classes with two class I HDACs, HDAC1 and HDAC2, being the most predominant in the nuclei of cells where they regulate the deacetylation of various genes involved in cell cycle progression (Yamaguchi et al., 2010). Another class of eraser protein are histone deubiquitylating proteases that regulate the transcription of genes associated with the cell cycle, DNA repair, and endocytosis by removing the ubiquitin molecule from the histone tails (Turcu et al, 2009). USP11 is a type of a deubiquitylase which specifically targets the H2AK119U epigenetic mark associated with heterochromatin, and is able to remove the ubiquitin molecule through its ubiquitin c terminal hydrolase that hydrolyses the peptide bond between the glycine 76 of ubiquitin and the ε-amino group of the lysine side chain (Zhang, 2011). This results in the chromatin loosening from its previously tightly packed stated into euchromatin, allowing genes to be transcribed (Ting et al, 2019).

The last subgroup of the histone modifying proteins are the reader proteins that recognize specific chemical modifications and transmit the epigenetic signal downstream (Milosevich and Hof, 2016). Unlike acetylation, methylation of lysine residues has no effect on their

charge, and thus would have no effect on the chromatin state. Moreover, methylation can either activate or repress transcription depending on the methyl groups position on the histone tail, with methylated H3K4 and H3K36 being associated with euchromatin while methylated H3K9 and H3K27 being generally associated with heterochromatin (Hyun et al, 2017). To add further complexity, lysine methylation can exist in 3 states: mono, di or tri. Each state differs in size, the distribution of the positive charge, and hydrophobicity, allowing methyl-lysine readers to differentiate between the methyl states (Bannister and Kouzarides, 2011). Methyl-lysine reader proteins are able to recognize the methylation marks via their recognition motif which is typically made up of 2-4 aromatic residues that create an aromatic cage, in which pi cation interactions between the aromatic residues of the methyl-lysine reader protein and the methyl group of the lysine side chain take place (Ng et al, 2008). Following recognition, the methyl-lysine reader protein will either recruit effector proteins to the site of action or utilise its catalytic domain to convey the appropriate epigenetic signal downstream, resulting in either heterochromatin or euchromatin (Milosevich and Hof, 2016).

1.3 Epigenetic Regulators and Disease

Dysregulation of histone modifications due to abnormal expression and activity of the histone modifying proteins has been associated with a variety of diseases including cancer; therefore, targeting these epigenetic proteins could prove to be a valid strategy for novel cancer therapies. For example, BRD4 an acetyl lysine reader protein part of the bromodomain and extra terminal protein family has been identified as a therapeutic target for breast, lung, colon and prostate cancer (Lu et al, 2020). Through its two bromodomains (BD1 and BD2), BRD4 recognizes H3K5,8 and 12 acetylation and recruits transcription cofactors such as the positive transcription elongation factor B (PTEF-B). PTEF-B initiates transcription by phosphorylating and activating the serine 2 of the carboxyl terminal domain of RNA polymerase II (Andrikopoulou et al, 2020., Chiang, 2009., Devaiah et al, 2016). BRD4 is known to upregulate the expression of several oncogenes such as *TWIST* which induces the transdifferentiating process by which epithelial cells gain the mesenchymal phenotype, *c-MYC* which is involved in regulating cell proliferation and *SNAIL* which plays a role in cancer metastasis (Lu et al, 2019). Currently BRD4 inhibitors, such as JQ1, that compete for the acetylated residues with the BRD proteins are under trial and are showing encouraging

results; such as inhibiting proliferation and inducing cell cycle arrest and apoptosis in a variety of solid tumours, including some incurable subtypes (Donati et al, 2018., Shorstova et al, 2021). Such studies demonstrate the potential of histone modifying proteins as therapeutic targets.

1.4 CBX HP1 Proteins

The chromobox (CBX) family of proteins are a group of epigenetic reader proteins that are mainly associated with repressing the transcription of genes, thereby regulating intricate biological processes such as the maintenance of pluripotency in embryonic stem cells and cell fate decisions. Their aberrant expression and activity have been correlated to the tumorigenesis and progression of various human cancers including breast, liver and gastrointestinal malignancies (Li et al,2020). The CBX family of proteins is made up of eight proteins that can be further divided into two subgroups based on their molecular structure and epigenetic function, the heterochromatin proteins (HP1) that consist of three homologs (CBX1, CBX3 and CBX5) and the polycomb group (PcG) which is made up of five homologs (CBX2, CBX4, CBX6, CBX7 and CBX8) (Zhang et al, 2021).

All three HP1 proteins are roughly comprised of 190 amino acids resulting in a size of around 22kD. Additionally, they are all composed of a N-terminal chromodomain (CD), a C-terminal chromo shadow domain (CSD) and a hinge/linker region which resides in-between the two domains (Figure 1.2) (Vad-Nielsen and Lade-Nielsen, 2015). All three HP1 proteins have an affinity for the H3K9me2/3 epigenetic mark and have high sequence homology. For example, the CD and CSD of CBX5 and CBX3 share 71% - 87% sequence identity. However, the three HP1 proteins can be found distributed in different chromatin states (Canzio et al, 2014). For example, CBX5 is primarily found in heterochromatic regions, CBX1 is associated with both hetero and euchromatic regions and CBX3 is localized in euchromatic regions (Vad-Nielsen and Lade-Nielsen, 2015). Mediating the binding to the di or tri methylated H3K9 mark is the CD, which is a hydrophobic cage-like structure which docks onto the methyl mark with high specificity yet low affinity. This affinity is believed to be increased through the phosphorylation of a serine residue within the N-terminal (Canzio et al, 2014). Although the CSD and CD are similar in structure, CSD is a non-polar groove and its main function is to assemble homo and heterodimers, thereby generating a Y-shaped interaction platform for HP1 binding partners that usually contain the consensus sequence known as

the pentapeptide motif (PxVxL) which is recognised by the conserved residues within the CSD (Lomberk et al, 2006). Out of the three structural elements it's the linker region that is the most diverse between the HP1 paralogs, it contains a nuclear localization sequence and is prone to post-translational modifications which affects the function and localization of the HP1 proteins, therefore, it could potentially be the central control region of HP1 proteins (Canzio et al, 2014). Moreover, the linker region is able to interact with RNA complexes such as RISC (RNA induced silencing complex) which then guide the HP1 proteins to the appropriate chromatin locations (Vad-Nielsen and Lade-Nielsen, 2015). To date the best studied mechanism by which the HP1 proteins repress gene transcription is via their interplay with the histone methyltransferase known as SUV39H1. Upon binding to the H3K9me2/me3 through the CD of the HP1 protein the SUV39H1 is recruited to the chromatin site where it will methylate adjacent H3K9 residues which will then serve as new binding sites for supplementary HP1 proteins which will recruit even more SUV39H1. Furthermore, the CSD can also recruit other DNA methyl transferases that will form complexes with the SUV39H1 and the HP1 proteins which will further propagate the spread of heterochromatin into neighbouring euchromatin, a phenomenon known as position effect variegation (PEV) (Vad-Nielsen and Lade-Nielsen, 2015). In cancer, abnormal expressions of HP1 proteins has been associated with poorer patient prognosis, yet the mechanisms by which HP1 proteins are potentially involved in the process of tumorigenesis remain unclear.

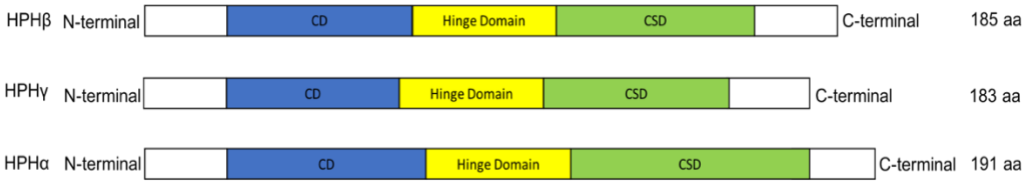

Figure 1.2 Size (aa = amino acid) and linear structure of the three heterochromatin proteins (HPHβ = CBX1, HPHγ = CBX3, HPHα = CBX5). The blue box represents the chromodomain and the green box represents the chromoshadow domain of the heterochromatin proteins.

1.5 The Polycomb Group

The polycomb group (PcG) of CBX proteins are a more diverse group of proteins in terms of their size, with the smallest member, CBX7, being made up of around 252 amino acids and the largest member, CBX4, being made up of approximately 560 amino acids (Ma et al, 2014). Unlike, the HP1 protein group the PcG group lack the C-terminal CSD and instead contain a polycomb repressor box (Pc Box). The PcG group also have a CD at the N-terminal and a central region which is enclosed between the PcBox and the CD (Figure 1.3) (Kawaguchi et al, 2017). These central regions, especially those of CBX2, CBX4, CBX6 and CBX8, are said to be simple in terms of their complexity, disordered and positively charged. The central region of CBX7 is also disordered however its positive charge is much smaller compared to the rest of PcG members due to its smaller size (Kim and Kingston, 2020). The Pc Box recruits and interacts with the subunits of the polycomb repressor complex 1 (PRC1), a multiprotein epigenetic regulatory complex that represses transcription via the monoubiquitylation of H2AK119 (Dobrinic et al, 2021).

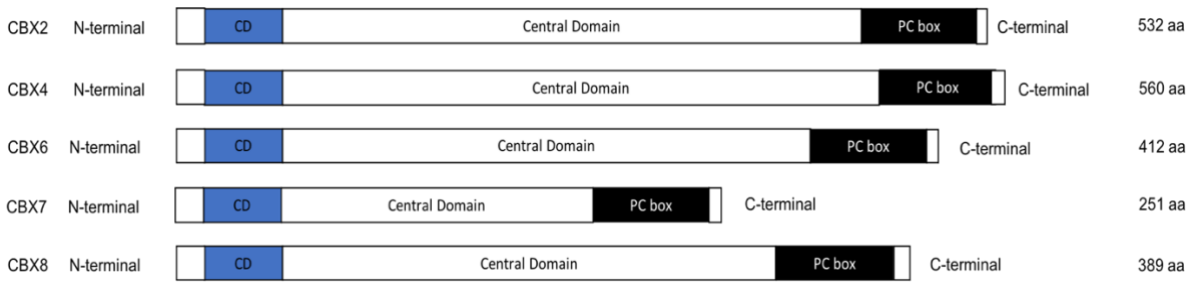

Figure 1.3 Size and linear structure of the five polycomb group CBX proteins. The blue box represents the chromodomain of the CBX proteins which recognize and bind to the H3K27me3 histone modification. The black box represents polycomb repressor box which recruits the subunits of the PRC1 complex to the H3K27me3 site.

Being one of the four protein subunits that make up the canonical PRC1 the CBX proteins (along with the PCGF, HPH and RING proteins) all have their distinct roles in repressing transcription (Figure 1.4). The CBX proteins via their CDs interact with the chromatin by locating and binding to the H3K27me3 epigenetic mark deposited beforehand by the EZH2 subunit of the PRC2 complex. Through the Pc Box the CBX proteins interact and recruit the other PRC1 complex subunits such as the HPH proteins which through their sterile alpha motif oligomerization domain facilitate the polymerization of the PRC1 complex. The RING component (a E3 ubiquitin ligase) of the PRC1 complex binds to one of the PCGF proteins to

enhance its own enzymatic activity and increase the efficiency of the ubiquitin transfer to the H2AK119 (Figure 1.5) (Geng and Gao, 2020). Moreover, the H2AK119U histone modification recruits additional PRC2 complexes thereby establishing a feedback loop between PRC1 and PRC2 that reinforces and maintains the transcriptional repression state (Brown et al, 2021).

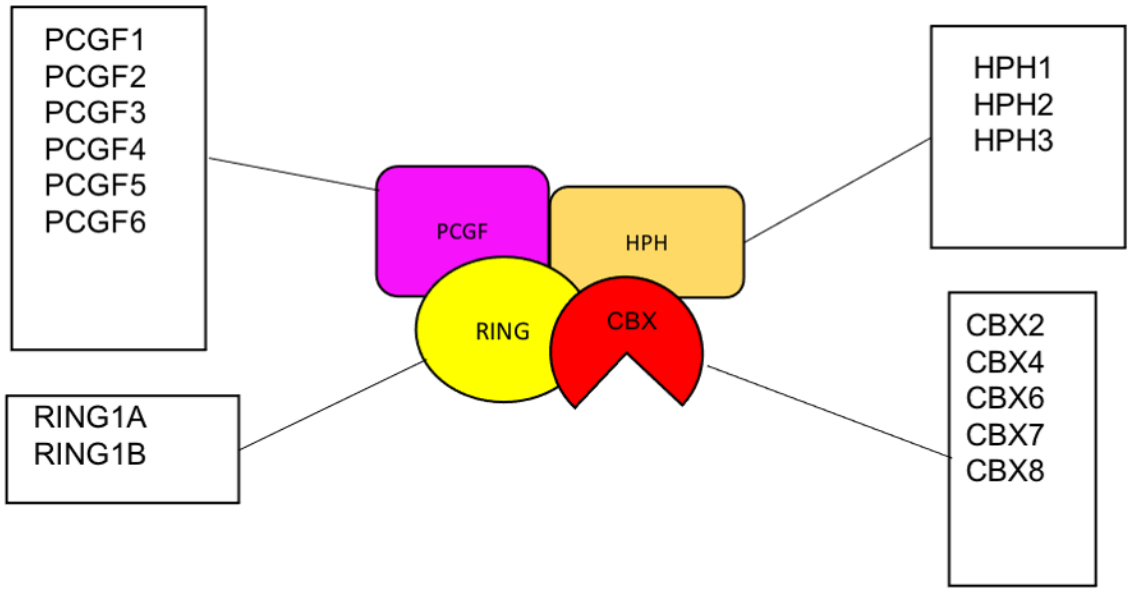

Figure 1.4 The four protein subunits and their orthologues that form the PRC1 complex.

Each subunit of the PRC1 complex has numerous orthologs: the five PcG CBX proteins, three HPH proteins (HPH1, HPH2, HPH3), two RING proteins (RING1A, RING1B) and six PCGF proteins (PCGF1, PCGF2, PCGF3, PCGF4, PCGF5, PCGF6) implying that there is a wide variety of differentially composed PRC1 complexes that may potentially have different effects on genes that they regulate (Gil and O'Loghlen, 2014). Out of all these subunits it's the CBX proteins, which bridge the epigenetic activity of the PRC2 and PRC1 complexes through chromatin interactions with the H3K27me3 mark, that are one of the most frequently up or downregulated PRC1 components in cancer; indicating a dualistic role in cancer progression and justifying research into their potential as therapeutic targets for the future (Wang et al, 2021).

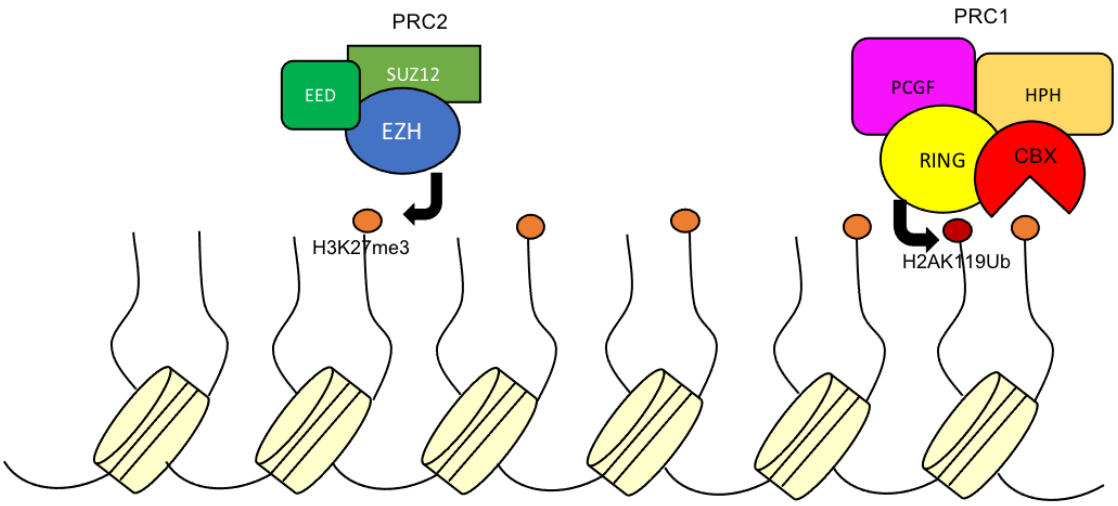

Figure 1.5 PRC2-PRC1 complex crosstalk. The CBX protein of the PRC1 complex recognize the H3K27me3 mark (orange circle), deposited by the PRC2 complex. The PRC1 complex then monoubiquitinates H2AK119 (red circle) via the RING protein to condense the chromatin.

1.6 CBX Proteins and Cancer

CBX7 has been found to be highly expressed in prostate cancer where it downregulates the *INK4B/ARF/INK4A* tumour suppressor gene (Li et al, 2021). The *INK4B/ARF/INK4A* gene codes for $p15^{INK4B}$ and $p16^{INK4A}$ which are cyclin dependent kinase (CDK) inhibitors that regulate the cell cycle and cellular senescence by binding to CDK4 and CDK6 and thus preventing retinoblastoma (pRB) from being phosphorylated resulting in G1 arrest (Popov and Gil, 2010). By repressing this gene, the CBX7 and PRC1 complex allow prostate cancer cells to bypass senescence and carry-on proliferating, suggesting that CBX7 acts as an oncogene in prostate cancer (Bernard et al, 2005). However, in pancreatic cancer CBX7 has tumour suppressive roles, and loss of CBX7 expression is correlated with poorer patient prognosis (Ni et al,2017). CBX7 counteracts the repression effect of histone deacetylase 2 (HDAC2) on the E-cadherin gene *CDH1*, which is responsible for maintaining the healthy epithelial cell phenotype. Due to a loss of expression of CBX7 in pancreatic cancer the epithelial cells are able to gain the invasive mesenchymal phenotype and set off the invasion and metastasis cascade (Pallante et al, 2015).

CBX8 is found to be overexpressed in cancers of the lung and liver where it is most commonly believed to facilitate tumorigenesis (Jia et al, 2020). In liver cancer CBX8 acts as a transcriptional activator of the early growth response protein (ERG1) which will over activate the beta catenin signalling pathway resulting in cytosolic accumulation of beta

catenin followed by nuclear localization, where it will activate oncogenes such as *LEF1* that will in turn promote cancer initiation (Zhang et al, 2018). In lung cancer CBX8 plays a role in augmenting metastasis by downregulating the protein kinase WNK2. This results in increased expression of MMP2 a matrix metalloproteinase that degrades the type IV collagen of the basement membrane of the extracellular matrix, as well as increase the expression of RAC1 which reorganizes the cytoskeleton via F actin polymerization in a way that promotes migration of the cancer cells (Jia et al, 2020).

CBX6 drives proliferation of hepatocellular carcinoma by activating the calcium binding protein S100A9 which activates numerous downstream signalling cascades such as the mitogen activated protein kinase (MAPK) pathway and the nuclear factor- kB (NFkB) pathway to drive the growth of the tumour (Zheng et al, 2017). CBX4 also plays a role in the progression of hepatocellular carcinoma by regulating the angiogenesis process by which the tumours are able to form new vasculature from pre-existing blood vessels in order to increase their blood flow, thereby increasing their uptake of nutrients needed for their excessive growth (Eelen et al, 2020). CBX4 is unique from the other CBX proteins as along with its CD at the N-terminal it also contains two SUMO interacting domains (SIM1 and SIM2) which SUMOylate HIF1 alpha at K391 and K477 increasing its transcriptional activity and resulting in the increased expression of the VEGF protein which promotes angiogenesis (Li et al, 2014).

1.7 CBX2 structural motifs and chromatin interactions

As well as the CD and the Pc Box CBX2 has several other motifs that contribute to its epigenetic activity (Figure 1.6). For example, the DNA binding motif known as the AT hook that resides beside the N-terminal CD is exclusive to CBX2. The other CBX proteins contain shorter variations called AT-hook like motifs (Ma et al, 2014). The AT hook contributes to CBX2 chromatin interactions by interacting with underlying DNA elements of chromatin and also stabilizing the CBX2 on the chromatin, suggesting that both the AT hook and the CD which identifies the H3K27me3 mark function cooperatively when binding CBX2 to chromatin (Kawaguchi et al, 2017). However, the AT hook has also been shown to bind CBX2 to unmodified chromatin promoting promiscuous chromatin binding (Kent et al, 2020).

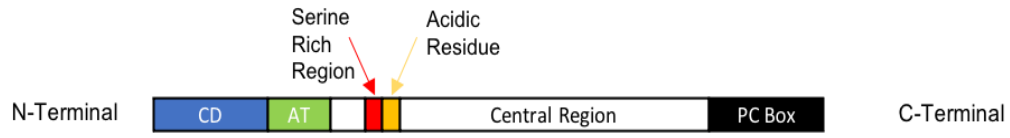

Figure 1.6 Linear structure of CBX2. Highlighting the different structural motifs that have been shown to play a role in CBX2 chromatin interactions or other CBX2 related function (CD – chromodomain, AT – AT hook, PC Box – Polycomb repressor box).

Within the central region of CBX2 there are numerous clusters that along with the CD are also believed to be important for CBX2 chromatin interactions. These clusters are either made up of consecutive positive or negative charged residues, such as the serine rich (SR) region made up of around fourteen consecutive serine residues, as well as an acidic residue (AR) cluster downstream of the SR region (Kawaguchi et al, 2017 and Plys et al, 2019). The AR cluster helps fix the CBX2 into position on the nucleosome, whereas the SR region has been found to be similar to the consensus target sequence of CK2 and therefore has been shown to be stably phosphorylated by this kinase. Phosphorylation of the SR region results in the serine residues mimicking the adjacent acidic residues which promotes the upstream serine residues to be phosphorylated as well. The phosphorylation of the SR region increases the nucleosome binding specificity of CBX2 but at the same time represses the AT-hooks nucleic acid binding activity (Kawaguchi et al, 2017).

Moreover, the SR and AR regions create electrostatic interactions that are one of the drivers of phase separation (Tatavosian et al, 2019). Phase separation involves the assembly of the CBX2-PRC1 into membrane-less compartments called condensates through the process of liquid-liquid phase separation, which is driven by CBX2 (Kent et al, 2020). These condensates accelerate the search for new specific binding sites (target genes marked with H3K27me3), as after leaving a transient site the PRC1 complex travels through the nucleus sampling through the genome for appropriate binding sites which typically takes approximately 70 seconds. The CBX2-PRC1 condensates are able to accelerate this target search by reducing the number of non-specific sites that are being sampled through, as usually the PRC1 complex samples around five non-specific binding sites before reaching the appropriate one (Brown et al, 2021). Upon identifying the appropriate binding site, the condensates localize at these sites and repress transcription. Furthermore, studies in mice embryonic stem cells have shown that through the interplay of different PRC1 complexes distal chromatin regions

are also brought into these condensates for repression. For example, CBX7-PRC1 complex has been shown to recruit distal chromatin regions marked with H3K27me3 into the CBX2-PRC1 condensates which will then be repressed in the condensate via RING protein mediated ubiquitylation (Tatasovian et al, 2019). Mutations and deletions of the SR region of CBX2 result in CBX2 not being able to phase separate implying this region is crucial for phase separation (Brown et al, 2021).

1.8 CBX2 and Cancer

CBX2 is consistently upregulated and associated with poor patient prognosis in a range of malignancies including glioblastoma, breast, prostate, liver and lung cancer (Clermont et al., 2015). In liver cancer, CBX2 regulates proliferation by promoting the expression of Wt-1 interacting protein (WTIP), which in turn inhibits the phosphorylation and inactivation of the oncogenic Yes-associated protein (YAP) which drives the proliferation of liver cancer cells and also induces metastasis (Mao et al, 2019). In prostate cancer CBX2 overexpression is associated with the proliferation of aggressive and metastatic cancers, with siRNA mediated CBX2 silencing inducing cell death in these prostate cancer cell lines (Clermont et al 2015). Gene expression profiling revealed CBX2 silencing negatively correlated to *PIK3R1* and *INPP5A* which are antagonists of the PI3K signalling pathway, suggesting that CBX2 regulates the PI3K/AKT signalling pathway in prostate cancer (Clermont et al, 2016). Such results are consistent with the findings of Wang et al who found that high CBX2 expression induces cell proliferation and invasion through the PI3K/AKT signalling pathway in glioma cells (Wang et al, 2021).

In breast cancer, overexpression of CBX2 has been shown to metabolically reprogram the breast cancer cells via the mTORC1 signalling pathway (Iqbal et al, 2020). Breast cancer cells expressing high levels of CBX2 have been associated with deregulated glycolysis and increased concentrations of glycolytic metabolites. By altering the metabolic pathways, the breast cancer cells are able to support their rapid proliferation (Iqbal et al, 2020). CBX2 has been shown to regulate the mTORC1 signalling pathway by also repressing the transcription of two mTORC1 inhibitors, *PRKAA2* and *TSC1*, with siRNA mediated CBX2 knockdown significantly upregulating the two genes. Additionally, CUT&RUN-qPCR revealed the promoter regions of the two genes to be enriched in CBX2, indicating that it may specifically be CBX2 that directly represses the transcription of the two genes via the PRC1 complex

(Bilton et al, 2022). Gene set enrichment analysis revealed high CBX2 expression to be positively correlated to genes associated with the PI3K/AKT oncogenic signalling pathway (Zheng et al, 2019). More specifically genes such as *PIK3CA* and *PIK3CD* which within the PI3K/AKT signalling pathway phosphorylate substrates associated with cell proliferation and invasion (Zheng et al, 2019., Fruman et al, 2017). CBX2 has been also shown to repress the transcription of the tumour suppressor gene *RBL2*, which encodes a pocket family protein that is able to form the DREAM complex with co-repressors such as MuvB, E2F4 and dimerization partner (DP) which repress E2F dependent genes resulting in cell cycle arrest (Bilton et al, 2022., Sasasivam et al, 2013). Western blot analysis showed an increase in RBL2 protein expression in CBX2 knockdown cells along with RNA-seq analysis showing a downregulation of DREAM target genes in CBX2 depleted cells. Additionally, ChIP-qPCR results in CBX2 knockdown cells revealed increased RBL2 enrichment at the promoters of its target genes. These results suggested that CBX2 may mediate RBL2 epigenetic silencing via the PRC1 complex and may prevent the formation of the DREAM complex, resulting in the upregulation of E2F target genes and allowing cancer cells to bypass cell cycle regulation (Bilton et al, 2022). High CBX2 expression may also be an indicator of resistance to the microtubule stabilizing chemotherapy drug paclitaxel, as a study investigating the overall survival time in patients expressing high CBX2 revealed that the overall survival time was significantly lower in the patient group that received the paclitaxel treatment when compared to the patient group that didn't receive the treatment (Chen et al, 2017).

Similarly to other cancers, CBX2 overexpression is mainly associated with the more aggressive breast cancer subtype such as the triple negative (TNBC) subtype, with siRNA mediated CBX2 knockdown reducing the cell growth in three different TNBC cell lines (Pique et al, 2019., Bilton et al, 2022.) Breast cancer is immunohistochemically classified into subtypes based on the expression of distinct molecular receptors such as the oestrogen and progesterone receptors (ER and PR) expressed in both luminal A and B subtypes, human epidermal growth factor receptor 2 (HER2) present in luminal B and HER2 subtypes whereas TNBC lacks the expression of all three molecular receptors (Dass et al, 2021). The absence of these molecular receptors results in the currently available endocrine therapies, commonly used against the other breast cancer subtypes, such as tamoxifen and aromatase inhibitors to be ineffective against TNBC. Moreover, TNBC displays high heterogeneity in relation to

chemotherapy sensitivity which alongside the endocrine therapy resistance prompted research to explore alternative therapy strategies (Aysola et al, 2013).

However, currently trialled therapies targeting molecular signatures associated with TNBC such as EGFR, VEGF, and PARP-1 were anticipated to be more clinically successful than they turned out to be. Limited treatment options for TNBC allows it to progress, become characteristically aggressive and eventually metastasize to the brain or the lungs (Dass et al, 2021). With TNBC being responsible for approximately 150,000 deaths in 2020 and 30% of breast cancer related deaths each year it is crucial for alternative therapeutic targets to be explored (Arnold et al, 2022., Saraiva et al, 2017). Variations in the chemical modifications of the histone tails driven by aberrant expression and activity of epigenetic regulatory protein have been recognised as potential prognostic markers as well as possible therapeutic targets for TNBC (Elsheikh et al, 2009). Reductions in modifications such as H4K16Ac and H4K20me3 at the promoters of various tumour suppressor genes increase the invasiveness of the breast cancer and are considered to be hallmarks of cancer (Li et al, 2021). While increased activity of epigenetic proteins such as SMYD3, a histone methyltransferase, results in increased H3K4me3 levels at the promoters of oncogenes such as *WNT10B* which initiates and drives the epithelial-mesenchymal transition in TNBC (Yang et al, 2021). Since CBX2 has been shown to contribute to chemotherapy resistance, regulate a variety of oncogenic pathways, and its overexpression is correlated to the aggressive and difficult to treat breast cancer subtypes, it could prove to be a viable therapeutic target for TNBC in the future.

1.9 Therapeutic strategies for targeting CBX2

One of the main strategies that is being explored for targeting CBX proteins is selective inhibition of their CD, as this is the structural element of CBX proteins that interacts with the chromatin by recognizing and binding to the H3K27me3 mark. Therefore, if the CD is inhibited the CBX proteins should not be able to locate and bind to the H3K27me3 mark and consequently be unable to interact with the chromatin. However, specifically targeting the CD of each individual CBX protein has proven to be challenging, with the aromatic cage of the CD that physically binds to the trimethylated lysine residue being almost identical between the CBX proteins (Milosevich et al, 2019). The only subtle differences observed are within the sidechain of the extended beta groove, therefore efforts into making CBX

selective inhibitors have focused on targeting these distinct areas within the CDs (Simhadri et al, 2016). Progress in designing, producing and testing the selective CD CBX protein inhibitors has been made for all five PcG CBX proteins. For example, a small molecule protein inhibitor with a weak affinity for the CBX7 CD has been developed, as well as peptidomimetic ligands with higher affinities and selectivity for the CDs of CBX4, CBX6 and CBX8 (Wang et al, 2021). More recently a CBX2 CD selective inhibitor, SW2-152F, has been developed which displays both high specificity and selectivity for CBX2 in cells and has been shown to significantly inhibit neuroendocrine prostate cancer cell proliferation, thus demonstrating the potential of these selective CD CBX protein inhibitors as viable therapeutic strategies in the future (Wang et al, 2021). Alternatively, instead of using peptidomimetic ligands to target the CD-H3K27me3 chromatin interaction, small molecule compounds that permeabilize through the cells more efficiently could be used. Two such small molecule inhibitors that bind to the H3K27me3 mark thereby blocking the CD mediated CBX2-H3K27me3 binding have already been identified (Lercher et al, 2022). If targeting the CD alone proves to be unsuccessful, alternative therapeutic strategies could include simultaneously targeting multiple CBX2 structural motifs that have been recently shown to also be required for CBX2s chromatin interaction (SR and AR region) and thus completely minimizing the ability for CBX2 to interact with the chromatin.

Another possible strategy could be targeting the proteins recruited to H3K27me3 mark by CBX2 instead, such as the RING proteins of the PRC1 complex that monoubiquitylate and consequently compact the chromatin. For example, a small molecule (RB3) that binds to the RING1B protein and reduces the level of H2A ubiquitylation has been developed (Shukla et al, 2021). However, CBX2 may be able to function independently of the PRC1 complex as its 321 amino acid shorter isoform which lacks the PC box that recruits the PRC1 complex is still able to regulate gene expression (Volkel et al, 2012). Another viable option could be to prevent the trimethylation of H3K27 by repressing the EZH2 subunit of the PRC2 complex thereby completely inhibiting the PRC1-PRC2 feedback loop. An EZH2 subunit inhibitor (EPZ005687) has already been developed and shown to inhibit the trimethylation of H3K27 in non-Hodgkin lymphoma cells (Wang et al, 2015). A more unconventional strategy for targeting CBX2 may be through its destabilization and proteasome-dependent degradation. Studies in leukemic cells have shown that the histone deacetylase known as SAHA induces

CBX2 SUMOylation via SUMO2 and SUMO3 which SUMOylate three key lysine residues: K60, K153 and K410, promoting CBX2's ubiquitylation and subsequently proteasomal dependent degradation resulting in impaired proliferation of the leukemic cells (Di Costanzo et al, 2018). Whether it will be through directly inhibiting CBX2 chromatin interactions by targeting one of its structural motifs, by proteasomal degradation, or by targeting one of the subunits of the PRC1 or PRC2 complexes more research will be required to investigate the impact of CBX2 depletion on both cancer and healthy cells.

Chapter 2: Thesis Aims

2.1 Hypothesis

CBX2 chromatin interactions are required for PRC1 mediated gene regulation and cell growth in TNBC.

2.2 Aims

Determine which specific domains of CBX2 are involved in coordinating its interactions with chromatin and are required for TNBC cell growth, PRC1 catalytic activity, and regulation of CBX2 target genes. This will be done by:

- Investigating the effect of overexpressing CBX2 variants, that contain or lack crucial domains, on the TNBC phenotype (cell counts), CBX2 target gene and protein expression (qPCR and western blot analysis) and the PRC1 mediated H2AK119U histone modification (western blot analysis and immunofluorescence).

- Determining whether the CBX2 plasmid variants can rescue the TNBC phenotype (cell counts, flow cytometry), CBX2 target gene expression (qPCR), and the PRC1 mediated H2AK119U histone modification (western blot analysis and immunofluorescence) when co-transfected with a CBX2 targeting siRNA.

2.3 Ethical Consideration

The project used cultured human triple negative breast cancer cells, MDA-MB-231 and MDA-MB-468, from the American Type Culture Collection (ATCC). Control of Substances Hazardous to Health (COSHH) forms were read and completed prior to any experiments.

Chapter 3. Materials and Methods

3.1.1 Making Agar plates and Luria Broth

Luria broth was made up in a schott bottle out of 500 ml of deionized water and 10 g of Luria broth (Thermofisher, UK). The solution was mixed using a magnetic stirrer until the Luria broth dissolved, once dissolved the bottle containing the Luria broth was autoclaved for sterility. After autoclaving the Luria broth was stored at room temperature for around a week after which another flask was made up if required.

Agar plates were made for the plasmid transformed competent *E. coli* cells to grow on and generate copies of the recombinant CBX2 variant plasmids. To make up the agar plates 10 g of Luria broth and 7.5 g of bacteriological agar (Sigma, UK) was measured and added to a schott bottle which was then filled with 450 ml of deionized water. The mixture was mixed with a magnetic stirrer until the Luria broth and the bacteriological agar dissolved. Once dissolved the mixture was topped up to 500 ml with deionized water, and then the bottle was autoclaved for sterility. Once autoclaved the schott bottle was placed in a bowl of cold water to cool and the bowl was placed on a magnetic stirrer to keep the agar mixing so that it didn't set in the schott bottle. Once cooled 50 mg/ml kanamycin was added to the agar in a 1:1000 dilution and the bottle was vigorously shook to mix the kanamycin in the agar. The agar was poured out into petri dishes just enough to cover the surface area of the petri dish. The petri dishes were left for 15 minutes at room temperature to set and then stored upside down at 4 ^{o}C.

3.1.2 Plasmid transformation and propagation

Day 1 (transformation)

Exactly 900 µl of Luria broth, per plasmid sample, was added to a universal tube and placed in a 42 ^{o}C water bath to warm up. Competent DH5α cells (Thermofisher, UK) were taken out the -80 ^{o}C freezer right before the procedure to minimize the loss of their competency. Once defrosted 75 µl of the competent *E. coli* cells were pipetted into an Eppendorf tube. Then, depending on the stock concentration of the CBX2 variant plasmids, either 0.5 µl or 1 µl of plasmid was added to the competent *E. coli* cells. If the plasmid stock concentration was 50 ng/µl or less 1 µl was added, if above 50 ng/µl 0.5 µl was added. The mixture was left on ice for 30 minutes. In the meantime, the petri dishes were taken out of the fridge

and placed upside down in a 37 ^{o}C incubator to warm up. Following the 30-minute ice incubation the plasmid and *E. coli* cell mixture was placed in the 42 ^{o}C water bath for 20 seconds resulting in a heat shock which induced the uptake of the exogenous CBX2 plasmid variant. Such sudden temperature change caused changes in the *E. coli* cells membrane fluidity causing the fusion between the cell membrane and cell wall pores which allowed the plasmid DNA to pass through. After the 20 second heat shock the transformed competent *E. coli* cells were placed on ice for 2 minutes. Then 900 µl of the preheated Luria broth was added to the samples and placed in a shaking incubator (Infors, US) at 225 rpm at 37 ^{o}C for 1 hour. Following the hour incubation, 200 µl of the sample was pipetted onto the petri dish. A glass spreader that was flamed before and after use was used to evenly distribute the sample around the petri dish. The petri dishes were then incubated upside down overnight at 37 ^{o}C (Zhang and Cahalan, 2007).

Day 2

The next day 5 ml of Luria broth was added to a universal tube along with 50 mg/ml kanamycin in a 1:1000 dilution. The petri dishes were taken out of the incubator and inspected for satellite colonies to ensure the bacteria hadn't overgrown. Next, using a flamed metal loop a single colony was picked up and dislodged into the universal tube which was then given a vigorous shake. The universal tube was then incubated overnight at 37 ^{o}C in a shaking incubator at 250 rpm until mid-morning of the next day. In preparation for the next day a 1000 ml flask with a cap made out of aluminium foil containing 200 ml of Luria broth was autoclaved and then stored at room temperature for the next day.

Day 3

The universal tubes were taken out of the shaking incubator and stored at room temperature until the afternoon. In the afternoon the tubes were placed back into the shaking incubator at 37 ^{o}C at 250 rpm for 15 minutes. Then, to the autoclaved 1000 ml flasks containing 200 ml Luria broth, 50 mg/ml kanamycin was added in a 1:1000 dilution. Following the 15 minutes 300 µl of the culture was added to the 1000 ml flasks containing 200 ml Luria broth. The flasks were then incubated at 37 ^{o}C in the shaking incubator at 250 rpm for 16 hours.

Glycerol Stocks

To make up glycerol stocks of the plasmid transfected bacteria culture, 1 ml of double strength Luria broth glycerol and 500 µl of culture from the universal tube was added into an Eppendorf tube which was then stored at -80 ^{o}C. The glycerol stabilizes the frozen bacteria protecting their membrane integrity.

Day 4

The next day the 200 ml of Luria broth from the 1000 ml flask was separated into four 50 ml polypropylene tubes (Sarstedt, UK) which were then centrifuged at 4000 x g for 10 minutes. Once centrifuged the supernatant was discarded leaving behind the cell pellet ready for the maxi prep procedure.

3.1.3 Maxi Prep

A maxi prep kit (Thermofisher, UK) was used to extract and purify the CBX2 plasmid DNA from the competent *E. coli* cells. Firstly, the column tube apparatus was set up by placing the maxi prep column tubes into the gravity/column tube rack. Once set up 30 ml of the Eq1 buffer was added to each column tube to equilibrate the column tube. While the Eq1 buffer was running through the column tube, 550 µl of 20 mg/ml of RNase A was added to the stock bottle of the R3 buffer which will remove any unwanted RNA from the sample. Then 10 ml of the R3 buffer was added to one of the falcon tubes containing the *E. coli* cell pellet. The solution was pipetted up and down to resuspend the pellet and then transferred across to the next falcon tube containing an *E. coli* cell pellet. The pellet was resuspended again and the process was repeated for the remaining two falcon tubes containing the *E. coli* cell pellets. To the last falcon tube that contained all four cell pellets resuspended in 10 ml of the R3 buffer, 10 ml of the lysis L7 buffer was added to lyse the cells. The falcon tube was then inverted five times and 10 ml of the N3 precipitation buffer was added and the tube was inverted five times again. The solution was then transferred to a glass centrifuge tube (autoclaved beforehand) and placed in the ultra-centrifuge for ten minutes at 10000 RPM at room temperature. Once centrifuged the supernatant was poured into the column tube and the pellet was discarded. After the supernatant had passed through the column tube 60 ml of the W8 wash buffer was added to the column tube in order to remove any impurities such as RNA and protein from the resin bound plasmid DNA. Next, 50 ml falcon tubes were placed under each column tube and 15 ml of the high salt concentrated E4 elution buffer

was added to each column tube to extract the plasmid DNA. Once all of the solution had passed through the column tube into the falcon tube 10.5 ml of isopropanol was added, mixed and then transferred into a new and clean glass centrifuge tube. The solutions were placed in the ultra-centrifuge for 30 minutes at 4 ^{o}C at 10000 RPM. Following centrifugation, the supernatant was poured out and 5 ml of 70% ethanol was added to the left behind pellet. The samples were then centrifuged again at 10000 RPM for 5 minutes at 4 ^{o}C. The isopropanol and ethanol desalt and precipitate the plasmid DNA from the solution. Next, the 5 ml of ethanol was carefully pipetted out without disturbing the pellet and the samples were left to air dry for 15 minutes. Following the 15 minutes the pellet was resuspended in 250 µl of TE buffer and stored at 4 ^{o}C for 72 hours. The plasmids DNA concentration (ng/µl), and the DNA protein contamination (260:280 and 260:230) was analysed by a Nanodrop 2000 (Thermo scientific, UK) machine.

3.2.1 Cell Culture

The MDA-MB-231 breast cancer cells were grown in the RPMI media 1640 (Gibco, UK) whereas the MDA-MB-468 breast cancer cells were grown in the DMEM media (Gibco, UK). Both media were supplemented with 10% (V/V) Fetal Bovine Serum (FBS) (Gibco, UK), which is required for the cell's attachment, maintenance and proliferation. 1% 10,000 µ/mL penicillin and 10,000 µg/mL streptomycin (Lonza, UK) was also added to prevent bacterial contamination that would result in the loss of cells. The cells were either grown in 12 ml of media in a T75 flasks (Sarstedt, Germany) or in 30 ml of media in a T175 flasks, in both instances the media was changed every three days and the cells were incubated in a humidified incubator at 37 ^{o}C with 5% CO_2 (Nuaire, UK).

3.2.2 Trypsinisation

The cells were trypsinised when the cell monolayer covered approximately 80% of the flask when viewed under a light microscope (Olympus CKX53, UK). This ensured the cells would maintain their exponential growth phase. Trypsinisation was done with 1x phosphate buffered saline (PBS) made up of 1 PBS tablet (Fisher, UK) and 200 ml ddH2O in an autoclaved flask, and 10x trypsin (Sigma, UK) which was diluted 1:10 with PBS for the MDA-MB-468 cells and 1:30 for the MDA-MB-231 cells. Prior to trypsinisation the media, the trypsin and the PBS were warmed in a bead bath at 37 ^{o}C, as using them cold may stimulate stress pathways in cells which may affect the outcome of experiments. Cells were split in a

class II biological safety cabinet. First, the media was removed from the flask, then the cells were washed with 5 ml of PBS if they were in the T75 flask or 10 ml of PBS if the cells were in the larger T175 flask. Following this either 3 ml of diluted trypsin was added to the T75 flask or 5 ml of diluted trypsin was added to the T175 flask. The flasks containing the trypsin were then placed into the humidified incubator for 3-5 minutes, allowing the cells to detach from the surface of the flask. The detached cells in the trypsin were then transferred from the flask into a 50 ml falcon tube and made up to 15 ml with either 10 ml or 12 ml of appropriate media. The cells were then centrifuged at 3000 x *g* (Eppendorf, UK) for 3 minutes resulting in a cell pellet at the bottom of the falcon tube. The media supernatant was removed and the cells were resuspended in 5 ml of fresh media, a fraction of which would then be added to a new T75/T175 flask with appropriate fresh media. For routine cell culture a 1:5 dilution was most commonly used.

3.2.3 Cell Counting (for seeding cells in transfection plate)

During trypsinisation after the cells had been resuspended in 5 ml of fresh media, 20 µl of the cell solution was pipetted into the space between the glass coverslip and the haemocytometer (Neubauer) and counted under a light microscope. To avoid counting the cells twice, cells found on the exterior border at the top and on the right of the 1 mm^2 square were not counted (Figure 3.1). The average was calculated following the cells being counted in 3 different 1 mm^2 squares which was then multiplied by 10^4 to find the approximate total number of cells.

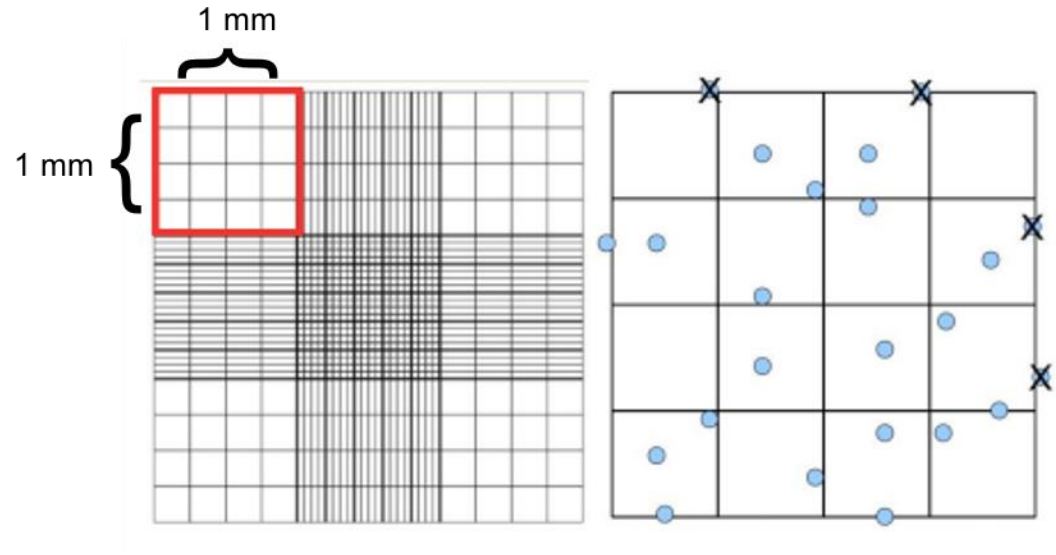

Figure 3. 1 Haemocytometer grid for counting cells. Made up of 9 1 mm^2 squares with 3 squares usually being used to count the cells and work out the average number of cells. When cells were found to be on the exterior border only those on the bottom and the left side were counted.

3.2.4 CBX2 plasmid transfection:

A day before the plasmid transfection the cells were trypsinised (as described in 3.2.2), counted and approximately 150,000 cells in a 2 ml cell suspension were seeded in each well of a six well plate and incubated overnight in a humidified incubator at 37 ^oC with 5% CO_2. The following day the CBX2 variant plasmids that beforehand have been made up to a DNA concentration of 100 ng/µl with the TE buffer (Thermofisher, UK) were introduced into the cells using the p3000 (Invitrogen) and lipofectamine 3000 (Invitrogen) reagents. In the class II biological safety cabinet for transfections in the MDA-MB-231 and the MDA-MB-468 cell lines the plasmid master mix comprising of 125 µl Opti-MEM media (Gibco, UK), 2 µl p3000 reagent and 10 µl of the plasmid was made up in 1.5 ml sterile polypropylene tubes (per well). In a separate set of Eppendorf tubes the lipofectamine 3000 master mix was made up per well with optimen media in a 4:125 ratio which was then added to the plasmid master mix to make up the transfection master mix which was incubated at room temperature for 15 minutes. After the 15-minute incubation 250 µl of the transfection master mix was added to the centre of the appropriate wells of the 6 well plate and then the cells were incubated for 72 hours in the humidified incubator at 37^oC.

3.2.5 CBX2 rescue experiment (plasmid and siRNA co-transfection)

For rescue experiments the plasmids were co-transfected into the cells with small interfering ribonucleic acids (siRNAs) that were used to knockdown CBX2 expression in order to observe whether the variant plasmids could rescue the cells ability to grow. A scrambled siRNA which is non-silencing was used as a control along with two discrete siRNAs that target CBX2; siCBX2-3 and siCBX2-4 (Table 3.1). The MDA-MB-231 cells were trypsinised, counted and 100,000 cells in a 2 ml cell suspension were seeded into the wells of a 6 well plate and incubated overnight in a humidified incubator at 37 ^{o}C. The following day in a class II biological safety cabinet the plasmid and siRNA master mix were made up into Eppendorf tubes consisting of 125 µl Opti-MEM media, 0.5 µl p3000 reagent, 1 µl siRNA (50 µM stock) and 2.5 µl of plasmid per well. In a separate set of Eppendorf tubes the lipofectamine 3000 master mix was made with the Opti-MEM media at a ratio of 1:125 per well. The two master mixes were then combined and incubated at room temperature for 15 minutes. Following the incubation 250 µl of the co-transfection master mix was dispensed into the centre of the appropriate wells of the 6 well plate and then incubated for 72 hours in a humidified incubator at 37 ^{o}C.

For the rescue experiments in the MDA-MB-468 cell line the knockdown using the siRNA was done first. In autoclaved Eppendorf tubes a transfection master mix consisting of basal media, RNAiMAX and the siRNA (50 µM stock) was made in a 100:2:1 ratio and left at room temperature for 15 minutes. During the incubation period the MDA-MB-468 cells were trypsinised and counted. Then the transfection master mix was pipetted into the centre of the wells of the 6 well plate and 150,000 cells in a 2 ml cell suspension were then seeded into each well and incubated overnight in the humidified incubator at 37 ^{o}C. The next day in autoclaved Eppendorf tubes the plasmid transfection master mix was made up consisting of 125 µl Opti-MEM media, 0.5 µl p3000 reagent and 2.5 µl plasmid per well. In a separate set of Eppendorf tubes the lipofectamine transfection mix was made up in a 1:125 ratio with the Opti-MEM media per well, which was then added to the plasmid transfection master mix. The master mix was then incubated at room temperature for 15 minutes. Following the 15 minutes 250 µl of the combined master mix was added to the appropriate wells of the 6 well plate and then incubated for 72 hours in the humidified incubator at 37 ^{o}C.

Table 3. 1. siRNA reagents.

siRNA	Company	Catalogue	Sequence (5'-3')
Scr	Sigma	HA11411080	UUCUCCGAACGUGUCACGU
CBX2-#3	Sigma	HA11411076	GCAAGGGCAAGCUGGAGUA
CBX2-#4	Sigma	HA11411078	CAAGGAAGCUCACUGCCAU

3.2.6 Cell Counts (Post transfection and co-transfection)

Following 72 hours after the plasmid transfection/co-transfection, the cells in the wells were counted to determine whether the combination of transfections affected the cells' growth. Firstly, in a class II biological safety cabinet the 2 ml of media was removed from each well and each well was then washed once with 1 ml of warm PBS. Next, 300 µl of 1:10 diluted trypsin was added to the centre of each well and the plates were then incubated in the humidified incubator at 37 ^{o}C until the cells were observed under the light microscope to have detached from the bottom of the well. Once the cells have detached 700 µl of the appropriate fresh media was added to each well and gently rocked to mix in with the trypsinised cells. Then 1 ml of the media and trypsinised cell mixture was transferred from the wells of the plate to sterile Eppendorf tubes. The Eppendorf tubes were then centrifuged (VWR, US) for 3 minutes at 3000 x *g* resulting in a cell pellet at the bottom of the Eppendorf tube. The media supernatant was removed and the cell pellets were resuspended in 500 µl of fresh media which was pipetted up and down to ensure the cells were properly resuspended. Then 20 µl of the cell mixture was dispensed onto the haemocytometer and the cells were counted. After the cells from all the samples had been counted the cell mixtures in the Eppendorf tubes were centrifuged at 3000 x *g* for 3 minutes. This time when the media supernatant was removed the cell pellets were resuspended in the appropriate buffer (protein lysis buffer or RNA extraction buffer) for downstream analysis.

3.3 Western Blot

3.3.1 Protein Lysis

Following the 72 hours of the transfection and/or co-transfection the media was removed from each well of the six well plate and the cells were washed with 1 ml of warm PBS. The cells were then lysed using RIPA buffer (Table 3.2). Depending on the cell density, 100-200 µl of the RIPA buffer was added to each well and the plate was then placed on ice and rocked for 30 minutes. After the 30 minutes the wells were scraped using a cell scraper which was sterilised with ethanol in-between scraping the different wells. The solution was then transferred to Eppendorf tubes and the samples were centrifuged at 16,000 x *g* for 3 minutes. Following centrifugation, the supernatant containing the protein was transferred to new Eppendorf tubes and the cell pellet left behind was discarded. The protein lysates were then stored at -20 ^{o}C for western blot.

Table 3. 2. Reagents used to make up the RIPA buffer used for protein lysis.

Reagents	**Stock Concentration**	**Volume added to make 100ml of RIPA buffer**
HEPES-KOH pH 7.5	0.5 M	10 ml
LiCl	2 M	25 ml
EDTA	0.5 M	200 µl
NP40	-	1 ml
Na-deoxycholate	-	0.7 g
H2O	-	63.8 ml

3.3.2 Bicinchoninic acid (BCA) assay

To quantify the amount of protein in the lysates to ensure equal amounts of protein were being loaded for the western blot analysis a BCA assay was performed using the Pierce BCA Assay kit (Thermofisher, UK). The lysates were compared to a set of serially diluted bovine serum albumin standards made up beforehand. Firstly, the lysates were diluted 1:8 in RIPA buffer with 10 µl of lysate and 70 µl of RIPA buffer being added to a new set of Eppendorf tubes. Next, 25 µl of the BSA standards (Table 3.3) and diluted lysates were loaded into a 96 well plate in triplicates. The working reagent (WR) was then prepared by calculating the

total volume of WR required: number of standards + number of samples * number of replicates * volume of WR added to each well. The WR was made by mixing reagent A and reagent B in a 50:1 ratio. Then 200 µl of the WR was added to each well and the plate was placed on a plate shaker for 30 seconds and then covered in aluminium foil due to the WR being light sensitive which would affect the results of the BCA assay. The covered plate was incubated for 30 minutes in a humidified incubator at 37 ^{o}C at 5% CO_2 concentration. Following the incubation, the plate was read by a BioTek Synergy HTX Multimode plate reader (Agilent Technologies, UK) at a 562 nm wavelength using the Gen5 software (Agilent Technologies, UK). The readings were used to plot a standard curve graph to calculate the unknown protein concentration of the lysates. Since the protein concentration of the lysates was relatively low, the volume needed to have the highest possible amount of protein in ug from the least protein concentrated lysate was calculated. Other lysates were then made to match the amount of protein in the least concentrated lysate by being diluted by the appropriate amount using the RIPA buffer. All lysates then had 10 µl of 5X protein lysis buffer (sodium dodecyl sulphate (SDS) 125mM Tris, 10% v/v glycerol, 2% w/v SDS, pH 6.8) added to them resulting in a total volume of 50 µl.

Table 3. 3. Final concentrations of the BCA standards used for the BCA assay. Made up of appropriate amounts of the BCA stock and the RIPA buffer.

Vial	**Final Concentration of BCA standard (µg/ml)**	**Volume of BCA stock (µl)**	**Volume of RIPA buffer (µl)**
A	2000	300	0
B	1500	375	125
C	1000	325	325
D	750	175 from vial B	175
E	500	325 from vial C	325
F	250	325 from vial E	325
G	125	325 from vial F	325
H	25	100 from vial G	400
I	0	0	400

3.3.3 Gel Electrophoresis:

SDS-polyacrylamide gel electrophoresis (SDS-PAGE) separated the proteins based on their molecular weight via an electric current that moves negatively charged proteins through the pores of the gel at a speed inversely proportional to their size towards the positive end of the gel. Since proteins aren't naturally negatively charged, they were mixed with SDS (as mentioned above) which coats the proteins with a negative charge allowing them to migrate down the gel. Once made up, the protein samples were boiled on a heat block (Stuart Scientific, UK) for 10 minutes at 100 ^{o}C. In the meantime, a glass back and middle electrophoresis plate (Biorad, UK) with a 1.5 mm integrated space were placed into a casting frame and the frame was then placed onto a casting stand. The plates were filled with distilled water to ensure the plates were set up correctly so when the resolving gel was added it wouldn't leak from the bottom of the plates. If the plates weren't leaking then a 10% resolving gel was made up (Table 3.4) and pipetted into the 1.5 mm gap between the glass back and middle electrophoresis plates to approximately 2 cm from the top. A 150 µl layer of isopropanol was then pipetted on top of the resolving gel to remove any air bubbles and level the top of the gel. Once the resolving gel had set the isopropanol layer was removed and the plates were filled to the top with the stacking gel (Table 3.4). Depending on the number of samples being used either a 10 or a 15 well comb (Biorad, UK) was placed into the stacking gel before it set. Once the stacking gel had set the gel was placed into an electrophoresis holder which was then placed into an electrophoresis tank which was filled with 1000 ml of 1x electro buffer made up of 200 ml of 5x electrophoresis buffer (Table 3.5) and 800 ml of ddH2O. The combs were then removed and 5 µl of the Spectra molecular protein ladder (Thermofisher, UK) of estimated molecular weights of proteins was loaded into the first well with the rest of the wells being loaded with 10 µl of the samples. The lid was then placed on top of the electrophoresis tank matching the coloured electrodes to each other and then connecting the lid to a power pack (Biorad, UK) that was then set to run at 110 V for approximately an hour and a half (Kielkopf et al, 2021).

Table 3. 4. Compositions of the resolving and stacking gels.

Reagent	Resolving Gel	Stacking Gel
ddH2O (ml)	7.5	3.1
Tris Buffer pH-8.5 (ml)	3.75	-
Tris Buffer pH-7.4 (ml)	-	1.25
40% Acrylamide (ml)	3.6	0.5
10% SDS (µl)	150	50
10% APS (µl)	69	30
99% TEMED (µl)	23	10

Table 3. 5. Composition of the 5x electrophoresis buffer used to make up 1x electrophoresis buffer for gel electrophoresis.

Reagent	Amount
ddH2O	1000 ml
Glycine	144 g
Tris Base	30 g
SDS	5 g

3.3.4 Gel Transfer:

Once the samples have migrated down to the bottom of the gel the electrophoresis was stopped and the gel was transferred onto a nitrocellulose membrane using a transfer cassette. The transfer cassette was opened up and a piece of sponge soaked in 1x transfer buffer was placed on top of the black side. The 1x transfer buffer was made up of 800 ml of ddH2O, 100 ml of 10x transfer buffer (Table 3.6) and 100 ml of methanol. Next two pieces of Whatman paper (Cytiva, UK) approximately the same size as the gel were soaked in the 1x transfer buffer and placed on top of the soaked sponge. Then the gel was taken out of the electrophoresis tank and using a gel releaser cautiously removed from the glass middle plate. The gel combs were cut off and the sides of the gels were carefully unstuck from the glass back plate using the gel releaser. The gel was then placed onto the soaked piece of

Whatman paper in the transfer cassette and the back plate was gently lifted off of the gel using the gel releaser. Next, the nitrocellulose membrane (GE Healthcare, UK) roughly the same size as the gel was soaked in the 1x transfer buffer and placed on top of the gel. Then, two more pieces of Whatman paper were soaked in the 1x transfer buffer and placed on top of the nitrocellulose membrane. A glass roller was then used to roll any air bubbles out of the gel membrane sandwich that would interfere with the protein bands upon visualization. Lastly, a piece of sponge was soaked in the 1x transfer buffer and placed on top of the two pieces of Whatman paper. The cassette was closed and placed into a transfer chamber ensuring the black side of the cassette is facing the black side of the chamber so that the negatively charged proteins move towards the positive charge and thus onto the nitrocellulose membrane. The transfer chamber was placed into a tank and the tank was filled with the 1000 ml of 1x transfer buffer. An ice pack was added to the transfer tank and the transfer was ran at 100 V for 1 hour.

Table 3. 6. Composition of the x10 transfer buffer used to make up the x1 transfer buffer.

Reagent	**Amount**
ddH2O	1000 ml
Glycine	111.75 g
Tris Base	24.24 g
SDS	10 g

3.3.5 Antibody incubation and visualization:

When the transfer was complete the membrane was removed from the sandwich and was blocked for an hour in 5% (w/v) milk which was composed of 5 g of milk powder (Marvel, UK) and 100 ml of tris buffered saline and tween (TBS-T) (Table 3.7). This prevented the primary antibodies from binding to proteins on the membrane non-specifically. The membrane was then incubated overnight on a roller at 4 ^{o}C in the appropriate primary antibody (Table 3.9) that was diluted 1:1000 in 5 ml of 5% milk. The next day the membrane was washed three times for 10 minutes in TBS-T and then incubated for an hour on a roller at room temperature in the appropriate secondary antibody that is bound to horseradish peroxidase (HRP). The secondary antibody detects and binds to the protein of interest-

primary antibody complex. The membrane was then washed three times for 10 minutes in TBS-T and once for 5 minutes in TBS. While washing the ECL substrate was made up with TBS and the two ECL substrate reagent (Biorad, UK) in a 2:1:1 dilution with 1ml of the mixture being added onto the membrane upon visualization. The ECL substrate contained an HRP substrate that detects the HRP bound secondary antibody which generated a chemiluminescent reaction which was then detected by the chemidoc XRS+ machine. The images were then viewed using the imagelab software and the protein of interest band was compared to the molecular weight protein ladder.

Table 3. 7. Compositions of TBS and TBS-T used for washing the membranes.

Reagent	**TBS**	**TBS-T**
ddH2O (ml)	900	900
X10-TBS (ml)	100	100
Tween (ml)	-	1

Table 3. 8. Composition of the x10 TBS.

Reagent	**Amount**
ddH2O	800 ml
NaCl	88 g
Tris Base	24.2 g

Table 3. 9. Types of different antibodies used for western blot analysis along with their company, catalogue number and the species they were raised in.

Antibody	Type	Dilution	Species	Company	Catalogue Number
CBX2	Primary	1:1000	Rabbit	Abcam	ab80044
	Secondary	1:1000	Goat-anti rabbit	Abcam	ab97051
Alpha Tubulin	Primary	1:1000	Mouse	Proteintech	6603I-I-Ig
	Secondary	1:1000	Goat anti-mouse	Abcam	ab97046
H2AK119U	Primary	1:1000	Rabbit	Cell Signalling Technology	D27C4
	Secondary	1:1000	Goat-anti rabbit	Abcam	ab97051
RBL2	Primary	1:1000	Rabbit	Cell Signalling Technology	D9T7SM
	Secondary	1:1000	Goat-anti rabbit	Abcam	ab97051

3.3.6 Densitometry

Western blot images were analysed using the ImageJ software to provide quantitative analysis of the protein band intensities. The western blot image was opened in the ImageJ software and using the rectangle option in the toolbar a rectangle was drawn around the first protein band. Then under the analyse option in the toolbar under the gel's category 'select first lane' was selected. The rectangle drawn around the first protein band was then moved to the next protein band and 'select next lane' was selected in the gels category in the analyse option on the toolbar. This was repeated for the rest of protein bands. Once all the lanes have been highlighted using the analyse option in the toolbar under the gel's category 'plot lanes' was selected and using the line option in the toolbar a line was drawn across the base of the peaks. Using the wand option in the toolbar the area of the peak was analysed by clicking the middle of the peak. This was repeated for the loading control protein band. The areas of the peaks were transferred to excel where they were made relative to the control sample and normalised to the relative density of bands of the loading control protein.

3.4 RT-qPCR

3.4.1 RNA Extraction

Following the 72-hour incubation period the plasmid transfected and/or plasmid and siRNA co-transfected cells had RNA extracted from them using the Qiagen RNeasy Mini kit (catalogue number 74104). Firstly, in the class II biological safety cabinet the media from the wells of the 6 well plate was removed and each well was washed with 1 ml of warm PBS. Then, 350 µl of the RLT buffer was added to each well to lyse the cells, the plate was gently rocked from side to side. The solution was transferred to sterile RNase free Eppendorf tubes to which 350 µl of ethanol was then added using DNA and RNA free pipettes and filter tips in order to precipitate the RNA out of solution. The solution was pipetted up and down so that it was properly mixed. The total 700 µl volume was then transferred from the Eppendorf tubes to the spin columns attached to the 2 ml collection tubes. The samples were then centrifuged at 8000 x g for 15 seconds. The flow-through in the collection tube was discarded and then 700 µl of the RW1 buffer was added to the spin tubes and the samples were centrifuged at 8000 x g for 15 seconds. The RW1 buffer removed any impurities such as carbohydrates or fatty acids. The flow-through was discarded and then 500 µl of the RPE buffer was added to the spin columns and the samples were centrifuged at 8000 x g for 15 seconds. The flow-through was discarded and 500 µl of the RPE buffer was added to the spin columns again and the samples were centrifuged at 8000 x g for 2 minutes. The RPE buffer is a mild washing buffer which was used to remove any traces of salts. The flow-through was discarded and the spin columns were placed in new 1.5 ml DNA and RNA free Eppendorf tubes. Next, 30 µl of RNA-free water was added directly onto the filter of the spin column and the samples were centrifuged at 8000 x g for one minute. The spin columns were then discarded and the ~30 µl of the RNA sample in the 1.5 ml Eppendorf tubes was heated on the heat block at 55 ^{o}C for ten minutes. The RNA in the samples was then analysed with the RNA concentration (ng/µl), and the nucleic acid protein contamination (260:280 and 260:230) being measured by a Nanodrop 2000 machine.

3.4.2 Reverse Transcription

To generate the complementary DNA (cDNA) needed for qPCR experiments, 1 µg of RNA was reverse transcribed into cDNA. The RNA concentration from the nanodrop reading was used to calculate the volume of RNA in µl needed to have the 1 µg of RNA, which was then

made up to a volume 12.7 µl with molecular grade water (GE Healthcare, UK). Next, a master mix consisting of 4 µl of 5xRT buffer (Promega, UK), 2 µl of deoxynucleotide triphosphates (DNTPs)(Bioline, UK), 1 µl of oligo dTs (Invitrogen, UK) and 0.3 µl of the reverse transcriptase (RT) enzyme (Promega, UK) per sample was made up in an Eppendorf tube. Next, 7.3 µl of the master mix was added to the 12.7 µl of the 1 µg RNA samples and the samples were then heated on the heat block at 37 ^{o}C for one hour and then at 95 ^{o}C for five minutes to denature the RT enzyme and therefore end the reverse transcription reaction. Finally, the samples were made up to 200 µl by the addition of 180 µl of molecular grade water and the cDNA samples were stored at -20 ^{o}C ready to be used for qPCR.

3.4.3 qPCR

For quantitative polymerase chain reaction (qPCR) master mixes for each gene of interest were made on ice in DNA and RNA free Eppendorf tubes. The master mix comprised of 5 µl of SYBR green (Sigma, UK), 2.1 µl molecular grade water, 0.1 µl ROX dye (Sigma, UK), and 0.4 µl of the forward and reverse primer (Table 3.10) per reaction and each sample was analysed in a triplicate for each gene. The master mixes were then vortexed and 8 µl was loaded in triplicate wells of the 96 PCR well plate (Applied Biosystems, UK). Next 2 µl of cDNA sample was pipetted into appropriate wells but this time onto the side of the well near the top. Molecular grade water was also loaded as a negative control. After the master mixes and cDNA samples were loaded a clear PCR plate coverslip was placed over the plate and made flat to remove any air bubbles. The plate was then spun using a plate spinner to ensure the 2 µl of the cDNA sample pipetted onto the side of the well moved down to the master mix at the bottom of the well. The plate was then placed onto the plate holder of the StepOne plus qPCR machine (Thermofisher, UK) and the following experiment settings were selected. For the experiment type the quantitative comparative CT setting was chosen and the reagent selected was SYBR green reagents with melt curve. The reaction volume per well was changed to 10 µl per well and the run was started. The reaction started off at 95 ^{o}C for ten minutes in order to denature the DNA into two single strands, then the temperature decreased to 60 ^{o}C for 1 minute to allow the primers to bind to the template DNA strand, and finally the temperature was raised to 72 ^{o}C for 1 minute which is the optimal temperature for the Taq polymerase enzyme to function and polymerize the new DNA strands. This was repeated for 40 cycles. Once the reaction was finished the results in the

form of amplification curves and scores were exported into excel and analysed using the cycle thresholds (CT) mean values to calculate the expression fold changes in the genes of interest via the delta-delta CT formula ($2^{-\Delta\Delta Ct}$).

Firstly, the delta CT value was found by calculating the difference in the average CT values between the control group (pFLAG) and the CBX2 plasmid transfected group for the gene of interest and the housekeeping gene. The delta-delta CT value was then calculated by subtracting the delta CT value of the housekeeping gene from the delta CT value of the gene of interest. The expression fold change was then calculated by using the delta-delta CT value as the negative power of 2.

Table 3. 10. Forward and reverse primers used for qPCR experiments.

Primer	**Company**	**Sequence**
RPL13A Forward Primer	Sigma	CCTGGAGGAGGAGAGGAAA-GAGA
RPL13A Reverse Primer	Sigma	TTGAGGACCTCTGTGTATTTGTCAA
CBX2 Forward Primer	IDT	GCTCCAAAGCCAGACTAACA
CBX2 Reverse Primer	IDT	CAGGGACAGACATCCTCATTTC
RBL2 Forward Primer	Sigma	AGTCCAAAGCACTTAGAATC
RBL2 Reverse Primer	Sigma	GAATCTGTTCCAGTTTCTCAC
AURKA Forward Primer	IDT	GGTGACAACAAACCCGACG
AURKA Reverse Primer	IDT	CCGGGTTCTTAGGGAGCAAG

3.5.1 Immunofluorescence

Using tweezers, glass coverslips were dipped into a beaker of methanol and left to air-dry for 15 minutes before being placed into the centre of an individual well of a six well plate. 100,000 MDA-MB-231 cells in the 2 ml cell suspension were then seeded into the wells onto the glass coverslip and incubated in a humidified incubator at 37 ^{o}C for 24 hours. Following 24 hours the cells were co-transfected with the plasmids and the CBX2 targeting siRNAs as described in 3.2.5 And then incubated in a humidified incubator for 72 hours.

Post 72 hours the 2 ml of media was removed from each well and the cells were washed with 1 ml of pre-warmed PBS and then fixed with 1 ml of ice-cold methanol for 15 minutes at room temperature. Once fixed, the methanol was removed and the cells were washed twice with 1 ml of ice-cold PBS. Since both the FLAG-tagged CBX2 protein and H2AK119U histone modification that were being investigated are expressed intracellularly the cells were permeabilized with 1 ml of 0.25% (v/v) triton X-100 for 10 minutes to improve antibody penetration. The 0.25% triton X-100 was removed and the cells were washed 3 times with 1 ml of ice-cold PBS for 5 minutes. The glass coverslips with the fixed cells were then transferred to a new six well plate using tweezers and then incubated for 30 minutes in 150 µl of goat serum to block unspecific antibody binding. In the meantime, a master mix consisting of 1 ml 1% (w/v) BSA in PBS-T and the mixture of the two primary antibodies was made with the pFLAG primary antibody being diluted 1:2000 and the H2AK119U primary antibody being diluted 1:1000. The goat serum was removed from the cells and 250 µl of the primary antibody mixture was added on top of the glass coverslips (Table 3.11). The cells were incubated in the primary antibody mixture for 1 hour in a humidified chamber. Following the 1 hour the primary antibody mixture was decanted from the glass coverslips and the cells were washed 5 times for 5 minutes with ice-cold PBS. The secondary antibody mixture was made with the green secondary fluorescent antibody complementary to the primary pFLAG antibody being diluted 1:2000 and the red secondary fluorescent antibody complementary to the primary H2AK119U antibody being diluted 1:250 in 1 ml of 1% BSA in PBST. The cells were incubated in 250 µl of the secondary antibody mixture for 1 hour in the dark. The secondary antibody mixture was removed and the cells were washed in the dark 5 times for 5 minutes with ice-cold PBS. Using tweezers, the glass coverslips with the fixed cells were taken out the well and gently dried on a paper towel. Glass slides were sterilised

with ethanol and appropriately labelled before a drop of DAP stainI was added onto them and the glass coverslip with the fixed cells was placed on top of the DAPI drop (cell side down). To seal the coverslips nail varnish was applied to the edges of the coverslips, the slides were then stored for 2 hours in the dark at 4 ^{o}C to allow the nail varnish to dry before the slides were visualized.

Table 3. 11. Types of antibodies used for immunofluorescence analysis along with their company, catalogue number and species they were raised.

Antibody	**Type**	**Dilution**	**Species**	**Company**	**Catalogue Number**
pFLAG	Primary	1:2000	Mouse	Sigma	F3165
	Secondary	1:2000	Goat-anti mouse	Invitrogen	A-11001
H2AK119U	Primary	1:1000	Rabbit	Cell Signalling Technology	D27C4
	Secondary	1:250	Goat anti-rabbit	Thermofisher	T-2767

3.5.2 Immunofluorescence Visualization

The slides were visualized using the Zeiss AXIO Vert.A1 inverted fluorescence microscope that was connected to a computer with the Zeiss Zen software. The eyepiece slider on the front of the microscope was fully pushed in to allow binocular viewing, a magnification of 40x was set and the slides were placed (coverslip side down) onto the stage. Before focusing the microscope, the lighting switch on the left-hand side of the microscope was switched to 'RL' (reflected light), and the shutter at the top was closed to minimize the background fluorescence of the green channel (GFP). Once focused the Zeiss Zen software was opened on the computer and the slider at the front of the microscope was pulled out to allow camera viewing. From the acquisition tab in the software the '3 colour + phase' setting was selected to view the cells using the camera. Next the boxes of the DAPI blue, GFP and Texas red were selected as the 3 filter colours that were going to be used to visualize the cells. Then using the 'Live' function the cells were viewed and focused using the microscope camera. Once focused the cells were photographed using the 'SNAP' function. Before obtaining an image, the filter wheel located below the objectives was set to the appropriate filter that was selected on the computer software.

3.6.1 Flow cytometry preparation and analysis

Following the 72-hour incubation period post the plasmid and siRNA co-transfection the 2ml of media from each well was transferred to FACS tubes (BD Biosciences, UK). The cells were then washed with 0.5 ml of pre-warmed PBS which was then transferred to the FACS tube. The cells were then trypsinised using the 1:30 diluted trypsin. Once detached the cell and trypsin solution was transferred to the FACS tube which was sealed with parafilm and centrifuged at 300 x g for 5 minutes. Once centrifuged the supernatant was carefully removed from the FACS tube and 0.5 ml of PBS was used to wash and resuspend the cell pellet before the samples were centrifuged for a second time at 300 x g for 5 minutes. The PBS supernatant was carefully removed and the cell pellet was resuspended in 100 µl citrate buffer (0.25 M sucrose, 40 nM sodium citrate, pH 7.6), 400 µl DNA staining and lysis buffer (PBS, 20 µg/ml propidium iodide, 0.5% NP-40 and 0.5 mM EDTA) and 5µl of 20 mg/ml RNase A. The FACS tubes were placed in a tube rack which was then entirely covered in aluminium foil and incubated in the dark at 4 ^{o}C for 40 minutes.

Cells were detected and gated using FL2-Area and FL2-W channels to remove doublet and clumped cells – ensuring only single cells were counted. 10,000 events/cells were counted and then the gated cells were then separated by FL2-A in a histogram to assess each phase of the cell cycle and gated once more to count the number of cells in sub-G1, G1, S and G2 phase.

3.7.1 Statistical Analysis

Using GraphPad a one-way ANOVA was used to determine the overall statistical significance of the cell count and qPCR results followed by the Tukey's multiple comparisons test to determine between which specific groups those significant results lie.

Chapter 4. Results

4.1.1 - Plasmid propagation, extraction and purification

Firstly, it was required to propagate the plasmid to have enough plasmid for the cell line transfection experiments. Plasmid stocks were kindly provided by Jun-ichi Nakayama (Nagoya City University) and were previously validated and reported in Kawaguchi et al, (2017). In order to increase the plasmid concentration, the plasmids were transformed via the heat shock method into competent *E. coli* cells that were then grown for 24 hours on kanamycin agar plates. Post incubation a single colony was selected and grown in Luria broth. The plasmid DNA was extracted from the *E. coli* cells and purified using a Maxi Prep kit. The plasmids were resuspended in TE buffer and then analysed by the nanodrop machine to determine the final plasmid DNA concentration, the 260/280 ratio to measure the purity of the plasmid DNA and the 260/230 ratio which is a secondary assessment of the nucleic acid purity. The concentration of the AR plasmid had increased ~14-fold from its initial concentration whereas the concentrations for the other five plasmids had increased ~50 fold from their initial concentrations (Table 4.1). The 260/280 ratios for the six plasmids were ~1.90 with a value >1.80 being considered to be the standard value for 'pure' DNA. Whilst, the 260/230 ratios were ~2.20 with 2-2.20 being accepted as the appropriate range for 'pure' nucleic acids indicating that the plasmids were relatively pure DNA and were not contaminated by any contaminants such as proteins or polyhydroxy compounds.

Table 4. 1. Initial and final DNA concentrations along with the 260/280 and 260/230 ratios of the six-plasmids used for the subsequent experiments.

CBX2 plasmid variant	Initial concentration (ng/ul)	Final concentration (ng/ul)	260/280	260/230
pFLAG	53.2	2763	1.89	2.24
FL	31.4	2754	1.90	2.28
SR	104	2672	1.90	2.25
AR	95.4	1327	1.91	2.29
SA	53	2902	1.90	2.22
CD	12.1	2493	1.90	2.26

Plasmid compositions: **pFLAG** – empty vector that only contained a flag tag. **FL** – contained the 'full length' wildtype sequence of CBX2. **SR** – deleted the 'serine rich' region that is stably phosphorylated which increases CBX2's nucleosome binding specificity. **AR** – deleted the 'acidic residue' that helps fix CBX2 into position on the nucleosome. **SA** – deleted both the serine rich region and acidic residue. **CD** – deleted the chromodomain that is responsible for recognizing the H3K27me3 mark.

4.1.2 - Verification of the plasmid DNA sequences

Next, it was required to verify the DNA sequences of the six plasmids to ensure they were either an empty vector, a full length CBX2 sequence or a mutant CBX2 that is missing the appropriate structural motifs that have been shown to play a role in CBX2 chromatin interactions. Plasmids were diluted to a concentration of 100 ng/ul with the TE buffer and sent away for Sanger sequencing by Azenta/GENEWIZ. The sequencing provided a quality score that indicated whether the quality of the samples was high or low, a trace file and a FASTA file that was used to analyse the differences between the nucleotide sequences of the plasmids (Figure 4.1). The sequencing confirmed that the 'pFLAG' plasmid that was treated as a transfection control was an empty vector that only contained a FLAG tag. Furthermore, the other five plasmids were also found to contain the FLAG tag. The 'FL' plasmid was validated to contain the complete sequence of the wildtype CBX2. The 'CD' plasmid was found to be missing the sequence for the chromodomain and the 'SR' plasmid was found to have the sequence for the serine rich region deleted as expected. However, the 'AR' plasmid that was supposed to have the sequence for the acidic residue deleted and

the ‘SA’ plasmid that was supposed to have both sequences for the serine rich region and the acidic residue deleted were labelled the wrong way round. Following this discovery, the labelling for the two plasmids was corrected.

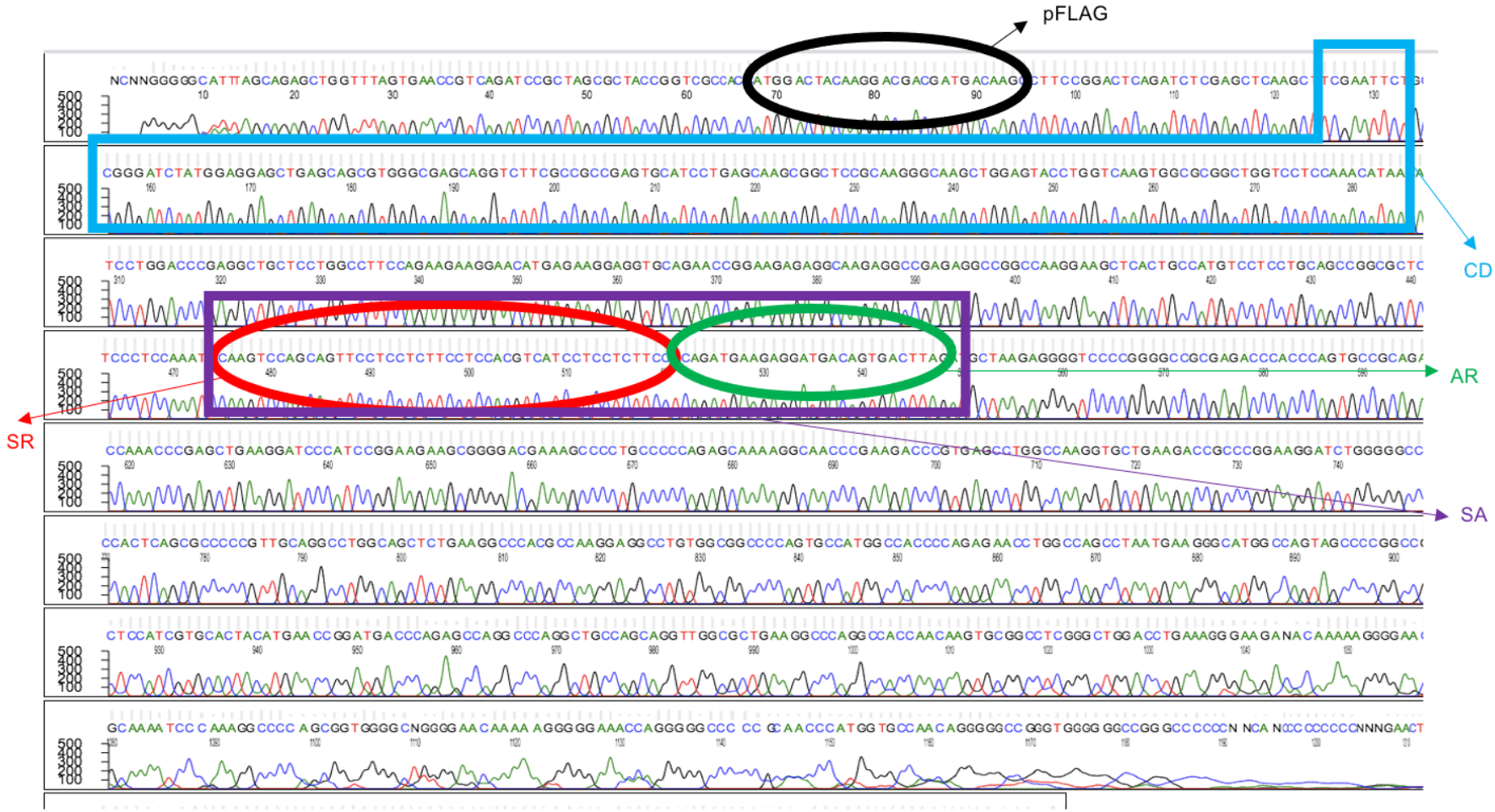

Figure 4. 1. Screenshot of the DNA sequence of the FL CBX2 plasmid from Genewiz highlighting the different structural motifs that were deleted in the mutant CBX2 plasmids. The sequence of the FLAG tag is highlighted by the black circle, the CD sequence is represented by the light blue, red illustrates the SR region sequence, green the AR cluster sequence and the purple square both the SR rich and AR cluster sequences. The rest of the sequence following the purple box encodes for the rest of the CBX2 (central region, PC repressor box etc).

4.1.3 - Confirmation of the protein molecular weight of the mutant CBX2 proteins

Following the verification of the plasmid DNA sequences, the transient expression of the plasmids was analysed at a protein level by western blot analysis (Figure 4.2). Since DNA sequencing showed the appropriate structural motifs were deleted the CBX2 wildtype and mutant proteins were expected to be at varying molecular weights. To assess this 1 µg of the plasmid was transfected into the MDA-MB-231 and MDA-MB-468 cells 24 hours after the cells were seeded. The cells were then incubated for 72 hours and afterwards the protein was extracted from them for western blot analysis to assess the molecular weight of the wildtype and mutant CBX2 proteins using CBX2 and alpha tubulin (used as a loading control) specific antibodies. In both cell lines the FL CBX2 appeared at the expected ~72kDA molecular weight and the mutant CBX2 proteins were observed at lower molecular weights, as anticipated, since the mutant CBX2s are shorter variations of the wildtype CBX2. The SA mutant CBX2 was observed at the lowest molecular weight in both cell lines. In the MDA-MB-468 cells the endogenous CBX2 is more prominent than in the MDA-MB-231 cells resulting in two CBX2 bands being observed, one demonstrating the endogenous CBX2 expression the other the transient CBX2 protein expression. Furthermore, the molecular weights that the mutant CBX2s appeared at complemented the molecular weights and the pattern observed by Kawaguchi et al (2017), who developed the plasmid constructs and calculated the predicted molecular weights.

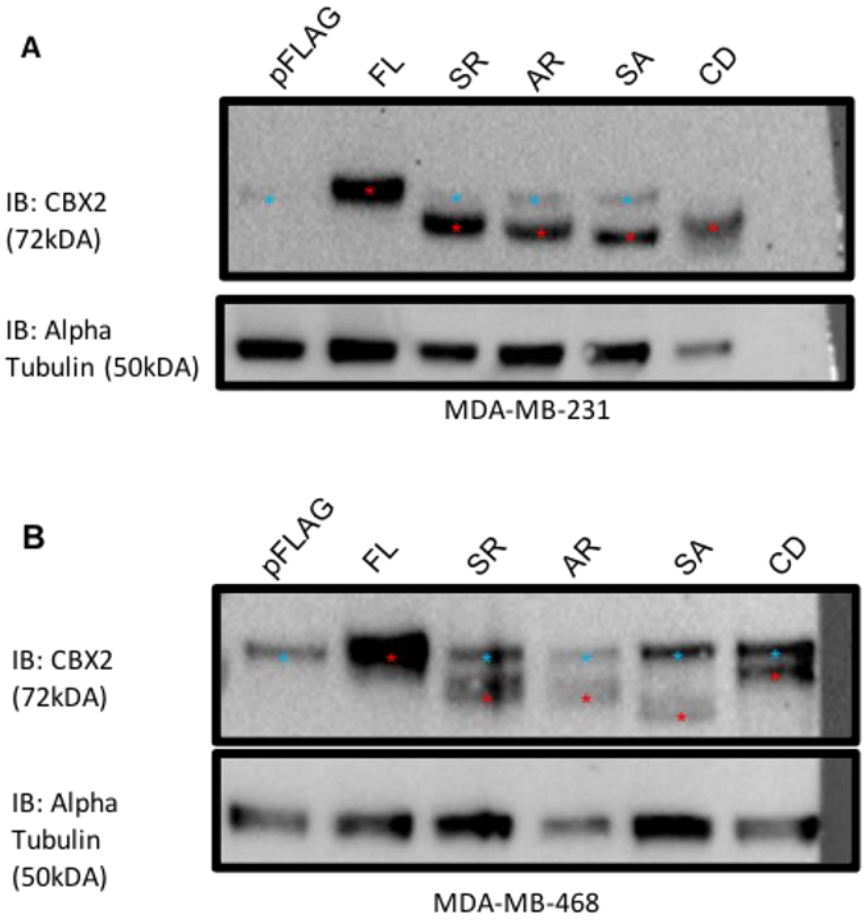

Figure 4. 2. Western blot showing the transient protein expression of the different CBX2 plasmids in MDA-MB-231 (A) and MDA-MB-468 (B) cell lines. The plasmids transfected into the cells are specified at the top above the relevant lanes, specific antibodies used and the protein molecular weights are noted to the left of the blot. * = plasmid CBX2 protein expression, * = endogenous CBX2 protein expression. N = 3 for blot A, N = 2 for blot B.

4.2.1 – CBX2 chromatin interactions and cell growth

Previous work from the group has shown that siRNA mediated knockdown of CBX2 reduced cell growth in TNBC cell lines indicating that CBX2 plays a role in TNBC proliferation. To determine whether it is the CBX2 chromatin interactions that are required for TNBC cell growth the wildtype and mutant versions of CBX2 were overexpressed in TNBC cell lines, to investigate whether their co-expression would enhance or impair the pro-proliferative activity of the endogenous CBX2 (Figure 4.3). The MDA-MB-231 and MDA-MB-468 cells were counted using a haemocytometer 72 hour post the 1 µg plasmid transfection. The cell count data was made relative to the pFLAG transfected cells and analysed using a one-way ANOVA test and the Tukey's multiple comparison test. In the MDA-MB-231 cell line (Figure 4.3 A), overexpression of the FL CBX2 plasmid compared to the empty vector pFLAG plasmid increased cell growth, and compared to the CD plasmid the FL significantly increased the cell growth ($p<0.01$). Overexpression of the SR, AR and SA mutant CBX2 plasmids had a lesser impact on cell growth with the cell number being similar to the cell number of the cells transfected with the pFLAG plasmid. Whereas, overexpression of the CD mutant CBX2 reduced cell growth compared to the pFLAG plasmid. In the MDA-MB-468 cell line (Figure 4.3 B), overexpression of the FL CBX2 significantly increased cell growth compared to the pFLAG transfected cells ($p<0.01$). Conversely, overexpression of the SR, SA and CD plasmid significantly depleted cell growth compared to the pFLAG transfected cells ($p<0.05$).

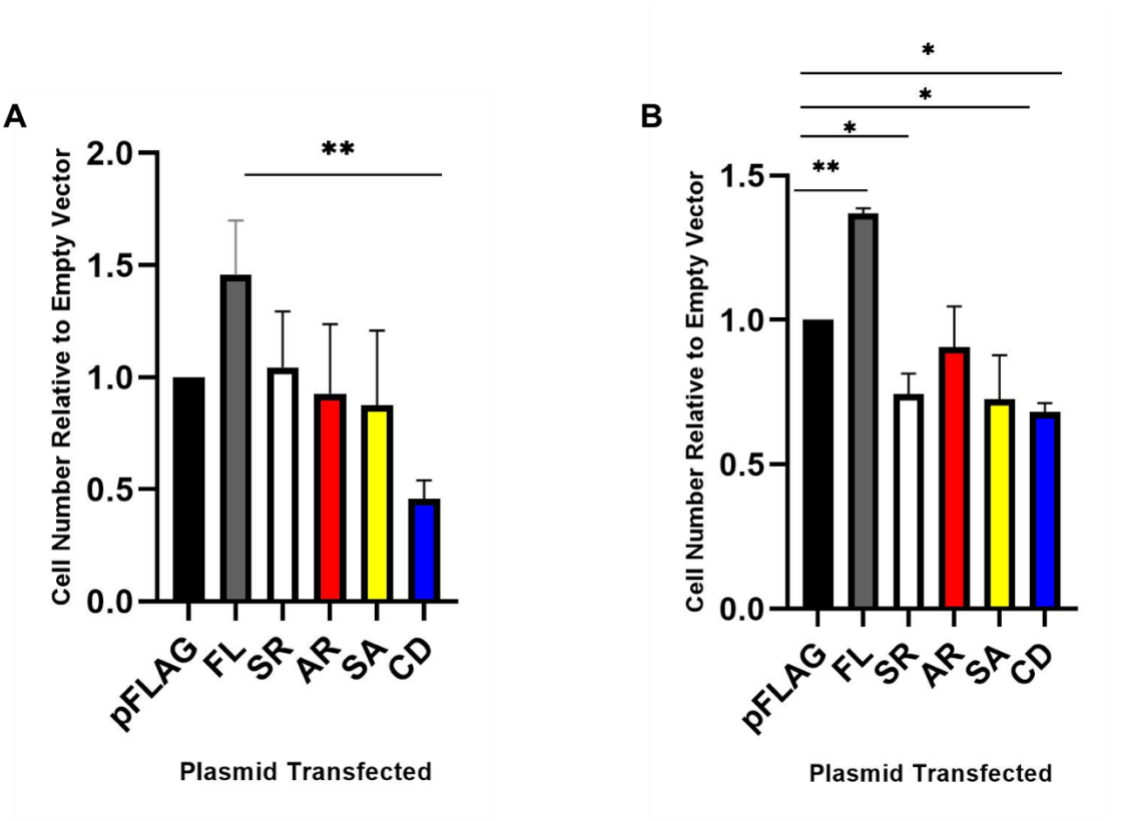

Figure 4. 3. Cell growth was analysed by cell counts 72 hours post the 1 µg plasmid transfection into the MDA-MB-231 cells (A) and MDA-MB-468 cells (B). Cell counts were an average of three triplicates of three independent experiments ± SEM and standardised to the cells transfected with the pFLAG plasmid. P-values were determined by Tukey's multiple comparisons test. **A** (3 repeats): ** = $p<0.01$. **B** (3 repeats): * = $p<0.05$, ** = $p<0.01$, *** = $p<0.001$, **** = $p<0.0001$.

4.2.2 – Validating CBX2 CD chromatin interactions being required for TNBC cell growth

To validate that the CBX2 chromatin interaction of the CD is required for TNBC cell growth, the CBX2 plasmids were co-transfected with CBX2 targeting siRNAs to determine whether the FL CBX2 and the CD mutant CBX2 could rescue TNBC cell growth following a siRNA mediated CBX2 knockdown. The rescue experiments were initially done with the pFLAG plasmid (which was used as a control), the FL and the CD plasmid, as the overexpression of those CBX2 plasmids elevated and depleted the TNBC cell growth, respectively (Figure 4.4). The MDA-MB-231 cells were co-transfected with 250 ng of the previously mentioned plasmids and with a non-silencing CBX2 siRNA (Scr) or a CBX2 targeting siRNA: either siCBX2-3(#3) or siCBX2-4(#4). For rescue experiments in the MDA-MB-468 cells the CBX2 knockdown was performed 24 hours prior to the 250 ng plasmid transfections as those cells have a longer doubling time and therefore a co-transfection at the same time resulted in a minimal knockdown effect. Also, only 250 ng of the plasmid was used for the rescue experiments as co-transfecting 1 μg of the plasmid as well as a siRNA was observed to result in cell death. The cell count data for the rescue experiments was standardised to the Scr-pFLAG co-transfected cells and analysed using a one-way ANOVA and Tukey's multiple comparisons test.

In MDA-MB-231 cells (Figure 4.4 A and B), co-transfection with #3/#4-pFLAG and #3/#4-CD did not rescue cell growth with the difference in cell number between the scr-pFLAG being significantly reduced ($p<0.001$ for #3-pFLAG, $p<0.05$ for #3-CD and $p<0.001$ for #4-pFLAG and #4-CD). Cells co-transfected with the #3/#4-FL did rescue cell growth, almost restoring it to similar numbers observed in the cells co-transfected with the non-silencing siRNA, and significantly increased the cell number compared to #3/#4-pFLAG and #3/#4-CD co-transfected cells ($p<0.01$ for #3-pFLAG, $p<0.05$ for #3-CD and $p<0.01$ for #4-pFLAG and #4-CD). Similarly, in MDA-MB-468 cells (Figure 4.4 C) co-transfected with #3-pFLAG and #3-CD did not rescue cell growth with the difference in cell number compared to the Scr-pFLAG co-transfected cells being significantly reduced ($p<0.01$ for #3-pFLAG and $p<0.001$ for #3-CD). Whereas, the #3-FL co-transfected cells managed to restore the cell growth and significantly increase it compared to the #3-CD co-transfected cells ($p<0.05$). Interestingly, cells co-transfected with the non-silencing siRNA and the FL plasmid also significantly increased cell growth compared the scr-CD co-transfected cells ($p<0.05$).

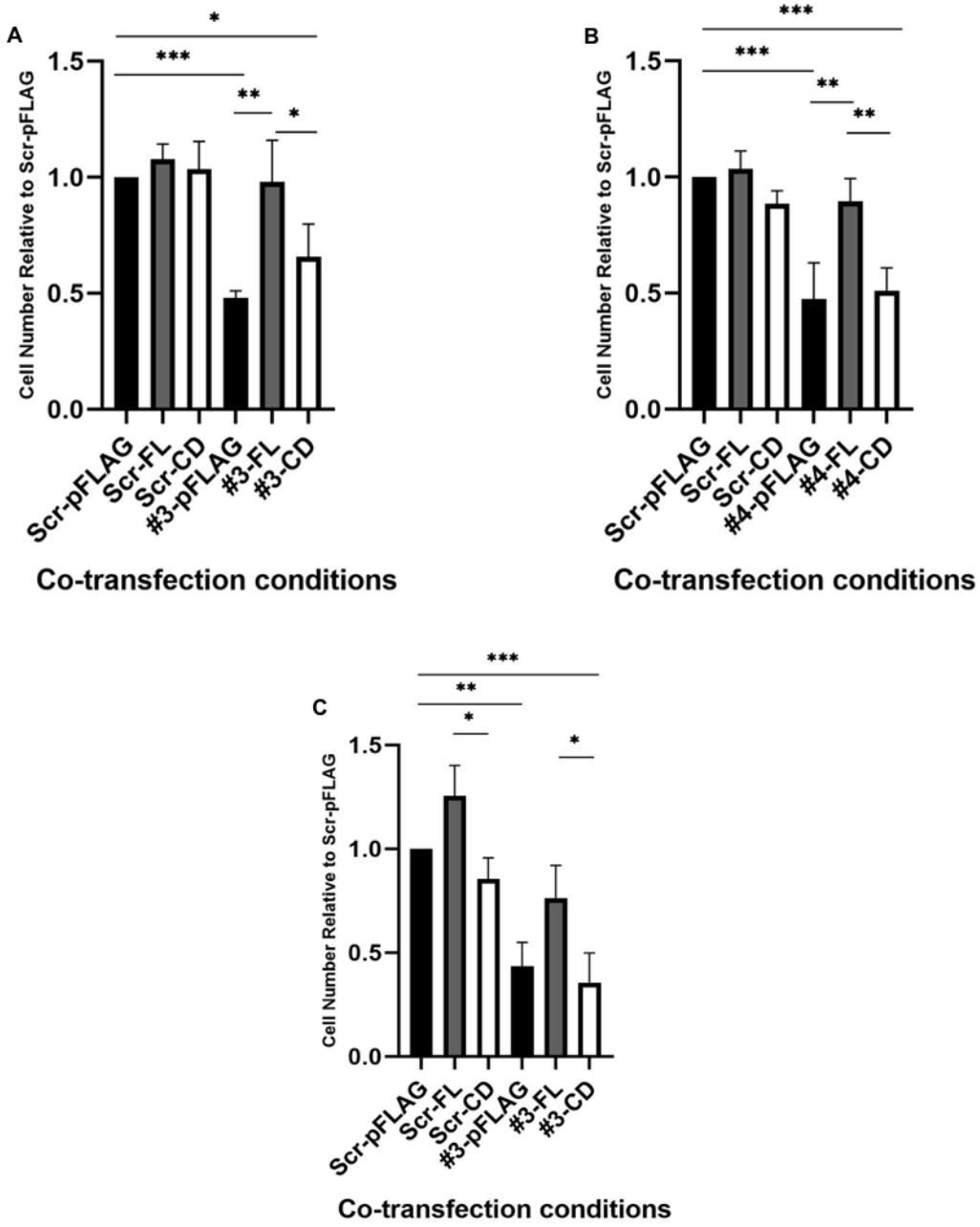

Figure 4. 4. Cell growth was analysed by cell counts in the MDA-MB-231 cells (A and B) and MDA-MB-468 cells (C) 72 hours post the co-transfection with 250ng of the pFLAG, FL and CD plasmid and the non-silencing siRNA and CBX2 targeting #3 (A and C) and #4 (B) siRNA. The cell count data was the average of three triplicates of three independent experiments ± SEM and standardised to the cell count of the scr-pFLAG co-transfected cells. P-values for all three sets of experiments were determined by Tukey's multiple comparison test: * = $p<0.05$, ** = $p<0.01$, *** = $p<0.001$, **** = $p<0.0001$.

4.2.3 – Co-transfection cell images

To further support the quantitative data above indicating the CD CBX2 chromatin interaction is required for TNBC cell growth the cells were viewed under the light microscope and photographed down a microscope eye-piece (Figure 4.5). MDA-MB-231 cells were seeded 24 hours prior to being co-transfected with 250 ng of the pFLAG, FL and CD CBX2 plasmid and either a non-silencing siRNA or a CBX2 targeting siRNA. After 72 hours the cells were viewed under a light microscope with the 40x magnification lens and photographed. A notable decrease in the number of cells can be observed in the #3-pFLAG and #3-CD co-transfected cells alongside a change in the cell morphology with cells appearing more round, suggesting that those cells are potentially dying. Cells co-transfected with the #3-FL appeared to have maintained their regular morphology and rescued their ability to grow and proliferate almost restoring the cell number to those observed in the cells co-transfected with the plasmids and the non-silencing siRNA.

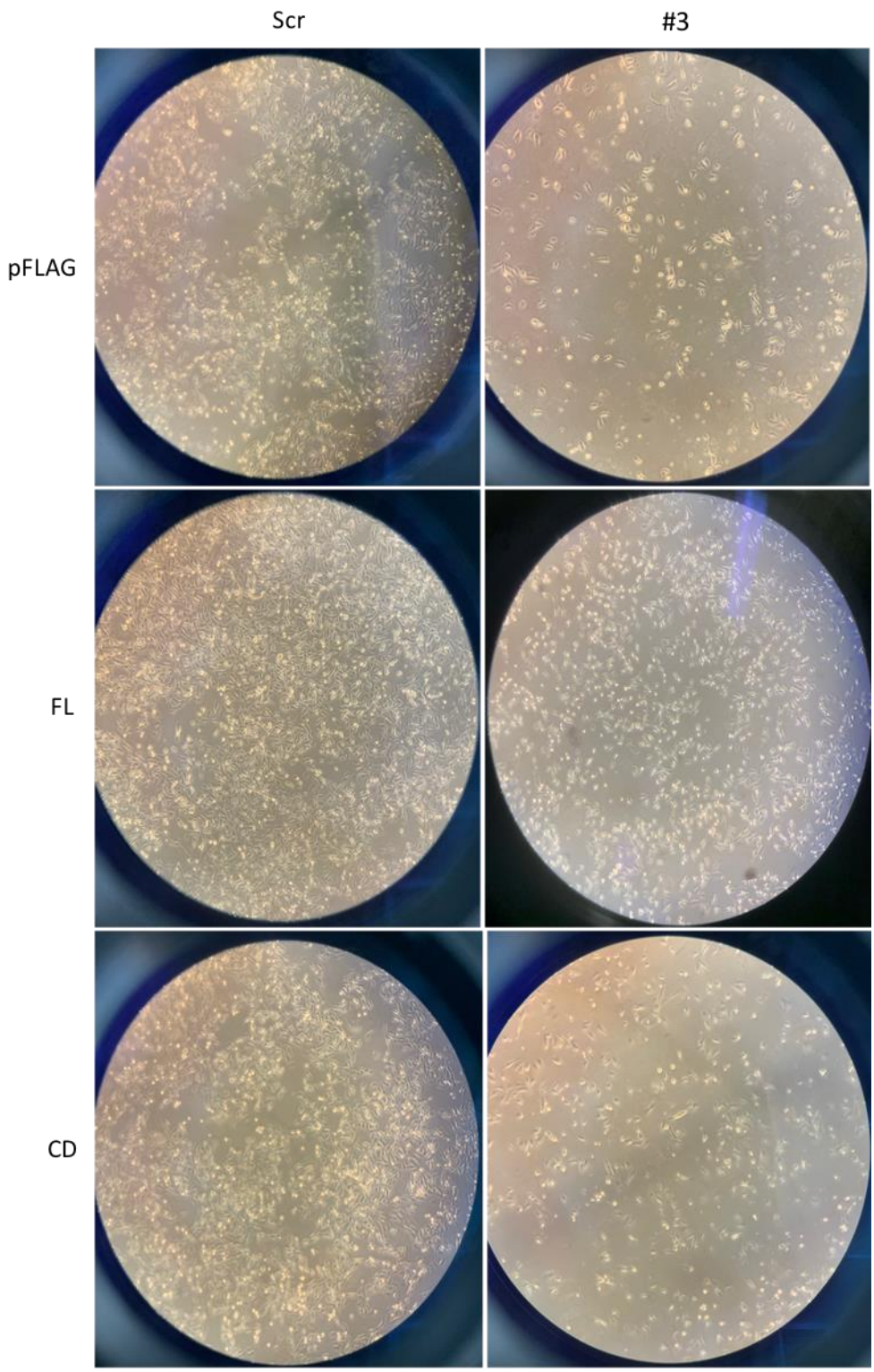

Figure 4. 5. Photographic images of the MDA-MB-231 cells co-transfected with the pFLAG, FL and CD plasmid and a non-silencing siRNA (Scr) or a CBX2 targeting siRNA (#3) using the 40x magnification lens of the light microscope. The transfected siRNA is indicated at the top and the transfected plasmid is specified to the left of the images.

4.2.4 – CBX2 CD chromatin interaction effect on stages of the cell cycle

To further understand the importance of the CD CBX2 chromatin interaction for TNBC cell growth the cell cycle phases of the co-transfected cells were analysed by propidium iodide flow cytometry. This would allow us to know whether the different transfection combinations were causing cell death or arrest in a particular phase of the cell cycle. MDA-MB-231 cells were stained with propidium iodide for flow cytometry analysis 72 hours post the 250 ng pFLAG, FL and CD plasmid co-transfection with the non-silencing siRNA or the CBX2 targeting siRNA. In cells co-transfected with the #3-pFLAG and #3-CD the percentage of cells in the sub G1 phase increased, decreased in the G1 phase and slightly increased in the S phase compared to the non-silencing siRNA co-transfected cells. An increase of cells in sub G1 phase indicates a potential increase in cell death. Whereas, for the #3-FL co-transfected cells the pattern observed for the percentages of cells in a certain cell cycle phase was similar to the pattern observed in the non-silencing siRNA co-transfected cells. No statistical analysis was performed due to this experiment only being performed once because the flow cytometry machine stopped working and was not repaired before the completion of this study.

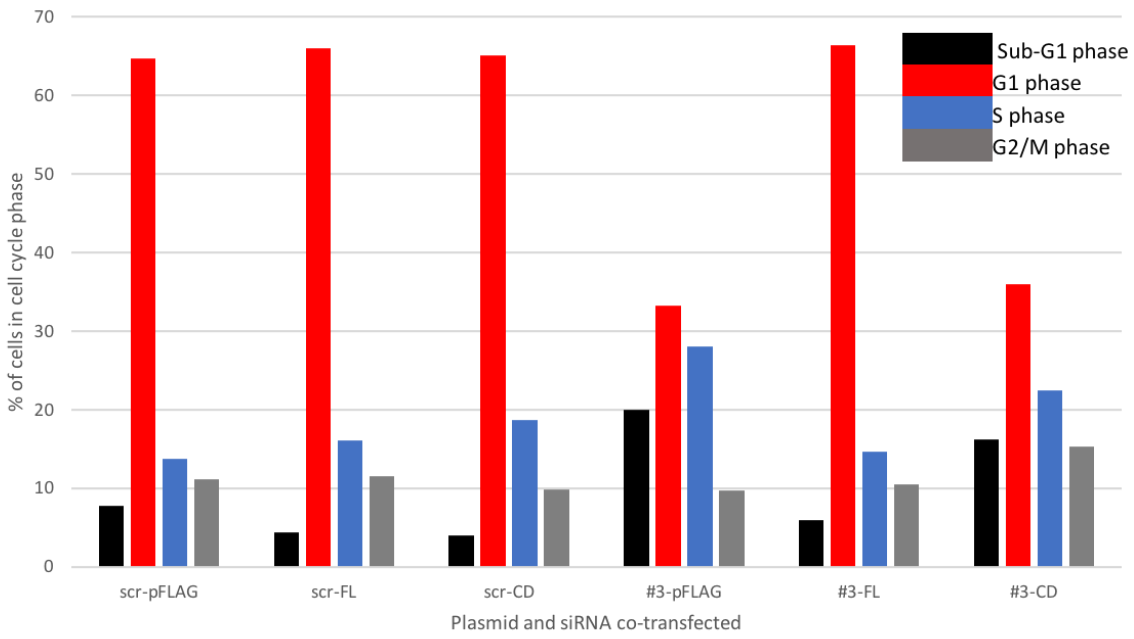

Figure 4. 6. Cell cycle analysis by flow cytometry displaying the percentage of cells in each phase of the cell cycle following the MDA-MB-231 cell co-transfection with 250 ng of the pFLAG, FL and CD plasmid and the non-silencing CBX2 siRNA or the CBX2 targeting siRNA.

4.2.5 - SR and AR chromatin interactions effect on TNBC cell growth

After confirming that FL CBX2 can rescue cell growth following CBX2 knockdown, but that the CBX2 mutant that is missing the CD responsible for the recognition of the H3K27me3 mark does not, the rescue experiment was expanded to the SR and AR mutant CBX2 plasmids. This was done to determine whether the chromatin interactions that the SR region and the AR have been shown to be involved in are also essential for TNBC cell growth. MDA-MB-231 cells were seeded 24 hours prior to the co-transfection with 250 ng of the pFLAG, SR or the AR plasmids and either a non-silencing CBX2 siRNA or a CBX2 targeting siRNA, incubated for 72 hours and then counted using a haemocytometer. The cell count results were made relative to the cell counts of the scr-pFLAG co-transfected cells and analysed using the one-way ANOVA and Tukey's multiple comparisons test. Both, the SR and AR mutant CBX2 plasmids rescued TNBC cell growth following the siRNA mediated CBX2 knockdown and significantly increased the cell number compared to the cells co-transfected with the #3-pFLAG ($p<0.05$ #3-SR and #3-AR).

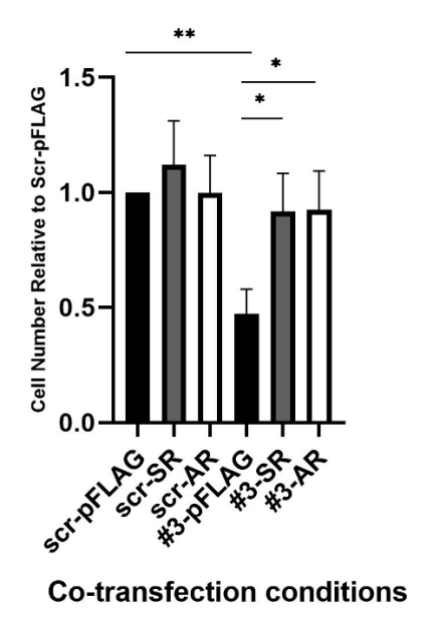

Figure 4. 7. Cell growth was analysed by cell counts in the MDA-MB-231 cells 72 hours post the co-transfection with 250ng of the pFLAG, SR and AR plasmid and the non-silencing siRNA and CBX2 targeting #3 siRNA. The cell count data was the average of three triplicates of three independent experiments ± SEM and standardised to the cell counts of the scr-pFLAG co-transfected cells. P-values for all three sets of experiments were determined by Tukey's multiple comparison test: * = $p<0.05$, ** = $p<0.01$.

4.3.1 Chromatin interactions and PRC1 complex activity

Validation of the CD CBX2 chromatin interaction being required for TNBC cell growth, suggested that the CBX2 chromatin interactions could therefore also be essential for regulating the expression of genes that CBX2 potentially regulates to augment TNBC proliferation. CBX2 regulates the expression of its target genes via the PRC1 complex which condenses the chromatin by monoubiquitinating H2AK119 following its CBX2 mediated recruitment to the H3K27me3 mark. It was therefore first required to investigate the importance of CBX2 chromatin interactions to PRC1 complex activity by assessing the ubiquitination of H2AK119 via western blot analysis. First, the effect on H2AK119 monoubiquitination was analysed following transfection of the pFLAG, FL and four mutant CBX2 plasmids. The MDA-MB-231 cells were seeded for 24 hours, then transfected with 1 µg of the plasmid and incubated for 72 hours. Afterwards the protein lysates were extracted from the cells and analysed by western blot using antibodies specific for H2AK119U, CBX2 and alpha tubulin (Figure 4.8A). The image was then semi-quantitatively analysed by densitometry using the ImageJ software (Figure 4.8B).

The FL CBX2 elevated the global H2AK119U modification resulting in a more intense band at 26kDA compared to the pFLAG and mutant CBX2 H2AK119U bands. This was supported by the densitometry analysis with the H2AK119U protein expression increasing by 1.5-fold following the overexpression of the FL CBX2 when compared to the pFLAG overexpression H2AK119U protein expression (Figure 4.8 B). The western blot appeared to show that the global H2AK119U histone modification was slightly increased by SR, AR and SA mutant CBX2 when compared to pFLAG. However, there was more protein present in the cells overexpressed with the FL CBX2 and SR and AR mutant CBX2 compared to the pFLAG transfected cells. This resulted in the densitometry analysis suggesting the H2AK119U protein expression decreased following the SR and AR CBX2 mutant overexpression but increased following the SA CBX2 mutant overexpression. No band was observed at 26kDA for the CD mutant CBX2 due to there being considerably less protein present indicated by the alpha tubulin band.

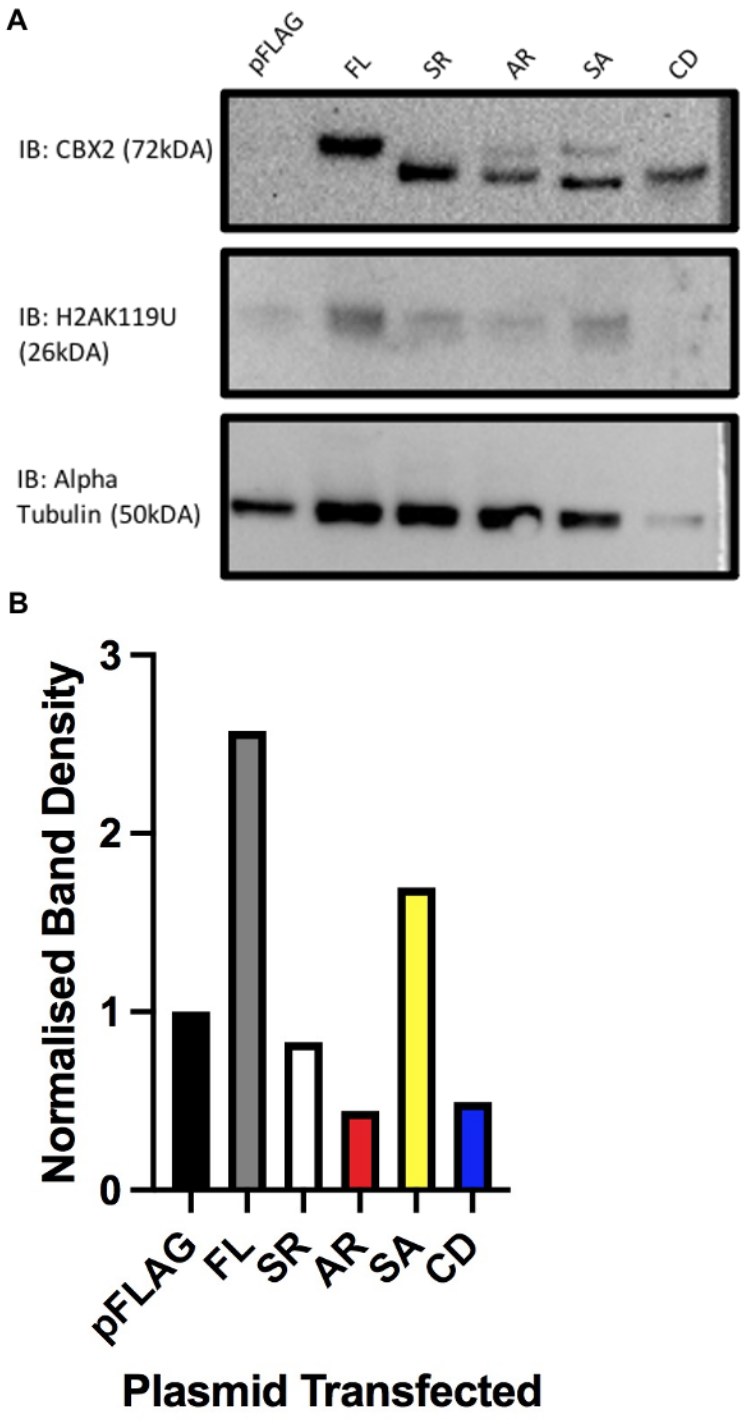

Figure 4. 8. A - Western blot probed for CBX2, H2AK119U and alpha tubulin illustrating the effect of the plasmid overexpression on the global H2AK119U histone modification in MDA-MB-231 cells. The plasmids transfected into the cells are specified at the top above the relevant lanes, specific antibodies used and the protein molecular weights are noted to the left of the blot. **B** - H2AK119U protein expression analysed by densitometry following 1 µg plasmid transfection into MDA-MB-231 cells. (N=1)

In an attempt to achieve a more reliable result for the H2AK119U histone modification of the CD mutant CBX2 the next plasmid overexpression experiments investigating H2AK119U mainly focused on the pFLAG, FL and CD plasmids. The protein lysates were extracted from the MDA-MB-231 cells 72 hours post the 1 µg plasmid transfection and analysed by western blot using CBX2, H2AK119U and alpha tubulin specific antibodies (Figure 4.9A). Using the ImageJ software, the images were semi-quantitatively analysed by densitometry (Figure 4.9 B). Overexpressing the FL CBX2 increased the H2AK119U levels resulting in a more intense band at 26 kDA when compared to the 26 kDA band of the pFLAG suggesting elevated PRC1 activity. Whereas, overexpressing the mutant CD CBX2 did not increase the levels of the H2AK119U modification resulting in a similar intensity band at 26 kDA to the pFLAG H2AK119U band. Other than for the N1 set of samples the alpha tubulin was similar across the rest of the samples indicating relatively equal amounts of protein were loaded. Densitometry analysis showed the FL CBX2 to significantly increase the H2AK119U histone modification compared to the pFLAG and CD deficient CBX2.

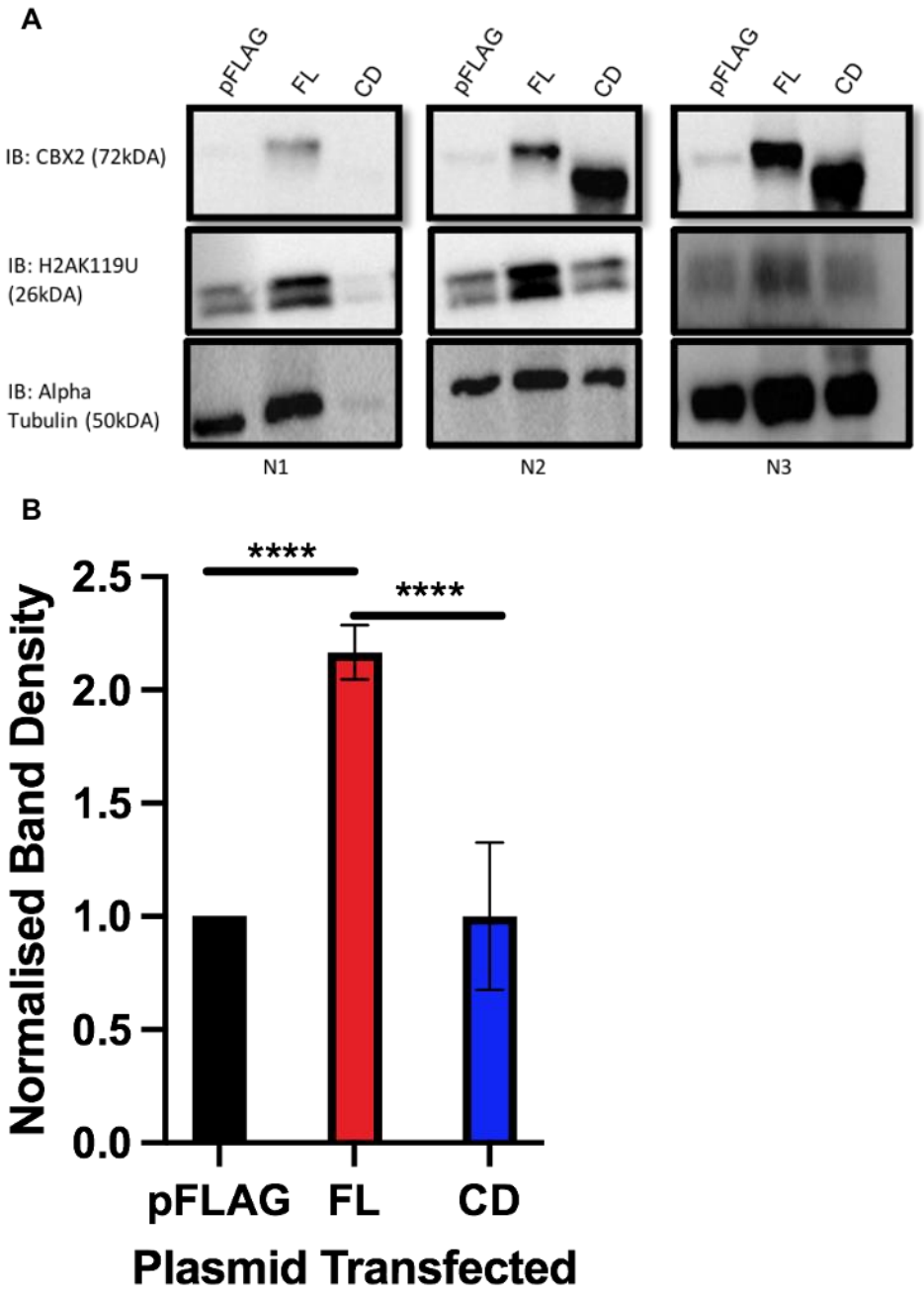

Figure 4. 9. A - Western blot depicting the effect of overexpressing the FL and CD mutant CBX2 on the global H2AK119U histone modification, experiment was repeated three times as represented in the figure. The plasmids transfected into the cells are specified at the top above the relevant lanes, specific antibodies used and the protein molecular weights are noted to the left of the blot. **B** - H2AK119U protein expression analysed by densitometry following 1 µg overexpression of the pFLAG, FL and CD plasmids in MDA-MB-231 cells. Data is the average of 4 replicates for the pFLAG and FL samples and 3 triplicates for the CD due to the alpha tubulin loading being inconsistent for one of the blots (**** = $p<0.0001$)

4.3.2 - Validating the CD CBX2 chromatin interaction being required for PRC1 complex activity

Overexpression of the FL CBX2 appeared to consistently increase the ubiquitination of H2AK119 but the CD mutant CBX2 did not, suggesting that the CD CBX2 chromatin interaction is required for PRC1 complex activity. To verify this the H2AK119U histone modification was assessed by western blot analysis following siRNA mediated CBX2 knockdown, to determine whether the FL and the mutant CD CBX2 could restore the H2AK119U histone modification to similar levels observed in the samples co-transfected with the non-silencing siRNA (Figure 4.10).

MDA-MB-231 cells were co-transfected with 250 ng of either the pFLAG, FL or the CD plasmid along with either a non-silencing CBX2 siRNA or a CBX2 targeting siRNA. CBX2 knockdown for the MDA-MB-468 cells was performed 24 hours prior to the plasmid transfection. Following the plasmid transfection both cell lines were incubated for 72 hours, with protein extracted subsequently which was then analysed by the western blot using antibodies specific for H2AK119U, CBX2 and alpha tubulin. The image was then semi-quantitatively analysed by densitometry using the ImageJ software.

The #3/#4-FL CBX2 managed to restore the monoubiquitination of H2AK119 to similar levels observed in the samples co-transfected with the plasmids and the non-silencing CBX2 siRNA in both cell lines. Whereas the H2AK119U band for the #3/#4-CD mutant CBX2 was less intense indicating a reduction in H2AK119U and thus the PRC1 complex activity. Alpha tubulin bands indicated the amount of protein present was not always equal particularly in Figure 4.10A and 4.10C. There was also difficulty in observing the CBX2 protein expression most likely due to transfecting only 250 ng of the plasmid CBX2 into the cells. Densitometry analysis complemented the result of the FL CBX2 restoring H2AK119U protein expression (Figure 4.11).

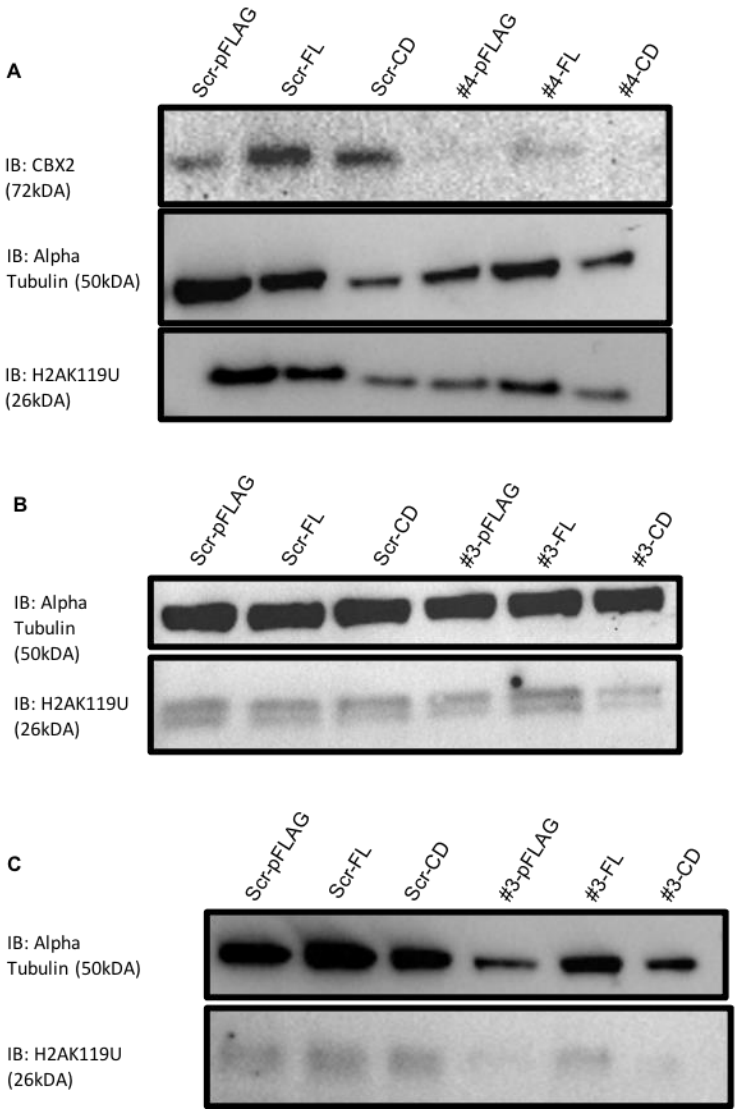

Figure 4. 10. Western blot showing the global H2AK119U histone modification following the co-transfection with 250 ng of the pFLAG, FL and CD plasmid and the non-silencing CBX2 siRNA or the CBX2 targeting siRNA in MDA-MB-231 cells (A and B) and MDA-MB-468 cells (C). The plasmids and siRNAs co-transfected into the cells are specified at the top above the relevant lanes, specific antibodies used and the protein molecular weights are noted to the left of the blot. N = 2 for blots B and C, N = 1 for blot A.

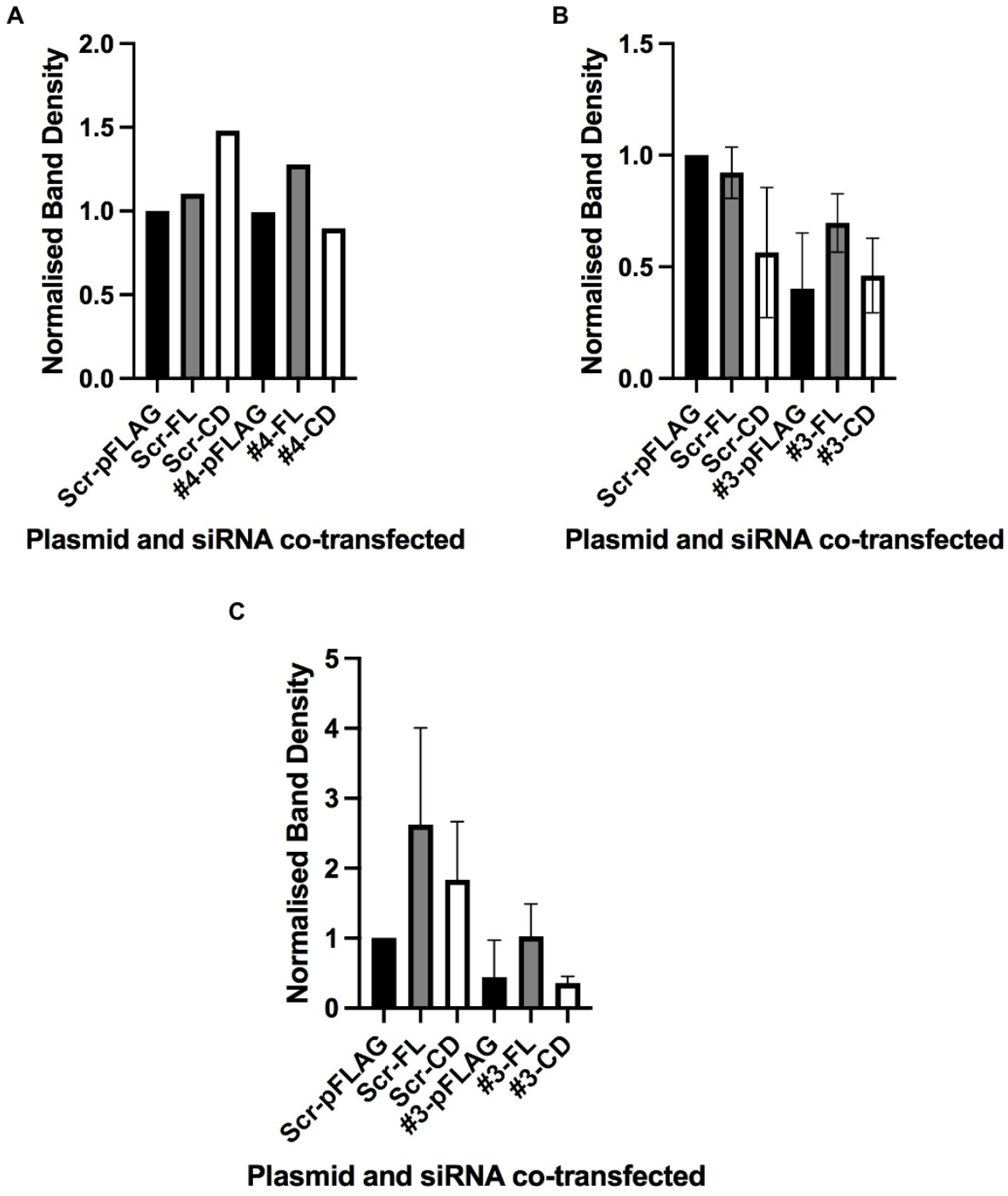

Figure 4. 11. H2AK119U protein expression analysed by densitometry following the plasmid and #3 (A and C) or #4 (B) siRNA co-transfection in MDA-MD-231 cells (A and B) and MDA-MB-468 cells (C). For B and C results are averages from two independent experiments.

4.3.3 - Further investigating the requirement of the CD chromatin interaction for the PRC1 complex activity by IF

To further support the CD CBX2 chromatin interaction being required for the catalytic activity of the PRC1 complex, the H2AK119U histone modification was also assessed by IF (Figure 4.12). MDA-MB-231 cells were seeded for 24 hours on glass coverslips and incubated for 72 hours after being co-transfected with the pFLAG, FL or the CD plasmid and a CBX2 targeting siRNA. Post the 72h hours the cells were fixed onto the coverslip and incubated in primary pFLAG and H2AK119U antibodies and subsequently in the secondary fluorescent green (pFLAG) and fluorescent red (H2AK119U) antibodies and counterstained with DAPI. The H2AK119U signal intensity of the siRNA and plasmid co-transfected cells was strikingly reduced when compared to the signal intensity of the negative control cells that were not transfected with neither the siRNA or plasmid. However, cells co-transfected with the #3-FL were found to have increased global H2AK119U indicated by a more intense red signal when compared to the #3-pFLAG and #3-CD co-transfected cells. Transient expression of the plasmid was detected using the pFLAG specific antibody suggesting that the small, intense green speckles in plasmid transfected cells was the plasmid tagged with the FLAG tag. These dots were not observed to be as clear in the negative control sample.

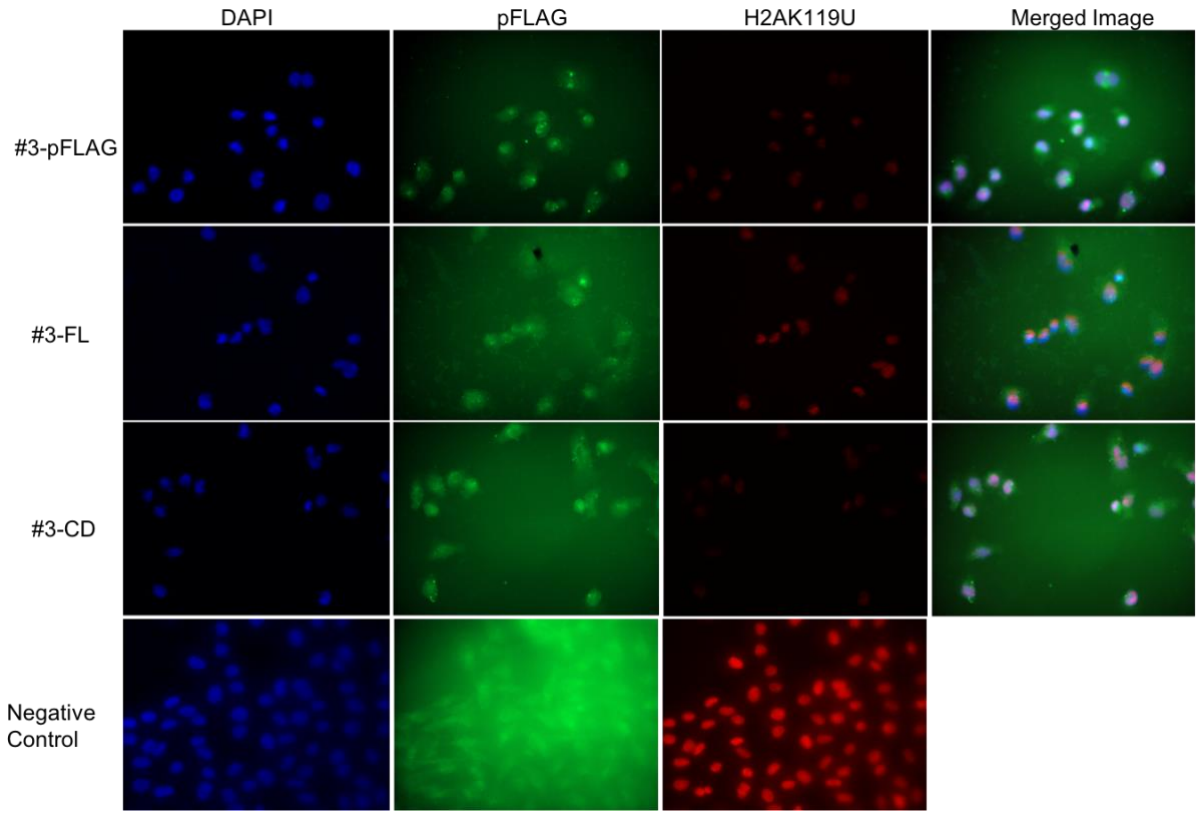

Figure 4. 12. Immunofluorescent images of MDA-MB-231 cells co-transfected with the 250 ng pFLAG, FL and CD plasmid and the CBX2 targeting #3 siRNA. The negative control cells were MDA-MB-231 cells fixed onto the coverslip not transfected with neither the siRNA or the plasmid. The pFLAG and H2AK119U were detected using primary pFLAG and H2AK119U antibodies that the complementary secondary fluorescent green (pFLAG) and red (H2AK119U) antibodies then bound to. Images are representative of the repeat experiment that showed a similar pattern in the H2AK119U red signal intensity. Co-transfection conditions are specified to the left of the images and what the images detected is stated above.

4.3.4 - SR and AR chromatin interactions effect on PRC1 complex activity

Since overexpression of the SR and AR mutant CBX2 did slightly increase the ubiquitination of H2AK119, it was required to investigate whether those mutant CBX2 proteins could restore H2AK119U levels following an siRNA mediated CBX2 knockdown. Thereby, determining whether the chromatin interactions of the SR region and the AR are required for PRC1 complex activity. The MDA-MB-231 cells were seeded for 24 hours and co-transfected with 250 ng of either the pFLAG, SR and AR plasmid and a non-silencing CBX2 siRNA or a CBX2 targeting siRNA. The cells were incubated for 72 hours post the plasmid and siRNA co-transfection. The protein was extracted and analysed by western blot using H2AK119U and alpha tubulin specific antibodies. Using the ImageJ software, the images were semi-quantitatively analysed by densitometry. The AR mutant CBX2 (#3-AR) did restore H2AK119U following CBX2 knockdown with the band at 26kDA being a similar intensity to the non-silencing siRNA and plasmid co-transfected samples. However, the SR mutant CBX2 did not with the H2AK119U band at 26kDA being less intense indicating a reduction in H2AK119U and subsequently the PRC1 complex activity. Densitometry analysis also found the SR mutant CBX2 not to be able to restore H2AK119U protein expression following siRNA mediated CBX2 knockdown. The alpha tubulin for the N2 samples was inconsistent but equal for the N1 set of samples.

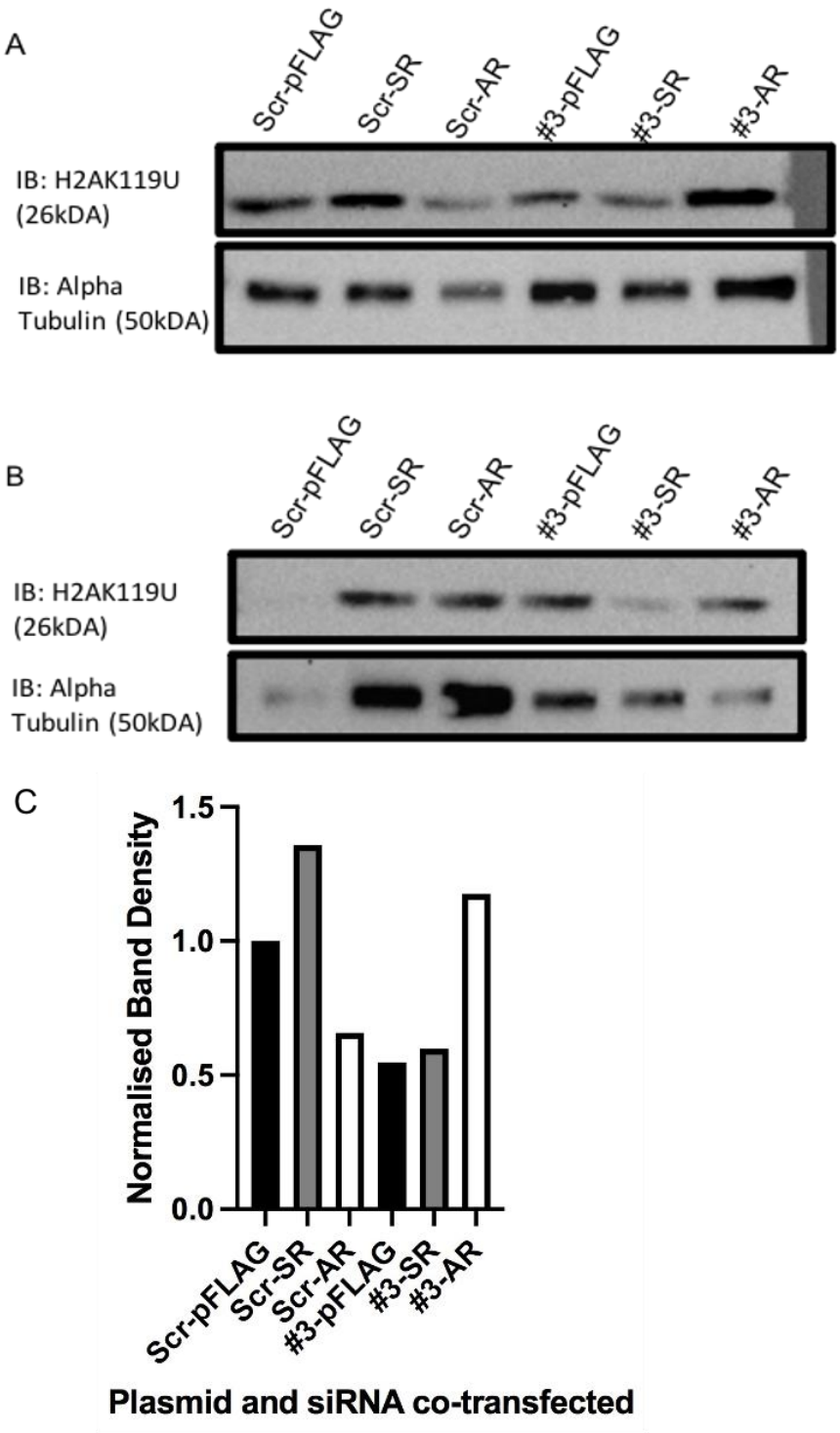

Figure 4. 13. A and B - Western blot showing the H2AK119U histone modification in MDA-MB-231 cells following the co-transfections with the pFLAG, SR and AR plasmids and the non-silencing CBX2 siRNA or the CBX2 targeting siRNA. The plasmids and siRNAs co-transfected into the cells are specified at the top above the relevant lanes, specific antibodies used and the protein molecular weights are noted to the left of the blot. **C** - H2AK119U protein expression in MDA-MB-231 cells analysed by densitometry for the western blot A image.

4.4.1 - CBX2 chromatin interactions effect on CBX2 target gene expression - RT-qPCR.

After demonstrating CBX2 chromatin interactions to be required for PRC1 complex activity by which CBX2 regulates the expression of its target genes, it was important to determine whether the impaired PRC1 complex activity had a consequent effect on the expression of an established CBX2 target gene. Previous work from the group has identified the *RBL2* tumour suppressor gene as a direct target gene that CBX2 represses in TNBC. Therefore, the need for CBX2 chromatin interactions for PRC1-mediated CBX2 gene regulation was investigated by qPCR which analysed the mRNA expression of *RBL2* following the overexpression of pFLAG, FL and the four mutant CBX2 plasmids (Figure 4.14).

The MDA-MB-231 cells were seeded for 24 hours, transfected with 1 µg of the CBX2 plasmid and then incubated for 72 hours. RNA that was extracted 72 hours post plasmid transfection and was reverse transcribed into cDNA which was then used to perform the qPCR. Primers for *RBL2, CBX2, RPL13A* (a normalising control gene) and *AURKA* (RBL2 target gene) were used to analyse the effect of overexpressing the FL and mutant CBX2 plasmids on the expression of both *CBX2* and its target gene *RBL2.* The average expression fold change results were analysed using a one-way ANOVA and Tukey's multiple comparisons test. For cells transfected with the FL and SR plasmids the CBX2 average expression fold change only slightly increased. Whereas, the CBX2 average expression fold change approximately doubled for the SA transfected cells, almost quadrupled for the AR transfected cells and increased 5-fold for the CD transfected cells (Figure 4.14 A). The *RBL2* expression fold change decreased for the FL, SR and AR plasmid transfected cells coincidentally, the *AURKA* expression fold change increased for the cells transfected with those three plasmids (Figure 4.14 B and C). Conversely for the SA and CD plasmid transfected cells the *RBL2* expression fold change had increased but the *AURKA* expression fold change for the SA and CD transfected cells also increased. Moreover, none of the results were found to be statistically significant.

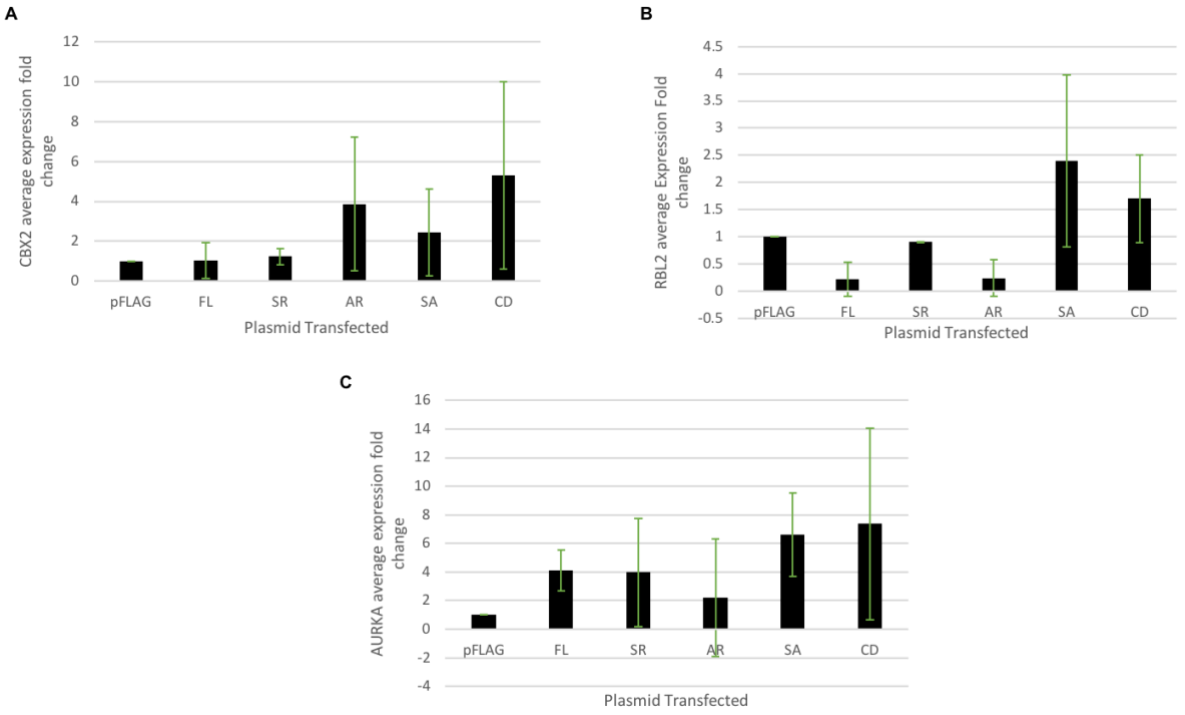

Figure 4. 14. Average mRNA expression fold change of CBX2 (A), RBL2 (B) and AURKA (C) in MDA-MB-231 cells following the overexpression of the six plasmids. Data is an average of two repeats ± SEM and expression fold change was standardised to the expression fold change of cells transfected with the pFLAG plasmid. Following analysis with Tukey's multiple comparisons test the differences observed in the expression fold change for CBX2, RBL2, and AURKA not significantly different ($p>0.05$).

4.4.2 CBX2 chromatin interactions effect on RBL2 protein expression

Next, the RBL2 protein expression was assessed following the overexpression of the pFLAG, FL and CD CBX2 plasmid, as it was the FL CBX2 and the CD mutant CBX2 that impacted the PRC1-mediated ubiquitination of H2AK119 the most at the protein level. MDA-MB-231 cells were seeded for 24 hours, then transfected with 1 μg of the plasmids and incubated for 72 hours. Protein was extracted and analysed by western blot using antibodies specific for CBX2, RBL2 and alpha tubulin (Figure 4.15A). The image was then semi-quantitatively analysed by densitometry using the ImageJ software (Figure 4.15B). The RBL2 band at 140 kDA was lost in cells overexpressed with the FL CBX2 compared to the cells transfected with the pFLAG plasmid suggesting enhanced PRC1 complex activity. Whereas, the RBL2 band for cells overexpressed with the CD mutant CBX2 was observed to be a similar intensity to the pFLAG transfected cells RBL2 band. The alpha tubulin band at 50 kDA for the three samples was similar indicating equal protein loading therefore the RBL2 protein expression was comparable. Although this was supported by the densitometry analysis this was only one experiment and repeat experiments are required.

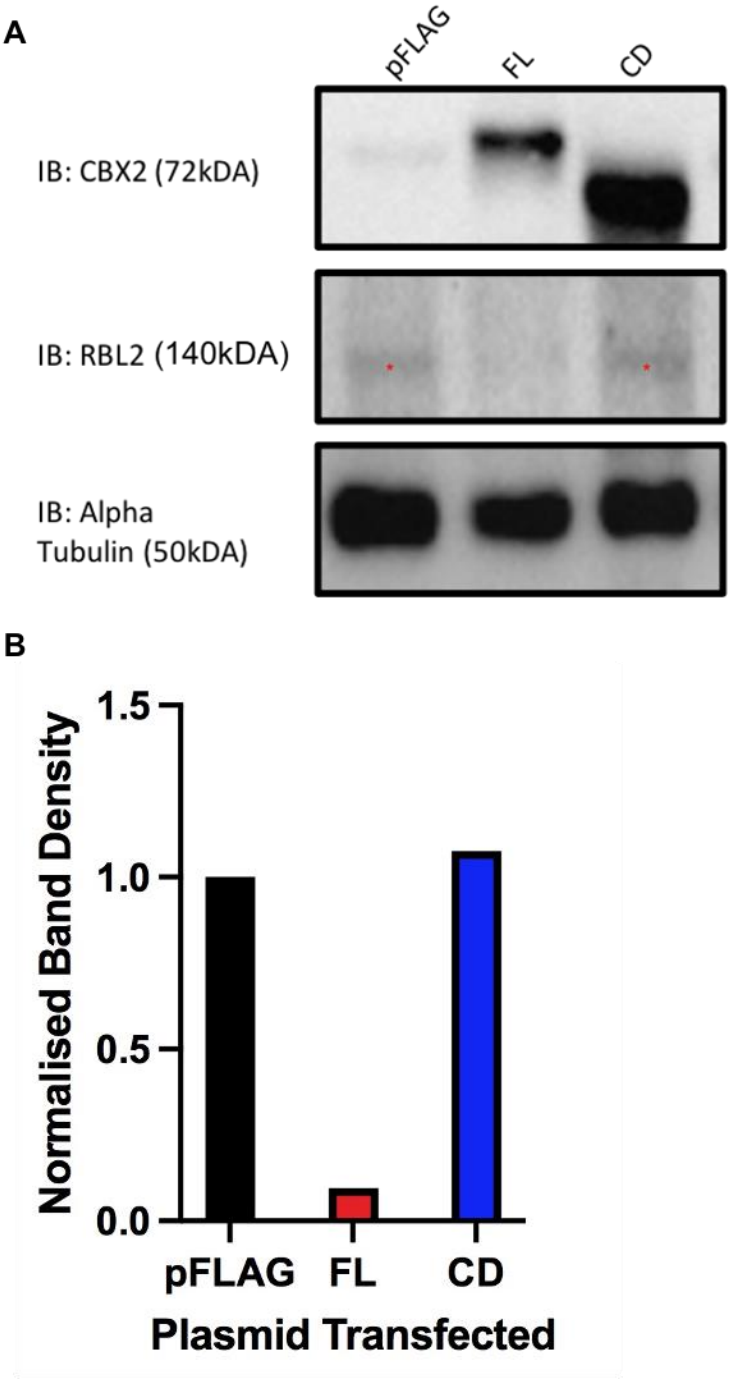

Figure 4. 15. A - Western blot probed for RBL2, CBX2 and alpha tubulin showing the effect of overexpressing the FL and CD mutant CBX2 on the RBL2 protein expression in MDA-MB-231 cells. The plasmids transfected into the cells are specified at the top above the relevant lanes, specific antibodies used and the protein molecular weights are noted to the left of the blot. N1 experiment therefore may need to be repeated. * = RBL2 protein expression at 140kDA. **B -** RBL2 protein expression in MDA-MB-231 cells analysed by densitometry following the 1 µg overexpression of the pFLAG, FL and CD plasmid.

4.4.3 - Validating the requirement of CBX2 chromatin interactions for CBX2 mediated RBL2 expression regulation.

In order to determine whether the FL or the CD mutant CBX2 could restore the transcriptional repression activity of the CBX2-PRC1 complex and reinforce the hypothesis that CBX2 chromatin interactions are required for CBX2 target gene regulation, the RBL2 protein expression was assessed following a siRNA mediated CBX2 knockdown and plasmid co-transfection. MDA-MB-231 cells were seeded for 24 hours and then co-transfected with 250 ng of either the pFLAG, FL and CD plasmid and a non-silencing CBX2 siRNA or a CBX2 targeting siRNA. After 72 hours protein was extracted and analysed by western blot using antibodies specific for alpha tubulin and RBL2 (Figure 4.16A). The RBL2 bands at 140 kDA appeared in the cells co-transfected with #3-pFLAG and #3-CD indicating an increase in RBL2 protein expression in those cells. Although bands are also present in the #3-FL co-transfected cells as well as the cells co-transfected with the non-silencing siRNA, those bands appear to be lower than the bands observed at 140 kDA in #3-pFLAG and #3-CD co-transfected cells. Suggesting that that is not RBL2 but non-specific antibody binding. A repeat of this experiment was done and a similar pattern was observed (figure 4.16B)

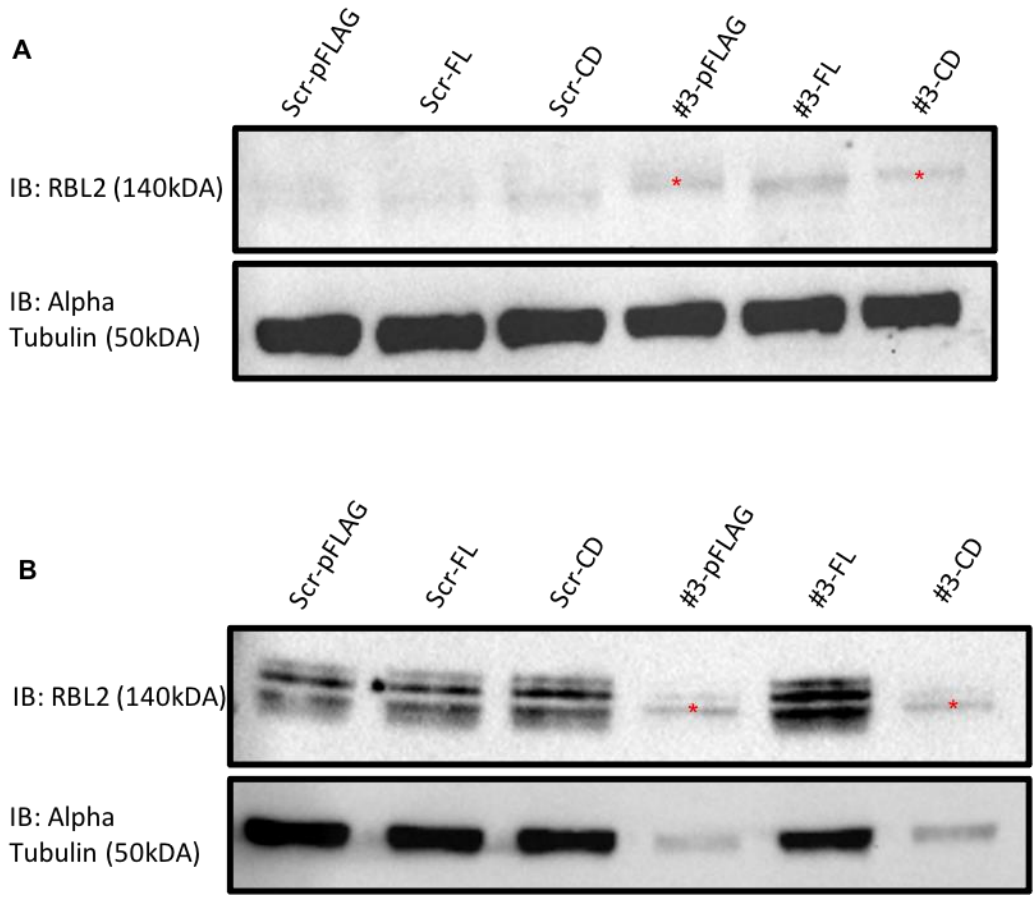

Figure 4. 16. Western blot representing RBL2 protein expression in MDA-MB-231 cells following the co-transfection with the pFLAG, FL and CD plasmid and the non-silencing siRNA or CBX2 targeting siRNA. The plasmids and siRNAs co-transfected into the cells are specified at the top above the relevant lanes, specific antibodies used and the protein molecular weights are noted to the left of the blot. Experiment was repeated (B) and a similar pattern in the RBL2 protein expression was observed. * = RBL2 protein expression at 140kDA

Chapter 5. Discussion

5.1 - CBX2 Chromatin Interactions and TNBC Cell Growth

Previous work from the laboratory highlighted the importance of CBX2 for TNBC cell growth with siRNA mediated CBX2 knockdown experiments reducing TNBC proliferation, and complementing the results of Zheng et al (2019) who found short hairpin RNA (shRNA) mediated CBX2 knockdown to also reduce TNBC cell growth (Bilton et al, 2022). This effect in TNBC correlates with studies that have shown CBX2 knockdown to have a similar effect on cell growth in other types of cancers such as prostate, glioma, liver and colon cancer (Clermont et al, 2016., Wang et al., 2021, Mao et al., 2019, Zhou et al., 2021). These studies have reinforced the relationship between CBX2's aberrant expression and activity to cancer progression and established CBX2 as a potential therapeutic target. However, the majority of those studies focused on knocking down the whole, multidomain CBX2 protein, instead of interrogating the structural motifs related to CBX2s chromatin interactions and thus, its epigenetic regulatory activity. Interrogation of the structural motifs would provide insight into the less extensively studied mechanistical and functional roles of CBX2 that could be exploited to improve potential strategies for therapeutically targeting CBX2 in the future (Simihadri et al, 2014).

The first aim of this study was to investigate the impact of overexpressing CBX2 and its structural motif deficient variants (Figure 5.1) on TNBC cell growth and which ectopically expressed CBX2 variants either augmented or diminished the endogenous CBX2 pro-proliferative effect in TNBC. The importance of the specific structural motifs was then validated by attempting to rescue the TNBC cell growth with the structural motif deficient variants following a siRNA mediated CBX2 knockdown.

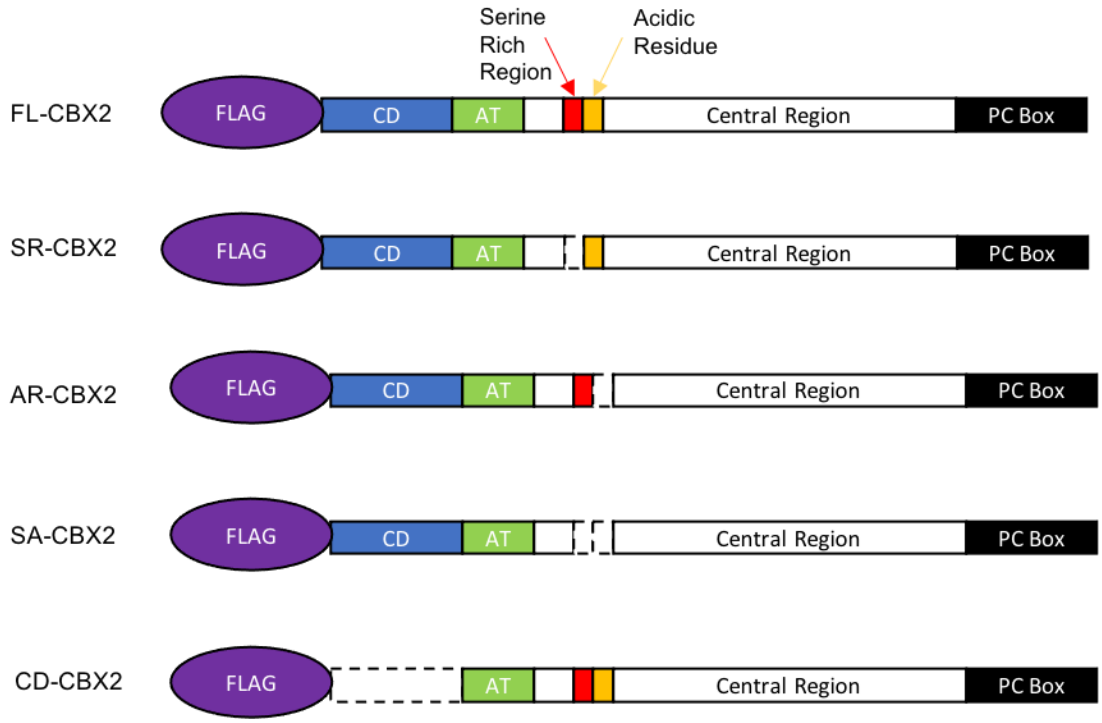

Figure 5. 1. Structural compositions of the FLAG tagged CBX2 plasmids used for transfection and co-transfection experiments.

After the MDA-MB-231 and MDA-MB-468 cells were transfected with the CBX2 plasmids it was observed that overexpressing FL CBX2 increased TNBC cell proliferation in both cell lines compared to the control pFLAG plasmid. A similar effect was observed by Wang et al (2021) who also found cell proliferation to be increased in LN224 glioma cells following CBX2 overexpression, suggesting CBX2 may be one of the key regulatory proteins driving cell proliferation in both TNBC and glioblastoma (GBM). Studies have shown CBX2 to regulate PI3K/AKT and mTORC oncogenic signalling pathways by suppressing inhibitors such as *PI3KR1* and *INPP5A* of the PI3K/AKT pathway and *PRKAA2* and *TSC1* of the mTORC pathway, as well as elevating the core drivers such as *PI3KCA, PI3KCD* and *GSK-3β* of the PI3K/AKT pathway and *p-mTOR* of the mTORC pathway and thus increasing cancer cell proliferation (Bilton et al, 2022., Wang et al, 2021 and Zheng et al, 2019). Additionally, CBX2 has been shown to accommodate for the increased energy demand of proliferating cancer cells by regulating the mTORC and PPAR signalling pathways to metabolically transform the cancer cells to sustain their proliferation (Hu et al, 2021., Iqbal et al, 2020). CBX2 mediated downregulation of *PPARG1*, a key regulator of the PPAR pathway, increases glutathione levels and the oxidation of pyruvate as well as decreases the levels of reactive oxygen

species (ROS) which biochemically adapts the cancer cells to increased cell proliferation (Srivastava et al, 2014). Moreover, the reduction in ROS levels further promotes cancer cell proliferation by upregulating anti-apoptotic factors and hyperphosphorylating the retinoblastoma protein (RB) which consequently inactivates RB resulting in cell cycle dysregulation (Arfin et al, 2021., Srivastava et al, 2014). Therefore, overexpression of FL CBX2 may have resulted in an upregulation of the above-mentioned oncogenic pathways which subsequently further facilitated the proliferation of TNBC cells.

Conversely, overexpressing the CD deficient CBX2 significantly reduced cell numbers in both MDA-MB-231 and MDA-MB-468 cell lines, suggesting that the chromatin interaction of the CD is required for regulating TNBC cell growth. This observation could potentially be due to a dominant negative effect, suggesting the overexpressed CD deficient CBX2 disrupts the activity of the normal, wildtype CBX2 within the cells. In the case of CBX2 this is most likely not due to the CD deficient CBX2 competing with the wildtype counterpart for the chromatin binding sites as, without the CD, the CBX2 is unable to bind to the H3K27me3 mark. Instead, this dominant negative effect may be due to the CD deficient CBX2 contesting the wildtype CBX2 for the protein subunits that constitute the PRC1 complex. Which upon formation with the CD deficient CBX2 is unable to function as it cannot bind to the chromatin and also prevents the wildtype CBX2 from forming the PRC1 complex hindering the wildtype CBX2s epigenetic regulatory function. This would also suggest that the PRC1 complex forms before the CBX2 binds to the chromatin while the currently accepted hypothesis for CBX2s mechanism of action is that the CBX2 binds to the H3K27me3 via the CD and then through its Pc Box recruits the rest of the components of the PRC1 complex (Hu et al, 2022).

To verify the importance of the CD chromatin interaction the FL and CD deficient CBX2 were introduced into the MDA-MB-231 cells along with two independent CBX2 targeting siRNAs (#3 and #4) and into MDA-MB-468 cells with one of the CBX2 targeting siRNAs (#3). In order to determine whether either of the CBX2s can rescue TNBC cell growth following the knockdown of the endogenous CBX2. In both cell lines the FL CBX2 was able to rescue TNBC cell growth and almost restore the cell number to the cell number observed in cells co-transfected with the CBX2 plasmids and non-silencing siRNAs. The CD deficient CBX2 was unable to rescue TNBC cell growth with the cell numbers found to be significantly reduced

when compared to the FL CBX2 rescue cells as well as compared to the cells co-transfected with the CBX2 plasmids and non-silencing siRNAs. Such results supplement the findings of Wang et al (2021) and Bilton et al (2022) who also targeted the CD chromatin interaction of CBX2 through the use of the recently developed CD-CBX2 inhibitor, SW2_15F, and also observed a reduction in proliferation in neuroendocrine prostate cancer and TNBC, respectively. Together these results imply that the loss of the CD chromatin interaction, by which CBX2 recognizes and localizes to the H3K27me3 mark, is responsible for CBX2s incompetence to effectively modulate and restore TNBC cell proliferation. Potentially due to CBX2 being unable to regulate the previously mentioned oncogenic signalling pathways that drive cancer cell proliferation without the CDs chromatin interaction.

Propidium iodide flow cytometry analysis revealed an increase in the percentage of MDA-MB-231 cells in the sub-G1 phase of the cell cycle following the co-transfection with the CBX2 targeting siRNA and the CD deficient CBX2, which is associated with increased cell apoptosis. This pattern was also observed in the cells co-transfected with the pFLAG plasmid and the CBX2 targeting siRNA but not in the cells rescued by the FL CBX2 suggesting that the fully functional CBX2 downregulates apoptosis in TNBC. With previous work from the laboratory also showing an increase in the percentage of TNBC cells in the sub-G1 phase following CBX2 knockdown (Bilton et al, 2022). The increase in apoptosis may be due to the CD deficient CBX2 being unable to upregulate the mTORC1 and E2F signalling pathways which have been shown to be downregulated following CBX2 knockdown (Bilton et al, 2022). mTORC1 signalling has been shown to inhibit apoptosis by downregulating GSK-3 preventing the caspase-3 apoptotic signalling cascade from activating, as well as upregulating antiapoptotic proteins such as BCL-2 (Zhou et al, 2020., Yan et al, 2021). Downregulation of the E2F signalling may also increase apoptosis by increasing ROS levels which is known for initiating apoptosis (Rouaud et al, 2018). Although mTORC1 is a downstream target of the PI3K/AKT signalling pathway this pathway was not identified to be significantly affected by CBX2 knockdown in TNBC even though it has been shown to be regulated by CBX2 in prostate cancer and GBM (Bilton et al, 2022). The PI3K/AKT signalling pathway is also known to block the apoptosis of cells by triggering the X-linked apoptosis protein (XIAP) to inhibit the activity of caspase-3 (Liu et al, 2020., Wang et al, 2021). Moreover, CBX2 has also been shown to directly regulate apoptosis with CBX2 knockdown

experiments found to increase the pro-apoptotic activity of caspase-8 in leukaemia cells, increase the phosphorylation and subsequent inactivation of the *YAP* oncogene that allows liver cancer cells to resist apoptosis, as well as triggering anoikis which is a different form of programmed cell death characterized by the detachment of cells from the ECM in ovarian cancer (Del Gaudio et al, 2022., Mao et al., 2019., Wheeler et al, 2018).

Together the cell count data following the overexpression and rescue experiments, as well as the propidium iodide flow cytometry analysis, potentially indicate that without the CD chromatin interaction which reads and recruits CBX2 to the H3K27me3 the CBX2 is no longer able to suppress apoptosis nor upregulate the oncogenic pathways that drive TNBC proliferation. However, the propidium iodide flow cytometry experiments should be repeated as they were only done once due to the machine breaking down after the first experiment. Experiments such as the MTS assay that quantifies the number of viable cells, could also be conducted in the future to further assess the requirement of the CD chromatin interaction for cell viability and proliferation. Additionally, to confirm cells containing the CD deficient CBX2 undergo apoptosis luminescent assays that measure the activity of the protein cleaving caspase 3 and 7 could also be performed, along with protein expression analysis by western blot of the cleaved PARP-1. Since PARP-1 cleavage is mediated by the two previously mentioned caspases and is widely considered to be an established hallmark of apoptosis. Alternatively, annexin V immunofluorescent staining could also be performed to detect cells undergoing apoptosis by the fluorescently tagged annexin V binding to the phosphatidylserine of the inner cell membrane which is exposed to the outside, in cells undergoing apoptosis (Crowley et al, 2016).

Overexpression of the SR, AR and SA deficient CBX2 had minimal effect on TNBC cell proliferation in MDA-MB-231 cells hinting that the chromatin interactions of those structural motifs are also required for TNBC cell growth, since their overexpression did not elevate cell proliferation. In the MDA-MB-468 cell line overexpression of the SR and SA deficient CBX2 had a bigger impact on the TNBC cell growth as they significantly reduced the TNBC cell proliferation. To further investigate the chromatin interactions of the SR region and AR cluster the SR and AR deficient CBX2 was co-transfected into MDA-MB-231 cells with a CBX2 targeting siRNA (#3). Unexpectedly, both the SR and AR deficient CBX2 managed to rescue TNBC cell growth with the rescue by the SR mutant CBX2 particularly interesting as

the SR region has been shown to be a major phosphorylation site of CBX2 and the phosphorylated CBX2 was hypothesized to be required for CBX2 activity (Kawaguchi et al, 2017). Therefore, it was expected the SR deficient CBX2 would not rescue TNBC cell growth. The rescue of TNBC cell growth by the SR deficient CBX2 may be due to the SR region not being the only phosphorylation site of CBX2, with studies showing that the serine 42 residue found within the CD of CBX2 to also be phosphorylated, which additionally increases CBX2s affinity for the H3K27me3 mark (Hatano et al, 2010). Although, the serine 42 residue within the CD of CBX2 is a minor phosphorylation site when compared to the whole SR region, perhaps its phosphorylation is sufficient to activate CBX2, which is then able to regulate TNBC cell proliferation as it possesses the CD. Experiments using shrimp alkaline phosphatase, which dephosphorylates proteins, to investigate whether the SR deficient CBX2 is still being stably phosphorylated would provide additional insight into the requirement of the SR region for CBX2 activation. Moreover, the rescue experiments for the SR deficient CBX2 could also be expanded to other cell lines such as the MDA-MB-468 cells, since its overexpression in those cells significantly reduced their growth. This was not done in this study due to time constraints.

The rescue of TNBC cell growth by the AR deficient CBX2 suggests that the chromatin interaction of the AR cluster is also not necessary for CBX2 functionality in regulating TNBC cell proliferation. However, the exact function of the AR cluster in relation to CBX2 chromatin interaction and activity is unclear. Some studies have hypothesised that the electrostatic interactions between the AR cluster and the neighbouring SR region results in further phosphorylation of additional upstream serine residues, whereas others speculate that the AR cluster located between basic residues helps fix CBX2 into position on the nucleosome as it also consists of acidic (DNA) and basic (histone proteins) components (Tatovosian et al, 2019., Kawaguchi et al, 2017).

5.2 - CBX2 Chromatin Interactions and PRC1 Complex Activity

Next, it was required to investigate the importance of the CBX2 chromatin interactions on PRC1 mediated H2AK119 ubiquitination, by which, CBX2 represses the transcription of its target genes. Thus, determining whether CBX2 chromatin interactions are required for the catalytic activity of the PRC1 complex. CBX2 and its variants were overexpressed in MDA-MB-231 cells and the H2AK119U histone modification was analysed by western blot, which was then quantified by densitometry. It was observed that overexpressing the cells with the FL CBX2 increased the H2AK119U histone modification when compared to the H2AK119U levels of the cells transfected with the pFLAG plasmid. This effect was expected since increasing CBX2 levels most likely increased the amount of CBX2-associated PRC1 complexes resulting in the observed increase of the H2AK119U histone modification. However, overexpression of the CD deficient CBX2 did not increase the H2AK119U histone modification suggesting that the CD CBX2 chromatin interaction that recognizes the H3K27me3 histone modification is required for the PRC1 complex activity. To further investigate the relationship between the chromatin interaction of the CD of CBX2 and the PRC1 complex activity, the FL CBX2 and CD deficient CBX2 were co-transfected into MDA-MB-231 cells with two independent CBX2 targeting siRNAs (#3 and #4) and into MDA-MB-468 cells with one of the CBX2 targeting siRNAs (#3). The H2AK119U histone modification was analysed by western blot to investigate whether either version of CBX2 could restore the H2AK119U histone modification following CBX2 knockdown. In both cell lines the FL CBX2 was able to rescue the H2AK119U histone modification to similar levels observed in the cells co-transfected with the non-targeting siRNA and plasmid, whereas the CD deficient CBX2 was unable to restore the H2AK119U histone modification to such levels. To further investigate the requirement of the CD chromatin interaction for the PRC1 complex activity the H2AK119U histone modification was analysed by immunofluorescence (IF). MDA-MB-231 cells were co-transfected with a CBX2 targeting siRNA (#3) and a pFLAG, FL or a CD plasmid and then probed with a primary pFLAG antibody to detect the plasmid transfected FLAG-tagged CBX2 which was stained with a green fluorescent secondary antibody. The cells were also probed with a H2AK119U primary antibody to detect the H2AK119U histone modification which was stained with a red fluorescent secondary antibody. The FLAG tagged CBX2 was believed to be the small bright green speckles observed within the cells, corresponding to the IF images of Tatavosian et al (2019), who assessed Halo-tagged CBX2

constructs in PGK12.1 mouse embryonic stem cells. The intensity of the red signal which corresponded to the H2AK119U histone modification was more intense for the cells rescued by the FL CBX2 compared to the H2AK119U red signal intensity of the cells co-transfected with the CBX2 targeting siRNA and the CD deficient CBX2 or the pFLAG. However, unlike the western blot results the H2AK119U histone modification rescued by the FL CBX2 was not restored to similar levels observed in the negative control sample (which was untransfected MDA-MB-231 cells). In summary, overexpression of the CD deficient CBX2 did not elevate the H2AK119U histone modification like the overexpression of the FL CBX2 did. Moreover, the CD deficient CBX2 was unable to restore the H2AK119U histone modification following CBX2 knockdown which was observed by western blot and IF. This suggests that without the CD chromatin interaction the CBX2 is unable to recognize, bind and subsequently recruit the PRC1 complex to the H3K27me3 resulting in a reduction in the H2AK119U histone modification.

Overexpression of the SR and AR deficient CBX2 did not increase the H2AK119U histone modification following western blot analysis. Suggesting the chromatin interactions of those two regions may be required for the PRC1 complex activity. Therefore, to further investigate these chromatin interactions in relation to the PRC1 complex activity the H2AK119U histone modification was assessed by western blot following the co-transfection of the SR and AR mutant CBX2 with a CBX2 targeting siRNA (#3) into MDA-MB-231 cells. Similarly, to the FL CBX2 the AR deficient CBX2 appeared to rescue and restore the H2AK119U histone modification to similar levels observed in the sample co-transfected with the plasmids and the non-silencing siRNA. Suggesting that the CBX2 is able to bind to chromatin and recruit the PRC1 complex without the speculative chromatin interaction of the AR cluster. Whereas, the SR deficient CBX2 appeared to be unable to rescue and restore the H2AK119U histone modification with the densitometry analysis of the protein band density being similar to the band density of the cells co-transfected with the CBX2 targeting siRNA (#3) and the pFLAG plasmid. This suggests that the SR region is required for chromatin interaction of the PRC1 complex and its subsequent ubiquitination activity. This result correlates to the findings of Kawaguchi et al (2017) who found the SR deficient CBX2 unable to restore the transcriptional repression of its target gene, *p21*, following CBX2 knockdown. Considering CBX2 regulates the transcription of its target genes by the PRC1 complex mediated

ubiquitination of H2AK119, it can be assumed that the SR deficient CBX2s inability to repress *p21* is a result of a reduction in the PRC1 complex activity.

As mentioned previously, the SR region is a major phosphorylation site of CBX2 which was linked to CBX2 activation. Its phosphorylation is also associated with increasing the nucleosome binding specificity of CBX2 by promoting the CD mediated chromatin binding over the AT-hooks DNA binding ability (Kawaguchi et al, 2017). Therefore, the lack of phosphorylation of the SR region may result in no increase in the nucleosome binding specificity of CBX2. Therefore, the CBX2 does not bind to the H3K27me3 and recruit the PRC1 complex as efficiently resulting in a reduction in the H2AK119U histone modification. Alternatively, without the SR region the CBX2 may be unable to phase separate into condensates in which CBX2 compartmentalizes the repression of its target genes located in distal chromatin regions. These condensates are able to localize on unmodified chromatin via the AT hook, with the HPH and RING protein of PRC1 being incorporated into these condensates to form a trimeric complex (Kent et al, 2020). The distal chromatin regions marked with H3K27me3 are then recruited into these condensates by CBX7 and CBX8 associated PRC1 complexes where they are condensed by the CBX2-HPH-RING trimeric complex (Tatovosian et al, 2019). Studies have highlighted the importance of the SR region to CBX2s ability to phase separate, with experiments mutating or deleting the SR region diminishing the formation of CBX2 condensates (Plys et al, 2019). Therefore, the SR deficient CBX2 may be unable to phase separate into condensates where it would ubiquitinate H2AK119 of distal chromatin regions resulting in a reduction in H2AK119U. Potentially these distal chromatin regions are not associated with genes regulating cell proliferation, hence the observed rescue of TNBC cell growth but not of the PRC1 complex activity by the SR deficient CBX2.

Interestingly, overexpression of the SA deficient CBX2 which lacks both the SR region and the AR cluster increased the H2AK119U histone modification. Since overexpression of the individual SR and AR deficient CBX2 decreased the H2AK119U histone modification it was expected that the loss of both of those regions would result in a greater reduction in the H2AK119U histone modification. Although, this was a singular experiment it correlates to the findings of Kawaguchi et al (2017) who found the SA deficient CBX2 to be able to partially restore the repression of the *p21* target gene, which suggests a rescue of the PRC1

complex activity by the SA deficient CBX2. Perhaps the loss of the electrostatic interactions between the SR region and the AR cluster results in a change in the overall structural charge of CBX2 helping it to stabilize on the chromatin more readily, or, it may reduce the inter/intramolecular interaction between the CD and the DNA binding AT hook to promote the CD mediated nucleosome binding.

5.3 - CBX2 Chromatin Interactions and CBX2 target gene regulation

The requirement of CBX2 chromatin interactions for CBX2 target gene expression regulation was investigated to determine whether the chromatin interactions which affected the activity of the PRC1 complex would consequently affect the expression of an established CBX2 target gene. As previous work in the laboratory identified *RBL2* to be a direct target gene of CBX2 in TNBC, the mRNA levels of *CBX2*, *RBL2* and *AURKA* (which is a gene downregulated by RBL2) were all investigated by qPCR following the overexpression of CBX2 and its variants in MDA-MB-231 cells (Bilton et al, 2022). It was observed that overexpression with the FL and SR deficient CBX2 only slightly increased CBX2 mRNA levels compared to the overexpression of the AR, SA and CD deficient CBX2, with a reason for this effect remaining unknown as the protein expression of CBX2 and its variants was consistently shown to be overexpressed to similar levels by western blot analysis.

However, the FL and SR deficient CBX2 along with the AR deficient CBX2 were able to repress *RBL2* resulting in a reduction in the mRNA expression fold change of *RBL2* which then as expected increased the expression fold change of *AURKA.* This suggests that the chromatin interactions of the SR region and AR cluster are not required for CBX2 mediated target gene regulation. Whereas overexpression of the CD and SA deficient CBX2 increased the expression fold change of RBL2 potentially due to the dominant negative effect, with the SA deficient CBX2 again having opposing effects to the individual SR and AR deficient CBX2. However, none of the results were found to be statistically significant therefore the changes observed in the *RBL2* and *AURKA* mRNA expression fold changes are interpreted as patterns and trends. Moreover, at the time of these experiments there were ongoing issues with the qPCR machine, therefore, the protein expression of RBL2 was investigated by western blot.

RBL2 protein expression was investigated following the overexpression of only the pFLAG, FL and CD deficient CBX2 in MDA-MB-231 cells, as the FL and CD deficient CBX2 were shown to affect the PRC1 complex activity most reliably. The RBL2 protein band almost completely

disappeared following the overexpression of the FL CBX2 with densitometry analysis revealing a 10-fold reduction in the RBL2 band density compared to the cells transfected with pFLAG. Which suggests increasing the expression of CBX2 results in an increase in CBX2 associated PRC1 complex which further downregulates RBL2. The CD deficient CBX2 on the other hand, was unable to further downregulate RBL2 resulting in almost no change in the RBL2 band densities between the cells transfected with the pFLAG and the CD deficient CBX2. This suggests that the chromatin interaction of CD may be required for regulating the expression of CBX2 target genes. To further investigate the requirement of the CD chromatin interaction for CBX2 target gene regulation, the RBL2 protein expression was analysed by western blot following the co-transfection of the pFLAG, FL and CD deficient CBX2 along with a non-silencing siRNA or a CBX2 targeting siRNA (#3) into MDA-MB-231 cells. An increase in the RBL2 protein expression was observed for CBX2 knockdown and rescue by the pFLAG and CD deficient CBX2 cells, but not in the non-knockdown cells or cells rescued by the FL CBX2. Although a band for the latter samples did appear, it was lower down compared to the band observed in #3-pFLAG and #3-CD suggesting potential non-specific binding of the antibodies. Restoration of the repression of RBL2 following CBX2 knockdown by the FL CBX2 but not by the CD deficient CBX2 suggests the recognition of the H3K27me3 by the CD may be required for the PRC1 complex activity to effectively repress its target genes.

RBL2, also known as p130, is a tumour suppressor gene part of the pocket family protein that along with E2F4, MuvB and DP constitute the DREAM complex, which coordinates cell cycle transitions and checkpoints by regulating cell cycle associated genes (Schade et al, 2019). RBL2 is mainly associated with the DREAM complex during the G0 and G1 stages of the cell cycle indicating RBL2 to play a role in regulating the G0/G1 cell cycle transition, where cells re-enter the cell cycle from their quiescent state (Tedesco et al, 2002). Our propidium iodide flow cytometry analysis illustrated a reduction in the % of cells in the G1 phase following the co-transfection with the CBX2 targeting siRNA and the pFLAG or the CD deficient CBX2. Potentially suggesting the CD deficient CBX2 being unable to repress RBL2 results in the restoration of the G0/G1 cell cycle checkpoint and the consequent reduction in % of cells being able to enter the G1 phase of the cell cycle. Conversely, since the FL CBX2 is able to restore the repression of RBL2 there is a loss of the G0/G1 cell cycle checkpoint

resulting in the TNBC cells being able to bypass quiescence and re-enter the cell cycle at the G1 phase. Moreover, the direct target gene RBL2 represses, *AURKA*, has been shown to prevent cells from entering the S phase of the cell cycle (Jantscher et al, 2011). With our propidium flow cytometry analysis demonstrating an increase in the percentage of cells in the S phase in cells co-transfected with the CBX2 targeting siRNA and the pFLAG or the CD deficient CBX2 but not the FL CBX2. Perhaps since the CD deficient CBX2 is unable to repress RBL2, it allows the RBL2 to downregulate AURKA resulting in the cells being able to enter the S phase of the cell cycle. Whereas, the FL CBX2 which represses RBL2 prevents the downregulation of AURKA which subsequently blocks the entry of cells into the S phase. Additionally, AURKA has been shown to phosphorylate p53 which promotes its MDM2 mediated ubiquitination and subsequent proteolysis, preventing the activation of pro-apoptotic proteins such as PUMA, NOXA and BAD, which facilitate apoptosis (Kutayama et al, 2013., Chen et al, 2011). Propidium iodide flow cytometry analysis showed an increase in the percentage of cells in the sub G1 phase which is associated with apoptosis in cells co-transfected with CBX2 targeting siRNA and the pFLAG or the CD deficient CBX2. Therefore, the upregulation of RBL2 due to the CD deficient CBX2 being unable to successfully repress RBL2, potentially results in the downregulation of AURKA preventing p53 degradation which is then able to induce apoptosis (Figure 5.2).

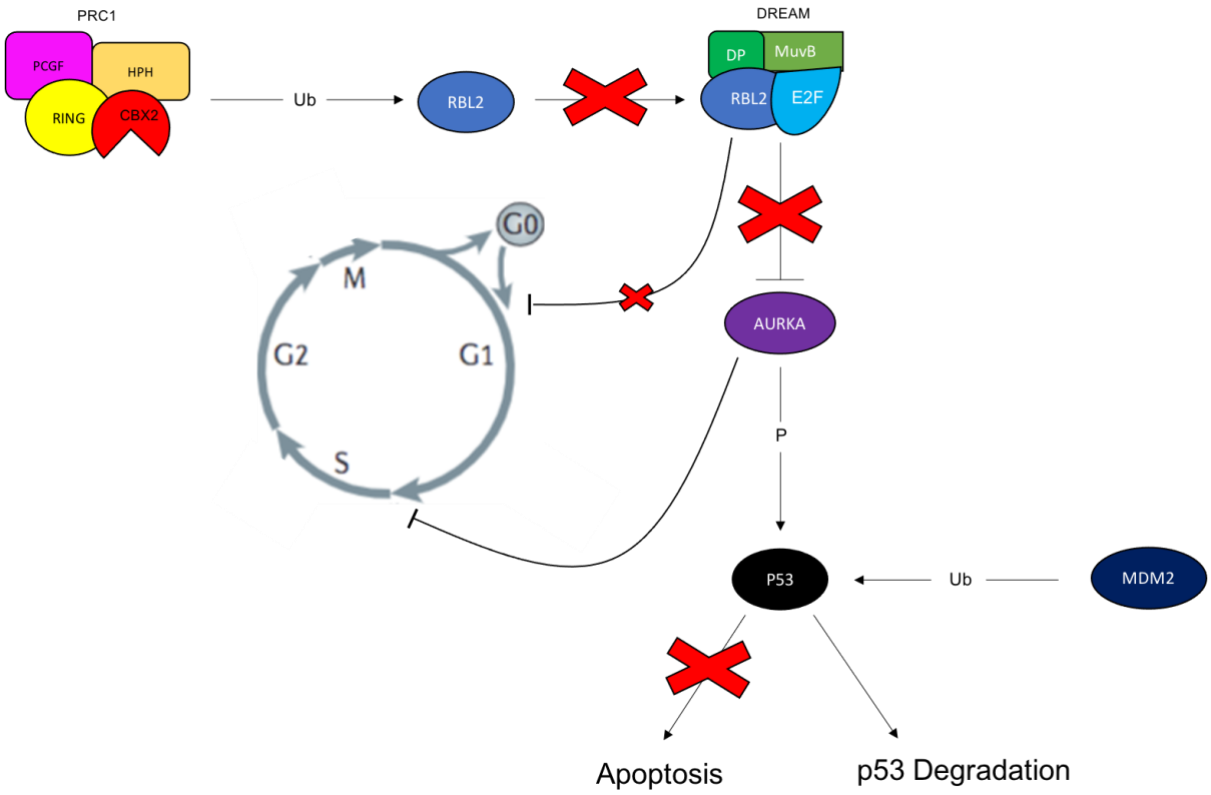

Figure 5. 2. Potential downstream effect of CBX2 repressing RBL2. The FL CBX2 represses RBL2 via the monoubiquitination activity of the PRC1 complex preventing the formation of the DREAM complex resulting in the loss of the G0/G1 checkpoint and upregulation of AURKA. AURKA prevents cells from entering the S phase of the cell cycle and phosphorylates p53 promoting its Mdm2 mediated ubiquitination and subsequent degradation inhibiting apoptosis.

The finding of the CD chromatin interaction being required for CBX2 target gene regulation in this study complements the findings of Wang et al (2021), who by inhibiting the CD chromatin interaction through the use of the CD antagonizing CBX2 specific inhibitor demonstrated a significant increase in the expression of two specific androgen receptor genes, *TMPRSS2* and *KLK3,* which are typically significantly downregulated in neuroendocrine prostate cancer. Moreover, Kawaguchi et al (2017) also found the CD deficient CBX2 to be unable to rescue the transcriptional repression of *p21* following CBX2 knockdown, further highlighting the importance of CD chromatin interaction for CBX2 target gene regulation. Additional experiments such as chromatin immunoprecipitation (ChIP) analysis of the CD deficient CBX2 could determine whether the CBX2 is able to localize at the promoter regions of its target genes without the CD. Moreover, since the SR deficient CBX2

was unable to restore the H2AK119U histone modification, it too could be investigated for CBX2 target gene regulation.

5.4 - Conclusion and future perspectives

In conclusion, the findings of this study highlight the importance of the CDs chromatin interaction for CBX2 to moderate TNBC cell growth, the catalytic activity of the CBX2 associated PRC1 complex and CBX2 target gene regulation. Advocating for the CD of CBX2 to be pharmacologically targeted in the future especially considering the past success of reducing cancer growth by targeting the reader domains of other epigenetic regulatory proteins such as: the bromodomains of the acetyl lysine reader BRD4, the tudor domain of the arginine methylation reader TDRD3, and the CD of the methyl lysine reader CBX7 (Sahni and Keri, 2019., Morettin et al, 2017., Wang et al., 2021).

In order to further validate targeting the CD of CBX2 as a viable therapeutic strategy these experiments should be repeated in additional TNBC cell lines, another subtype of breast cancer and even other types of cancers. The recently developed CD-CBX2 inhibitor could also be pivotal in demonstrating that it is specifically the chromatin interaction of the CD that is crucial for CBX2 functionality, by repeating the rescue experiments performed in this study but using the inhibitor as an alternative to knocking down the CBX2 with siRNAs. However, further research should not neglect the other structural motifs of CBX2 with the chromatin interaction of the SR region requiring further investigation, as it was shown to be potentially important for the catalytic activity of the PRC1 complex. Further research is also required to identify the exact role of the AR cluster. The chromatin interaction of the AT-hook, not investigated in this study, should also be explored as it has been shown to promote promiscuous binding of CBX2 to chromatin. This potentially suggests that CBX2 may not be limited to regulating genes tagged with the H3K27me3 mark, and thus, may not exclusively be a transcriptional repressor. With some studies showcasing CBX2 to activate transcription by associating with JDMJ3 to demethylate H3K27me3 (Sun et al, 2019). Affirming these other structural motifs to not be crucial to CBX2 and that targeting the CD alone nullifies the chromatin interactions of CBX2 to a degree that impairs its ability to function, will dispel concerns of whether targeting only the CD will be enough to inhibit CBX2.

Chapter 6. References

Andrikopoulou, A., Liontos, M., Koutsoukos, K., Dimopoulos, M. A., & Zagouri, F. (2020). The emerging role of BET inhibitors in breast cancer. *Breast (Edinburgh, Scotland)*, *53*, 152–163.

Arfin, S., Jha, N. K., Jha, S. K., Kesari, K. K., Ruokolainen, J., Roychoudhury, S., Rathi, B., Kumar, D. (2021). Oxidative stress in cancer cell metabolism. *Antioxidants*, *10*(5), 642.

Arnold, M., Morgan, E., Rumgay, H., Mafra, A., Singh, D., Laversanne, M., Vignat, J., Gralow, J., Cardoso, F., Siesling, S., Soerjomataram, I. (2022). Current and future burden of breast cancer: Global statistics for 2020 and 2040. *The Breast*, *66*, 15-23.

Aysola, K., Desai, A., Welch, C., Xu, J., Qin, Y., Reddy, V., Matthews, R., Owens, C., Okoli, J., Beech,D., Piyathilake, C., Reddy, S., Rao, V. N. (2013). Triple negative breast cancer–an overview. *Hereditary genetics: current research*, *2013*(Suppl 2).

Bannister, A. J., & Kouzarides, T. (2011). Regulation of chromatin by histone modifications. *Cell research*, *21*(3), 381–395.

Bernard, D., Martinez-Leal, J.F., Rizzo, S., Martinez, D., Hudson, D., Visakorpi, T., Peters, G., Carnero, A., Beach, D. and Gil, J., 2005. CBX7 controls the growth of normal and tumor-derived prostate cells by repressing the Ink4a/Arf locus. *Oncogene*, *24*(36), 5543-5551.

Bilton, L. J., Warren, C., Humphries, R. M., Kalsi, S., Waters, E., Francis, T., Dobrowinski, W., Beltran-Alvarez, P., Wade, M. A. (2022). The Epigenetic Regulatory Protein CBX2 Promotes mTORC1 Signalling and Inhibits DREAM Complex Activity to Drive Breast Cancer Cell Growth. *Cancers*, *14*(14), 3491.

Brockers K, Schneider R. (2019) Histone H1, the forgotten histone. *Epigenomics.* (4):363-366

Brown, K., Andrianakos, H., Ingersoll, S. and Ren, X., 2021. Single-molecule imaging of epigenetic complexes in living cells: insights from studies on Polycomb group proteins. *Nucleic Acids Research*, *49*(12), 6621-6637.

Buocikova, V., Rios-Mondragon, I., Pilalis, E., Chatziioannou, A., Miklikova, S., Mego, M., Pajuste, K., Rucins, M., Yamani, N. E., Longhin, E. M., Sobolev, A., Freixanet, M., Puntes, V., Plotniece, A., Dusinska, M., Cimpan, M. R., Gabelova, A., & Smolkova, B. (2020). Epigenetics in Breast Cancer Therapy-New Strategies and Future Nanomedicine Perspectives. *Cancers*, *12*(12), 3622.

Canzio, D., Larson, A. and Narlikar, G.J., 2014. Mechanisms of functional promiscuity by HP1 proteins. *Trends in cell biology*, *24*(6),377-386.

Chen, J. (2016). The cell-cycle arrest and apoptotic functions of p53 in tumor initiation and progression. *Cold Spring Harbor perspectives in medicine*, *6*(3), a026104.

Chen, W.Y., Zhang, X.Y., Liu, T., Liu, Y., Zhao, Y.S. and Pang, D., 2017. Chromobox homolog 2 protein: A novel biomarker for predicting prognosis and Taxol sensitivity in patients with breast cancer. *Oncology letters*, *13*(3), 1149-1156.

Chiang, C. M. (2009). Brd4 engagement from chromatin targeting to transcriptional regulation: selective contact with acetylated histone H3 and H4. *F1000 biology reports*, *1*.

Clermont, P.L., Crea, F., Chiang, Y.T., Lin, D., Zhang, A., Wang, J.Z., Parolia, A., Wu, R., Xue, H., Wang, Y. and Ding, J., 2016. Identification of the epigenetic reader CBX2 as a potential drug target in advanced prostate cancer. *Clinical epigenetics*, *8*(1), 1-14.

Clermont, P.L., Lin, D., Crea, F., Wu, R., Xue, H., Wang, Y., Thu, K.L., Lam, W.L., Collins, C.C., Wang, Y. and Helgason, C.D., 2015. Polycomb-mediated silencing in neuroendocrine prostate cancer. *Clinical epigenetics*, *7*(1), 1-13.

Crowley, L. C., Marfell, B. J., Scott, A. P., Waterhouse, N. J. (2016). Quantitation of apoptosis and necrosis by annexin V binding, propidium iodide uptake, and flow cytometry. *Cold Spring Harbor Protocols*, *2016*(11), pdb-prot087288.

Dass, S. A., Tan, K. L., Selva Rajan, R., Mokhtar, N. F., Mohd Adzmi, E. R., Wan Abdul Rahman, W. F., Din, T., Balakrishnan, V. (2021). Triple negative breast cancer: A review of present and future diagnostic modalities. *Medicina*, *57*(1), 62.

Del Gaudio, N., Di Costanzo, A., Liu, N. Q., Conte, L., Dell'Aversana, C., Bove, G., Benedetti, R., Montella, L., Ciardiello, F., Corafa, V., Ambrosino, C., Tucci, C., Conte, M., Martens, J., Stunnenburg, H., Nebbioso, A., Altucci, L. (2022). CBX2 shapes chromatin accessibility promoting AML via p38 MAPK signaling pathway. *Molecular Cancer*, *21*(1), 1-15.

Devaiah, B. N., Case-Borden, C., Gegonne, A., Hsu, C. H., Chen, Q., Meerzaman, D., Dey, A., Ozato, K., Singer, D. S. (2016). BRD4 is a histone acetyltransferase that evicts nucleosomes from chromatin. *Nature structural & molecular biology*, *23*(6), 540-548.

Di Costanzo, A., Del Gaudio, N., Conte, L., Dell'Aversana, C., Vermeulen, M., de Thé, H., Migliaccio, A., Nebbioso, A. and Altucci, L., 2018. The HDAC inhibitor SAHA regulates CBX2 stability via a SUMO-triggered ubiquitin-mediated pathway in leukemia. *Oncogene*, *37*(19), 2559-2572.

Dobrinić, P., Szczurek, A.T. and Klose, R.J., 2021. PRC1 drives Polycomb-mediated gene repression by controlling transcription initiation and burst frequency. *Nature Structural & Molecular Biology*, *28*(10),811-824.

Donati, B., Lorenzini, E., & Ciarrocchi, A. (2018). BRD4 and Cancer: going beyond transcriptional regulation. *Molecular cancer*, *17*(1), 164.

Eelen, G., Treps, L., Li, X. and Carmeliet, P., 2020. Basic and therapeutic aspects of angiogenesis updated. *Circulation research*, *127*(2), 310-329.

Elsheikh, S. E., Green, A. R., Rakha, E. A., Powe, D. G., Ahmed, R. A., Collins, H. M., Soria, D., Garibaldi, J., Paish, C., Ammar, A., Grainge, M., Ball, G., Abdelghany, M.,Pomares, L., Heery, D., Ellis, I. O. (2009). Global histone modifications in breast cancer correlate with tumor phenotypes, prognostic factors, and patient outcome. *Cancer research*, *69*(9), 3802-3809.

Fruman, D.A., Chiu, H., Hopkins, B.D., Bagrodia, S., Cantley, L.C. and Abraham, R.T., 2017. The PI3K pathway in human disease. *Cell*, *170*(4), 605-635.

Geng, Z. and Gao, Z., 2020. Mammalian PRC1 complexes: compositional complexity and diverse molecular mechanisms. *International journal of molecular sciences*, *21*(22),8594.

Gil, J. and O'Loghlen, A., 2014. PRC1 complex diversity: where is it taking us? *Trends in cell biology*, *24*(11), 632-641.

Haque ME, Jakaria M, Akther M, Cho DY, Kim IS, Choi DK. (2021) The GCN5: its biological functions and therapeutic potentials. *Clinical Science (London).* 15;135(1):231-257.

Hatano, A., Matsumoto, M., Higashinakagawa, T., Nakayama, K. I. (2010). Phosphorylation of the chromodomain changes the binding specificity of Cbx2 for methylated histone H3. *Biochemical and biophysical research communications*, *397*(1), 93-99.

Hergeth, S. P., & Schneider, R. (2015). The H1 linker histones: multifunctional proteins beyond the nucleosomal core particle. *EMBO reports*, *16*(11), 1439–1453.

Hu, F. F., Chen, H., Duan, Y., Lan, B., Liu, C. J., Hu, H., Dong, X., Zhang, Q., Cheng, Y., Liu, M., Guo, A., Xuan, C. (2022). CBX2 and EZH2 cooperatively promote the growth and metastasis of lung adenocarcinoma. *Molecular Therapy-Nucleic Acids*, *27*, 670-684.

Hu, J., Zheng, Z., Lei, J., Cao, Y., Li, Q., Zheng, Z., Chen, C. (2021). Targeting the EZH2-PPAR Axis Is a Potential Therapeutic Pathway for Pancreatic Cancer. *PPAR research*, *2021*.

Hyun, K., Jeon, J., Park, K. (2017) Writing, erasing and reading histone lysine methylations. *Exp Mol Med* 49**,** e324

Iqbal, M.A., Siddiqui, S., Rehman, A.U., Siddiqui, F.A., Singh, P., Kumar, B. and Saluja, D., 2020. CBX2 and CBX7 antagonistically regulate metabolic reprogramming in breast cancer. *bioRxiv*.

Jantscher, F., Pirker, C., Mayer, C. E., Berger, W., Sutterluety, H. (2011). Overexpression of Aurora-A in primary cells interferes with S-phase entry by diminishing Cyclin D1 dependent activities. *Molecular Cancer*, *10*(1), 1-12.

Jia, Y., Wang, Y., Zhang, C. and Chen, M.Y., 2020. Upregulated CBX8 promotes cancer metastasis via the WNK2/MMP2 pathway. *Molecular Therapy-Oncolytics*, *19*, 188-196.

Katayama, H., Sasai, K., Kawai, H., Yuan, Z. M., Bondaruk, J., Suzuki, F., Fujii, S., Arlinghaus, R., Czerniak, B., Sen, S. (2004). Phosphorylation by aurora kinase A induces Mdm2-mediated destabilization and inhibition of p53. *Nature genetics*, *36*(1), 55-62.

Kawaguchi, T., Machida, S., Kurumizaka, H., Tagami, H. and Nakayama, J.I., 2017. Phosphorylation of CBX2 controls its nucleosome-binding specificity. *The Journal of Biochemistry*, *162*(5),343-355.

Kent, S., Brown, K., Yang, C.H., Alsaihati, N., Tian, C., Wang, H. and Ren, X., 2020. Phase-separated transcriptional condensates accelerate target-search process revealed by live-cell single-molecule imaging. *Cell reports*, *33*(2),108248.

Kielkopf, C. L., Bauer, W., Urbatsch, I. L., 2021. Sodium dodecyl sulfate–polyacrylamide gel electrophoresis of proteins. *Cold Spring Harbor Protocols*, *2021*(12), pdb-prot102228.

Kim, J. and Kingston, R.E., 2020. The CBX family of proteins in transcriptional repression and memory. *Journal of Biosciences*, *45*(1),1-8.

Kim, S., & Kaang, B. K. (2017). Epigenetic regulation and chromatin remodeling in learning and memory. *Experimental & molecular medicine*, *49*(1), e281

Lee, Y.H., Liu, X., Qiu, F., O'Connor, T.R., Yen, Y. and Ann, D.K., 2015. HP1β is a biomarker for breast cancer prognosis and PARP inhibitor therapy. *PloS one*, *10*(3), e0121207.

Lercher, L., Simon, N., Bergmann, A., Tauchert, M., Bochmann, D., Bashir, T., Neuefiend, T., Riley, D., Danna, B., Krawczuk, P., Pande, V., Patrcik, A., Steele, R., Wang, W., Rupnow, B., Tummino, P., Sharma, S., Finley, M. (2022). Identification of Two Non-Peptidergic Small Molecule Inhibitors of CBX2 Binding to K27 Trimethylated Oligonucleosomes. *SLAS Discovery*.

Li, J., Ouyang, T., Li, M., Hong, T., Alriashy, M.H.S., Meng, W. and Zhang, N., 2021. CBX7 is Dualistic in Cancer Progression Based on its Function and Molecular Interactions. *Frontiers in Genetics*, *12*.

Li, J., Xu, Y., Long, X.D., Wang, W., Jiao, H.K., Mei, Z., Yin, Q.Q., Ma, L.N., Zhou, A.W., Wang, L.S. and Yao, M., 2014. Cbx4 governs HIF-1α to potentiate angiogenesis of hepatocellular carcinoma by its SUMO E3 ligase activity. *Cancer cell*, *25*(1), 118-131.

Li, Q., Pan, Y., Cao, Z., Zhao, S. (2020) Comprehensive analysis of prognostic value and immune infiltration of chromobox family members in colorectal cancer. *Frontliers in oncology,*1901.

Li, W., Wu, H., Sui, S., Wang, Q., Xu, S., Pang, D. (2021). Targeting histone modifications in breast cancer: A precise weapon on the way. *Frontiers in cell and developmental biology*, *9*, 736935.

Lomberk, G., Wallrath, L. and Urrutia, R., 2006. The heterochromatin protein 1 family. *Genome biology*, *7*(7),1-8.

Lu L, Chen Z, Lin X, Tian L, Su Q, An P, Li W, Wu Y, Du J, Shan H, Chiang CM, Wang H. (2020) Inhibition of BRD4 suppresses the malignancy of breast cancer cells via regulation of Snail. *Cell Death Differ*.;27(1):255-268.

Ma, R.G., Zhang, Y., Sun, T.T. and Cheng, B., 2014. Epigenetic regulation by polycomb group complexes: focus on roles of CBX proteins. *Journal of Zhejiang University Science B*, *15*(5), 412-428.

Mao, J., Tian, Y., Wang, C., Jiang, K., Li, R., Yao, Y., Zhang, R., Sun, D., Liang, R., Gao, Z. and Wang, Q., 2019. CBX2 regulates proliferation and apoptosis via the phosphorylation of YAP in hepatocellular carcinoma. *Journal of Cancer*, *10*(12), 2706.

Marmorstein, R., & Zhou, M. M. (2014). Writers and readers of histone acetylation: structure, mechanism, and inhibition. *Cold Spring Harbor perspectives in biology*, *6*(7), a018762.

Menon, S.S., Guruvayoorappan, C., Sakthivel, K.M. and Rasmi, R.R., 2019. Ki-67 protein as a tumour proliferation marker. *Clinica Chimica Acta*, *491*,39-45.

Milosevich N, Hof F. (2016) Chemical Inhibitors of Epigenetic Methyl lysine Reader Proteins. Biochemistry;55(11):1570-83.

Milosevich, N., McFarlane, J., Gignac, M.C., Li, J., Brown, T.M., Wilson, C.R., Devorkin, L., Croft, C.S., Hof, R., Paci, I. and Lum, J.J., 2020. Pan-specific and partially selective dye-labeled peptidic inhibitors of the polycomb paralog proteins. *Bioorganic & Medicinal Chemistry*, *28*(1), p.115176.

Milosevich, N., Wilson, C.R., Brown, T.M., Alpsoy, A., Wang, S., Connelly, K.E., Sinclair, K.A., Ponio, F.R., Hof, R., Dykhuizen, E.C. and Hof, F., 2021. Polycomb paralog chromodomain inhibitors active against both CBX6 and CBX8. *ChemMedChem*, *16*(19), 3027-3034.

Morettin, A., Paris, G., Bouzid, Y., Baldwin, R. M., Falls, T. J., Bell, J. C., Côté, J. (2017). Tudor domain containing protein 3 promotes tumorigenesis and invasive capacity of breast cancer cells. *Scientific reports*, *7*(1), 1-13.

Ni, S., Wang, H., Zhu, X., Wan, C., Xu, J., Lu, C., Xiao, L., He, J., Jiang, C., Wang, W. and He, Z., 2017. CBX7 suppresses cell proliferation, migration, and invasion through the inhibition of PTEN/Akt signaling in pancreatic cancer. *Oncotarget*, *8*(5), 8010.

Pallante, P., Forzati, F., Federico, A., Arra, C. and Fusco, A., 2015. Polycomb protein family member CBX7 plays a critical role in cancer progression. *American journal of cancer research*, *5*(5), 1594.

Piqué, D.G., Montagna, C., Greally, J.M. and Mar, J.C., 2019. A novel approach to modelling transcriptional heterogeneity identifies the oncogene candidate CBX2 in invasive breast carcinoma. *British journal of cancer*, *120*(7), 746-753.

Plys, A.J., Davis, C.P., Kim, J., Rizki, G., Keenen, M.M., Marr, S.K. and Kingston, R.E., 2019. Phase separation of Polycomb-repressive complex 1 is governed by a charged disordered region of CBX2. *Genes & development*, *33*(13-14),799-813.

Popov, N. and Gil, J., 2010. Epigenetic regulation of the INK4b-ARF-INK4a locus: in sickness and in health. *Epigenetics*, *5*(8), 685-690.

Reyes-Turcu, F. E., Ventii, K. H., & Wilkinson, K. D. (2009). Regulation and cellular roles of ubiquitin-specific deubiquitinating enzymes. *Annual review of biochemistry*, *78*, 363–397.

Rouaud, F., Hamouda-Tekaya, N., Cerezo, M., Abbe, P., Zangari, J., Hofman, V., Ohanna, M., Mograbi, B., El-Hachem, N., Benfodda, Z., Lebeau, A., Tulic, M., Hofman, P., Bertolotto, C., Passeron, T., Annicotte, J., Ballotti, R., Rocchi, S. (2018). E2F1 inhibition mediates cell death of metastatic melanoma. *Cell death & disease*, *9*(5), 1-12.

Sahni, J. M., Keri, R. A. (2018). Targeting bromodomain and extraterminal proteins in breast cancer. *Pharmacological research*, *129*, 156-176.

Saraiva, D., Cabral, M. G., Jacinto, A., & Braga, S. (2017). How many diseases is triple negative breast cancer: the protagonism of the immune microenvironment. *Esmo Open*, *2*(4), e000208.

Schade, A. E., Oser, M. G., Nicholson, H. E., DeCaprio, J. A. (2019). Cyclin D–CDK4 relieves cooperative repression of proliferation and cell cycle gene expression by DREAM and RB. *Oncogene*, *38*(25), 4962-4976.

Shorstova, T., Foulkes, W. D., Witcher, M. (2021). Achieving clinical success with BET inhibitors as anti-cancer agents. *British Journal of Cancer*, *124*(9), 1478-1490.

Shukla, S., Ying, W., Gray, F., Yao, Y., Simes, M.L., Zhao, Q., Miao, H., Cho, H.J., González-Alonso, P., Winkler, A. and Lund, G., 2021. Small-molecule inhibitors targeting Polycomb repressive complex 1 RING domain. *Nature chemical biology*, *17*(7), 784-793.

Simhadri, C., Gignac, M.C., Anderson, C.J., Milosevich, N., Dheri, A., Prashar, N., Flemmer, R.T., Dev, A., Henderson, T.G., Douglas, S.F. and Wulff, J.E., 2016. Structure–activity relationships of Cbx7 inhibitors, including selectivity studies against other Cbx proteins. *ACS omega*, *1*(4), 541-551.

Sun, D., Cao, X., Wang, C. (2019). Polycomb chromobox Cbx2 enhances antiviral innate immunity by promoting Jmjd3-mediated demethylation of H3K27 at the Ifnb promoter. *Protein & cell*, *10*(4), 285-294.

Tatavosian, R., Kent, S., Brown, K., Yao, T., Duc, H.N., Huynh, T.N., Zhen, C.Y., Ma, B., Wang, H. and Ren, X., 2019. Nuclear condensates of the Polycomb protein chromobox 2 (CBX2) assemble through phase separation. *Journal of Biological Chemistry*, *294*(5),1451-1463.

Tedesco, D., Lukas, J., Reed, S. I. (2002). The pRb-related protein p130 is regulated by phosphorylation-dependent proteolysis via the protein–ubiquitin ligase SCFSkp2. *Genes & development*, *16*(22), 2946-2957.

Ting, X., Xia, L., Yang, J., He, L., Si, W., Shang, Y., & Sun, L. (2019). USP11 acts as a histone deubiquitinase functioning in chromatin reorganization during DNA repair. *Nucleic acids research*, *47*(18), 9721–9740.

Toft, D.J. and Cryns, V.L., 2011. Minireview: Basal-like breast cancer: from molecular profiles to targeted therapies. *Molecular Endocrinology*, *25*(2), 199-211.

Vad-Nielsen, J. and Nielsen, A.L., 2015. Beyond the histone tale: HP1α deregulation in breast cancer epigenetics. *Cancer biology & therapy*, *16*(2),189-200.

Wang, L., Ren, B., Zhuang, H., Zhong, Y. and Nan, Y., 2021. CBX2 Induces Glioma Cell Proliferation and Invasion Through the Akt/PI3K Pathway. *Technology in Cancer Research & Treatment*, *20*, 15330338211045831.

Wang, S., Alpsoy, A., Sood, S., Ordonez-Rubiano, S.C., Dhiman, A., Sun, Y., Jiao, G., Krusemark, C.J. and Dykhuizen, E.C., 2021. A potent, selective CBX2 chromodomain ligand and its cellular activity during prostate cancer neuroendocrine differentiation. *ChemBioChem*, *22*(13), 2335-2344.

Wang, S., C. Ordonez-Rubiano, S., Dhiman, A., Jiao, G., Strohmier, B.P., Krusemark, C.J. and Dykhuizen, E.C., 2021. Polycomb group proteins in cancer: multifaceted functions and strategies for modulation. *NAR cancer*, *3*(4), zcab039.

Wang, W., Qin, J.J., Voruganti, S., Nag, S., Zhou, J. and Zhang, R., 2015. Polycomb group (PcG) proteins and human cancers: multifaceted functions and therapeutic implications. *Medicinal research reviews*, *35*(6),1220-1267.

Wheeler, L. J., Watson, Z. L., Qamar, L., Yamamoto, T. M., Post, M. D., Berning, A. A., Spillman, M., Behbakt, K., Bitler, B. G. (2018). CBX2 identified as driver of anoikis escape and dissemination in high grade serous ovarian cancer. *Oncogenesis*, *7*(11), 1-14.

Yamaguchi, T., Cubizolles, F., Zhang, Y., Reichert, N., Kohler, H., Seiser, C., Matthias, P. (2010). Histone deacetylases 1 and 2 act in concert to promote the G1-to-S progression. *Genes & development*, *24*(5), 455-469.

Yan, J., Xie, Y., Si, J., Gan, L., Li, H., Sun, C., Di, C., Zhang, J., Huang, G., Zhang, X., Zhang, H. (2021). Crosstalk of the caspase family and mammalian target of rapamycin signalling. *International Journal of Molecular Sciences*, *22*(2), 817.

Zhang, S., Cahalan, M. D., 2007. Purifying plasmid DNA from bacterial colonies using the QIAGEN Miniprep Kit. *Journal of visualized experiments: JoVE*, (6).

Zhang, C., Chang, L., Yao, Y., Chao, C., Ge, Z., Fan, C., Yu, H., Wang, B. and Yang, J., 2021. Role of the CBX Molecular Family in Lung Adenocarcinoma Tumorigenesis and Immune Infiltration. *Frontiers in genetics*, *12*,771062-771062.

Zhang, C.Z., Chen, S.L., Wang, C.H., He, Y.F., Yang, X., Xie, D. and Yun, J.P., 2018. CBX8 exhibits oncogenic activity via AKT/β-catenin activation in hepatocellular carcinoma. *Cancer research*, *78*(1), 51-63.

Zheng, H., Jiang, W.H., Tian, T., Tan, H.S., Chen, Y., Qiao, G.L., Han, J., Huang, S.Y., Yang, Y., Li, S. and Wang, Z.G., 2017. CBX6 overexpression contributes to tumor progression and is predictive of a poor prognosis in hepatocellular carcinoma. *Oncotarget*, *8*(12), 18872.

Zheng, S., Lv, P., Su, J., Miao, K., Xu, H. and Li, M., 2019. Overexpression of CBX2 in breast cancer promotes tumor progression through the PI3K/AKT signaling pathway. *American Journal of Translational Research*, *11*(3), 1668.

Zhou, H., Xiong, Y., Liu, Z., Hou, S., Zhou, T. (2021). Expression and prognostic significance of CBX2 in colorectal cancer: database mining for CBX family members in malignancies and vitro analyses. *Cancer Cell International*, *21*(1), 1-16.

Zou, Z., Tao, T., Li, H., Zhu, X. (2020). mTOR signaling pathway and mTOR inhibitors in cancer: Progress and challenges. *Cell & Bioscience*, *10*(1), 1-11.

Chapter 7. Appendices

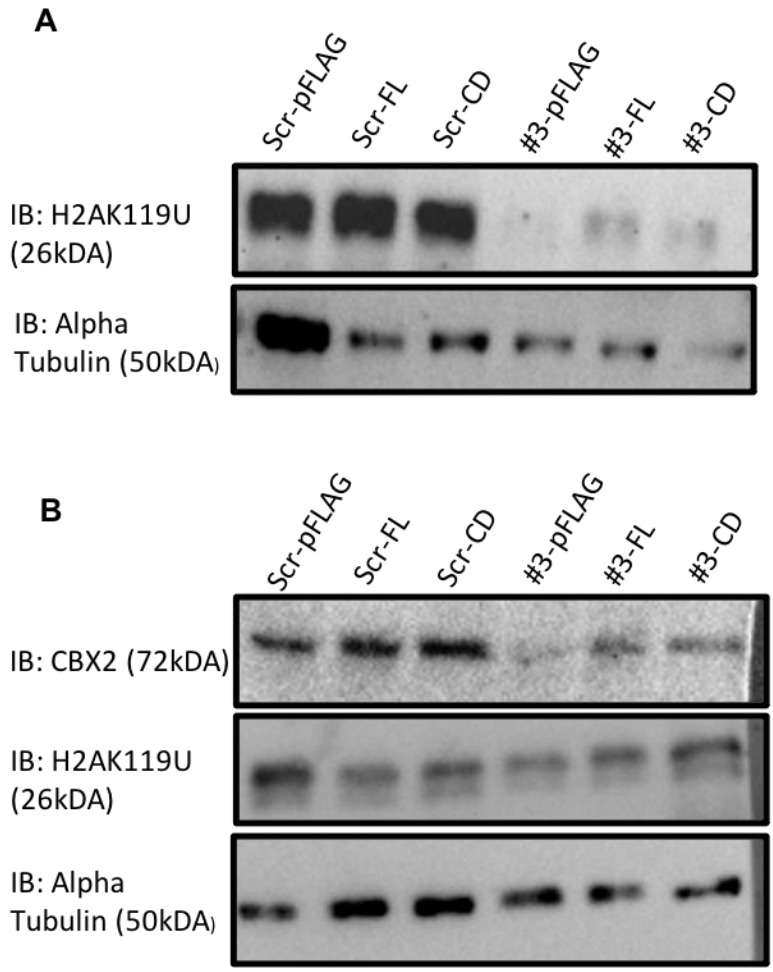

Supplementary figure 1.1. Western blot showing the global H2AK119U histone modification following the co-transfection with 250 ng of the pFLAG, FL and CD plasmid and the non-silencing CBX2 siRNA or the CBX2 targeting siRNA in MDA-MB-468 cells (A) and MDA-MB-231 cells (B). Alpha tubulin loading not equal.